A STUDY OF THE CONSTITUTION OF THE TERNARY SYSTEM

Na_2O-MnO-SiO_2

Thesis submitted by

SANAT KUMAR KABI, M.Sc., D.I.I.Sc.

to

The University of Glasgow

for

The Degree of Ph.D.

March, 1956.

I N D E X.

CHAPTER I.

INTRODUCTION.

INTRODUCTION.

A knowledge of multi-component systems containing sodium oxide is of considerable interest to both glass and heavy industries. Whereas sodium oxide is a major constituent of glasses, its application in the heavy industries is mainly as a refining agent and its use for desulphurisation and dephosphorisation of iron and steel is well known. Desulphurisation of pig iron may be effected through the use of manganese, lime or sodium carbonate as shown in the following equations.

$$\underline{FeS} + \underline{Mn} = \underline{Fe} + MnS$$

$$\underline{FeS} + CaO = FeO + CaS$$

$$\underline{FeS} + Na_2O = FeO + Na_2S$$

(The underlining of a reactant indicates that it is in solution in molten iron).

Unusually high manganese contents would be required for the efficient desulphurisation of pig iron by manganese. Thus nearly 3 percent manganese would be required to lower the sulphur content below 0.1 per cent at 1400°C. The available data(1,2) on the formation of sulphides are not sufficiently reliable to establish whether lime or soda would be the more efficient desulphurising agent for pig iron. The use of soda has the advantage of giving rise to liquid slags at iron-making temperatures, although Giedroyc and Daney(3) have examined and discussed the possibility of using solid lime to desulphurise pig iron. Soda has the further advantage in that it appears able

to replenish itself by the following secondary reaction

$$Na_2CO_3 + Na_2S + 2FeO = 2Na_2O + 2Fe + SO_2 + CO$$

On the other hand soda tends to be lost by volatilisation, the loss being greater the higher the basicity of the slag.

The use of soda for desulphurisation has made it possible to utilise certain low grade iron ores notably Northamptonshire ore in England and Dogger ore in Germany. Because of the relatively high alumina content of these ores, it was found necessary to operate with lime/silica ratios of about one instead of the higher ratio of about 1.4 used in normal practice, in order to obtain a sufficiently low melting slag. This acid burdening resulted in pig iron of higher sulphur content than usual. By the addition of sodium carbonate(4,5), it was possible to obtain iron with sulphur contents suitable for subsequent steel making operations.

There also exists the possibility of dephosphorisation of pig iron by means of soda slags. The extent of dephosphorisation depends on the temperature, the degree of oxidation and basicity of slags and the ability of the bases present to lower the activity of phosphorus pentoxide in the slag which is related to the stability of their respective phosphates. The free energy curves of Richardson, Jeffes and Withers(6) indicate that of the more common basic oxides, sodium oxide has by far the greatest dephosphorising power. This has been confirmed by Oelsen and Wiemer(7), who investigated the effect of sodium oxide addition to $Fe\text{-}3CaO.P_2O_5$ melts and by Maddocks and Turkdogan(8)(9), who pointed out that a basicity ratio of 1.5 to 2.0

gave a phosphorus distribution factor almost zero in lime slags, whereas under soda slags of similar basicity, distribution ratios of 100-200 could be attained. Dephosphorisation was found to be most efficient when the Na_2O/SiO_2 ratio approached unity. It would, however, be expected that the dephosphorising power of the slag would increase continuously with slag basicity. The most probable reason that an optimum dephosphorising power is observed at Na_2O/SiO_2 ratio ~ 1 is the tendency of the more basic slags to lose sodium oxide by the reaction

$$(Na_2O) + \underline{Fe} = 2Na + (FeO).$$

Dephosphorisation is therefore only possible if the slag composition is kept within certain limits.

The deleterious effect of alkali oxides on ladle and furnace linings has led to the study of multi-component systems containing sodium oxide. Another most important reason for the study of such systems is their use in elucidating the principles of Geochemistry.

It is the aim of the present work to further our knowledge of soda-containing slags by investigating phase relationships in the Na_2O-MnO-SiO_2 system.

CHAPTER 2.

THE BINARY SYSTEMS Mn-O, $MnO-SiO_2$, Na_2O-SiO_2 and Na_2O-MnO.

Temperature °C →
800
1000
1200
1400
1600
1800
Percent Magnesium oxide →
Mg
2
10
20
30
40
50
60
70
MgO + MgO
L + L' + MgO
L

Fig 1

THE BINARY SYSTEMS Mn-O, $MnO-SiO_2$, Na_2O-SiO_2, and Na_2O-MnO.

The only phase diagram which has been put forward for the system Mn-O is that of Benedicks and Lofquist(10), which is shown in Fig.1. These authors utilized the following information in constructing the diagram, which is in consequence somewhat tentative.

(1) The results of an experiment by Oberhoffer and D'hurt(11) who passed oxygen into molten manganese and from a microscopic examination of the slag showed that a eutectic was present.

(2) The similarity between FeO and MnO compounds.

(3) The similarity between MnO and MnS.

MnO, according to this diagram, has a congruent melting point at approximately 1700°C. Hay, Howat and White(12) have since determined the melting point as 1785°C. MnO has a sodium chloride structure and in view of the lower stability of trivalent manganese as compared with ferric iron, it would be expected that the Mn:O ratio is nearer the stoichiometric ratio (as indicated by the diagram of Benedicks and Lofquist), than the Fe:O ratio in FeO, where there is a considerable excess of oxygen. A recent investigation(13) has suggested that MnO is, like FeO, an oxygen excess compound. Thus when $p_{O_2} = 0.01$ atmosphere, the formula of the oxide was found to be $MnO_{1.044}$ at 1650°C. However, the present work was carried out in Armco-iron crucibles at temperature less than 1350°C, corresponding to partial pressures of oxygen less than 10^{-10}. Under such conditions, no great error should be incurred by assuming the stoichiometric formula.

Fig 2

Fig 3

Fig 4

Fig 5

Manganese Oxide-Silica.

The earliest investigation of this system was that of Doerinckel(14) who found that two compounds were formed, tephroite ($2MnO.SiO_2$) and rhodonite ($MnO.SiO_2$), both of which melted incongruently at 1323°C and 1215°C respectively. Greig(15) showed that a region of liquid immiscibility occurred in this system with silica-rich compositions above 1700°C. With the help of these data, Benedicks and Lofquist(16) constructed the diagram shown in Fig.2. The phase diagram presented by Herty(17) Fig.3, shows the same features as that of Benedicks and Lofquist but differs in certain details, principally in the position of the tephroite-rhodonite eutectic point. These differences led White, Howat and Hay(18) to reinvestigate the system. Their diagram is given in Fig.4, and in general is intermediate between those of Benedicks and Lofquist and Herty. In another investigation, Glaser obtained evidence of a third compound $3MnO.2SiO_2$ melting incongruently at 1194-1200°C. Glaser's work is suspect, however, for his slags were melted in pythagoras ware and were probably contaminated with Al_2O_3.

Certain inconsistencies in the form of the proposed diagram led Murad(19) to re-examine the system. The diagram obtained by Murad Fig.5, showed that both tephroite and rhodonite melt congruently. Evidence was also obtained for the formation of $3MnO.2SiO_2$ which melted incongruently at 1260°C and also appeared to decompose very easily in the solid state into tephroite and rhodonite, for even after quenching no new X-ray lines, other than those of tephroite and rhodonite, were obtained. The microstructure showed a dark etching phase which was

Weight percent of SiO_2 →
100
90
80
70
60
50
40
30
$K_2O.Al_2O_3 + 2Na_2O.SiO_2$
1700
1600
1500
1400°
1300°
1200°
1100°
1000°
900°
800°
700°
β. $Na_2O.2SiO_2$
α. $Na_2O.2SiO_2$
α. $Na_2O.2SiO_2$ + α. quartz
α. quartz + liquid
$Na_2O.SiO_2$ + α. $Na_2O.2SiO_2$
$Na_2O.2SiO_2$ + liquid
$Na_2O.SiO_2$ + liquid
$2Na_2O.SiO_2$ + $Na_2O.SiO_2$
$2Na_2O.SiO_2$ + liq.
Na_2O + liq.
α. Triclinite + liquid
α. cristobalite + liquid

Fig 6

suggested to correspond to a fine duplex structure of tephroite and rhodonite.

Sodium Oxide-Silica.

The presently accepted diagram for this system is that of Kracek(20) based partly on the earlier work of Morey and Bowen(21). According to this diagram, given in Fig.6, three binary compounds occur $Na_2O.SiO_2$, $Na_2O.SiO_2$ and $2Na_2O.SiO_2$. The former two melt congruently at 874°C and 1089°C respectively, the latter incongruently at 1120°C. Loffler(22) indicated the existence of a pyrosilicate 3 $Na_2O.2SiO_2$ with a congruent melting point at 1122°C. Zintl (23) also reported the existence of this compound. No evidence for it was obtained by Kracek; it is possible that the compound obtained by Loffler and Zintle was in fact $2Na_2O.SiO_2$. Kracek also reported the presence of two enantiomorphic inversions of $Na_2O.2SiO_2$ at 678°C and 707°C.

Sodium Oxide-Manganous Oxide.

No work on this system has been reported. Oelsen(24) reported the existence of a eutectic in the Na_2O-FeO system and it is possible that this also is a eutectiferous system.

Sodium Oxide-Manganous Oxide-Silica.

No previous work appears to have been carried out on the ternary system.

CHAPTER 3.

INTERIONIC ATTRACTION IN SILICATES.

INTERIONIC ATTRACTION IN SILICATES.

The investigation of silicate systems has proceeded along two main lines. The first of these is the study of the structure of solid and liquid silicates from a consideration of the individual and mutual behaviour of the ions concerned. The second is the study of the phase diagrams of silicate systems. As yet no definite relationships exist which can be used to deduce the latter from the former or vice versa. However, useful qualitative relationships have been formulated whereby the tendency to glass formation, compound formation and liquid immiscibility in poly-component systems can be derived approximately from the characteristics of the ions concerned. In the present Chapter a brief summary will be given of existing knowledge of the interaction of ions in silicate structures and its application to silicate systems. The behaviour of the Na_2O-MnO-SiO_2 system will be discussed later in the light of this knowledge.

It is well established that the structure and stability of both solid and liquid silicates depend on the capacity of the cations present to co-ordinate with oxygen ions. The coordination number of the ions in silicates has been most profitably discussed in terms of ionic interactions (coulombic, Van der Waals, etc.,) and the ionic nature of silicate crystals. The stability of the silicate structure therefore depends on the size and valency of the ions present and the geometry of the spatial distribution of the ions.

Dietzel(25) pointed out that the possibility of the formation of binary or ternary silicate compounds is determined by the ionic field strength Z/a_2 where Z is the valency and a is the distance between cation and anion. He also showed that the tendency to form compounds generally decreased with increasing attraction between cations (other than silicon) and oxygen anions. Thus if the behaviour of manganese with regard to the tendency of its oxide to form compounds with silica is compared with that of other common divalent cations such as Ca^{++}, Mg^{++}, Fe^{++} it is found that the number of binary silicate compounds formed decreases in the following order:-

Ion	Ionic Radius(A°) (Pauling)	Compound formed
Ca^{++}	0.99	$CaO.SiO_2$, $3CaO.2SiO_2$, $2CaO.SiO_2$, $3CaO.SiO_2$
Mn^{++}	0.80	$MnO.SiO_2$, $3MnO.2SiO_2$, $2MnO.SiO_2$
Mg^{++}	0.65	$MgO.SiO_2$, $2MgO.SiO_2$.
Fe^{++}	0.75	$2FeO.SiO_2$.

According to Dietzel, the number of compounds should decrease in the order $Ca^{++} > Mn^{++} > Fe^{++} > Mg^{++}$. The presence of three compounds in the $MnO-SiO_2$ system is not incompatible with the interionic attraction corresponding to the above ionic radii. The fact that the activity of silica in $MnO-SiO_2$ melts is intermediate between that in $FeO-SiO_2$ and $CaO-SiO_2$ melts(26) corroborates the above data. To explain the apparently anomalous position of Mg^{++}, two other factors must be considered. Firstly Pauling(18) has pointed out that if the ratio of the radius of the cation to that of the anion falls below

0.414, anion-anion contact rather than cation-anion contact will occur. In such cases the equilibrium distance between cation and anion will be larger than that calculated from the sum of their radii. Pauling in discussing the structure of MgO found that $R_{Mg^{++}} + R_{O^{--}}$ (where R = radius) was slightly larger than the calculated value, whereas in other cases, e.g., CaO, SrO, BaO, agreement was very satisfactory. The ratio $R_{Mg^{++}}/R_{O^{--}} = 0.46$ which is in the region where double repulsion becomes operative, and consequently the value of $R_{Mg^{++}} + R_{O^{--}}$ in MgO would be expected to be larger than calculated theoretically.

The second factor which must be considered is the effect of polarization and counter polarization. Fajans and Kreidl(27), from an examination of the molecular refraction of oxygen ions in silicates containing different cations, showed that electrons of polarizable anions can penetrate the outer electronic shell of "non-noble" gas type cations more readily than that of "octet-cations". Thus electrons of oxygen anions can penetrate the electron cloud of Mn^{++} or Fe^{++} with greater ease than that of, e.g., Mg^{++}. This will tend to increase the cation-anion attractive force in the case of Mn^{++} and Fe^{++}.

It will be seen that whereas the first factor tends to raise Mg^{++} to a higher position in the order $Ca^{++} > Mn^{++} > Fe^{++} > Mg^{++}$ by decreasing Z/a_2 because a is larger than that expected, the second factor tends to move both Mn^{++} and Fe^{++} down the scale by increasing the interionic attraction. These two factors could therefore give

the order of compound formation as $Ca^{++} > Mn^{++} > Mg^{++} > Fe^{++}$. A similar order should be applicable in comparing the different ternary systems, Na_2O-RO-SiO_2 where R = CaO, MnO, MgO, FeO.

In the above discussion it has been assumed that the cation-anion bond in silicates is completely ionic. This is not necessarily true, since it may possess a certain amount of mixed bonding (partly ionic and partly covalent) conferring some directional property to the bond. This is particularly true in the case of highly polarizable ions like Mn^{++}, Fe^{++}. The sodium ion, on the other hand, is almost completely ionic in character, so that Na_2O has the effect of supplying oxygen ions which can attach themselves preferentially to either Si^{4+} or other cations such as Mg^{++}, Ba^{++}, Ca^{++}, Mn^{++}, Fe^{++}, because of their higher covalency factor. This particular property of Na_2O of supplying oxygen is noticed when Na_2O is added to fayalite, $2FeO.SiO_2$. With very small additions of Na_2O to fayalite, FeO and $Na_2O.2SiO_2$ are formed. This property of Na_2O is also shown by the absence of liquid immiscibility in the Na_2O-SiO_2 system, although the tendency to two liquid formation in the high silica region is shown by the "S" shaped liquidus curve.

From the above considerations the following characteristics of the ions concerned can be summarized.

(1) Mn^{++} ion is highly polarizable. The bond between Mn^{++} and O^{--} is much stronger than that between Na^{+} and O^{--}.

(2) The oxygen ions from Na_2O have a tendency to attach themselves preferentially to Mn^{++} and Si^{++++}.

(3) The Na^{+} ions occupy the holes in the network of the silicate structure and show almost no tendency as a "network former".

(4) Mn^{++} and Fe^{++} have a tendency to give mixed bonding and Mn^{++} like Fe^{++} will stabilize glass.

CHAPTER 4.

PREPARATION OF RAW MATERIALS AND TERNARY SLAGS.

PREPARATION OF RAW MATERIALS AND BINARY SLAGS.

Manganous Oxide.

Manganous oxide was prepared by heating manganous oxalate in vacuum at 1000°C for an hour. Whilst the temperature was still 1000°C cracked ammonia was passed for about an hour. It was allowed to cool in the atmosphere of cracked ammonia. Manganous oxide of equal purity could be prepared by heating manganous oxalate at a temperature of 1000°C in an atmosphere of cracked ammonia, but the product required to be reheated in cracked ammonia at 1000°C for two to three hours.

Manganous oxalate is usually prepared either by the action of sodium oxalate or ammonium oxalate on manganous sulphate. In the preparation of manganous oxide the latter product was used because impurities present as ammonium salts volatilise, leaving a purer product.

The arrangement of the apparatus used is shown in Fig.7.

Silica.

Ground silica sand of more than 99 per cent purity was heated with hydrochloric acid (1:1) to dissolve any iron present as impurity. The sand was then washed with water. This procedure of alternate boiling with hydrochloric acid and washing with water was repeated till no appreciable iron was present in the leaching solution. The washed silica was dried in a muffle at 900°C to remove any carbonaceous impurities. The product contained 99.9 per cent SiO_2.

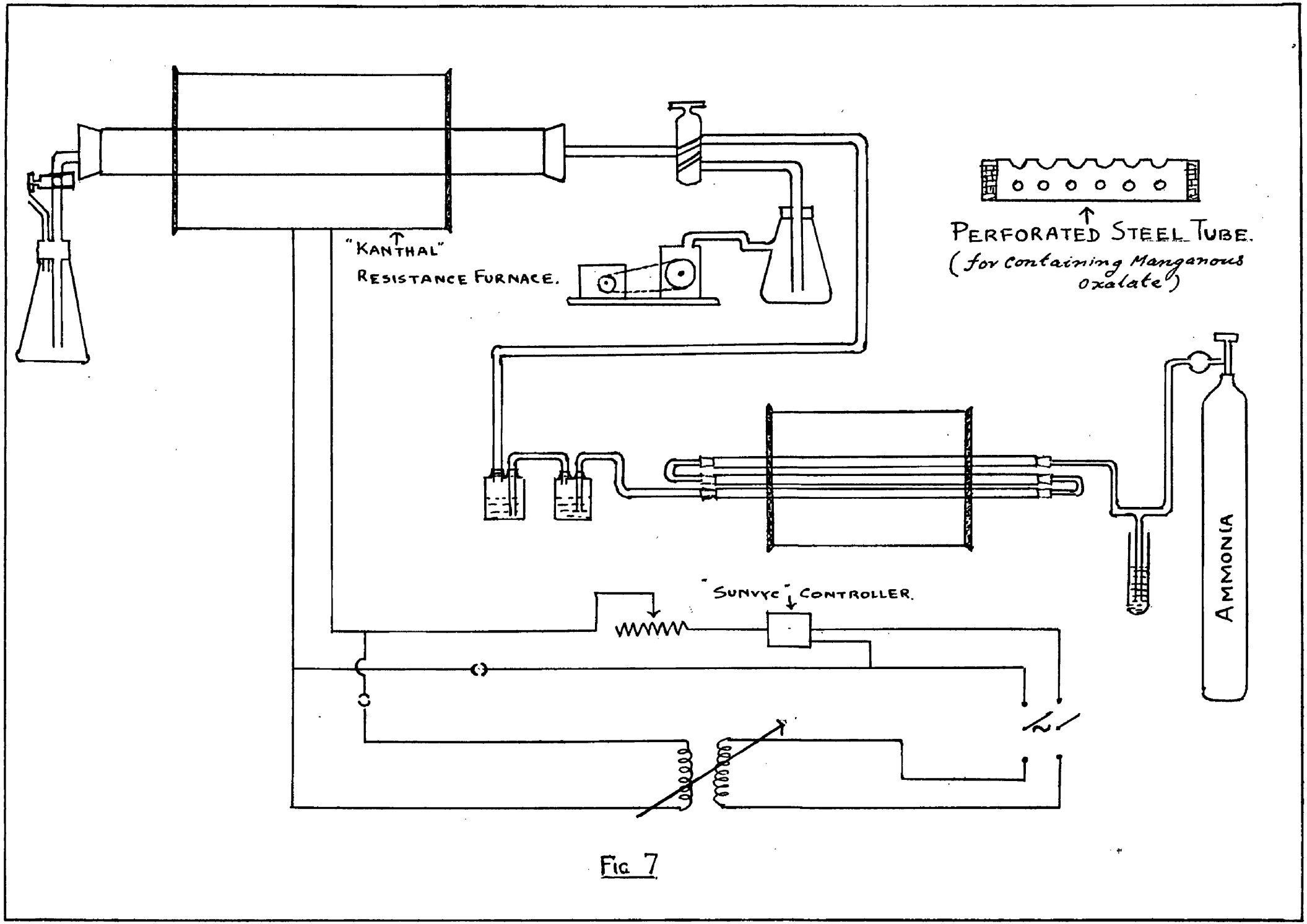
"KANTHAL"
RESISTANCE FURNACE.
PERFORATED STEEL TUBE.
(for containing Manganous oxalate)
AMMONIA
"SUNVYC" CONTROLLER.

Fig 7

Tephroite ($2MnO.SiO_2$).

Manganous oxide and silica in the proportion corresponding to the composition of Tephroite were melted in an Armco iron crucible in a platinum resistance furnace. An atmosphere of purified nitrogen was maintained in the furnace tube. The product was crushed and remelted.

Sodium Silicates.

The systems $R_2O-SiO_2-CO_2$ (R = K, Na, Li) have been studied by numerous authors because of their importance in experimental petrology. Niggli(28) compared the three systems $Li_2O-SiO_2-CO_2$, $Na_2O-SiO_2-CO_2$ and $K_2O-SiO_2-CO_2$ and concluded that only potassium disilicate, sodium metasilicate and lethium orthosilicate may be directly prepared by melting the ingredients together. Huttig and Dimoff(29), investigating the reaction between Na_2CO_3, Na_2O and amorphous silica, found that evolution of CO_2 was not continuous, neither did it take place at one temperature. About half was evolved between 610° and 765°C, the remainder above about 875°C (Fig.8). Turner(30) also investigated volatilization from sodium silicate. His results, Fig.9, show that volatilization increases sharply as the sodium oxide content increases beyond that corresponding to sodium disilicate. This was confirmed by Carter and Ibrahim(31). Consequently no attempt was made to make sodium metasilicate or sodium disilicate of exact composition.

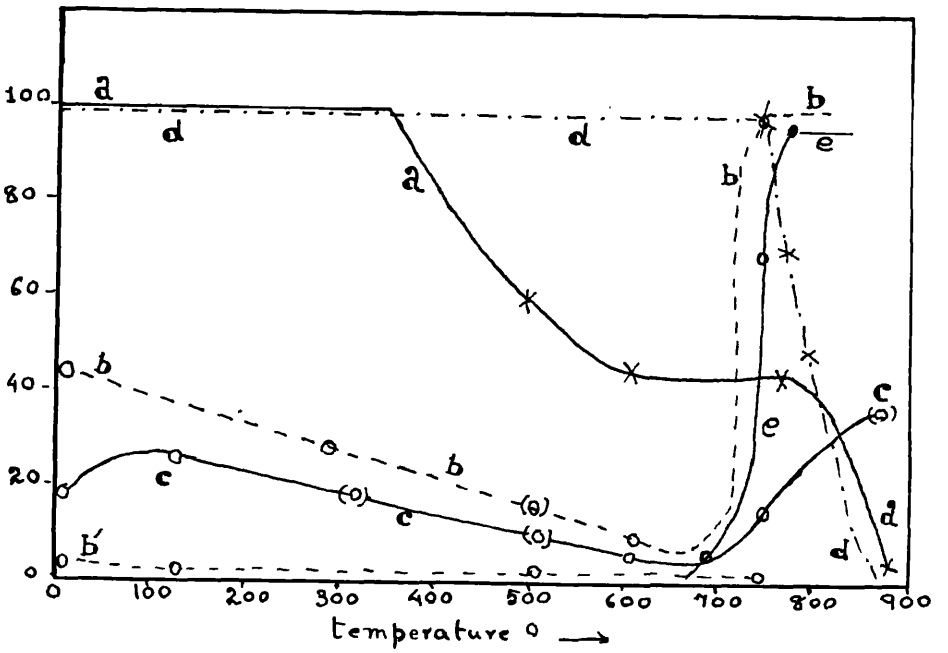

Reaction between Sodium Carbonate and Silica. (Huttig and Dimoff)

FIG 8

Curve "a" = Residual CO_2 in the crystalline phases.

Curve "b" = Percentage amounts of soluble silica in the presence of Na_2CO_3.

Curve "b'" = " " " " " in the absence of Na_2CO_3

Curve "c" = Percentage amounts of hygroscopic water.

line "d" = Intensity of characteristic x-Ray interference lines of Na_2CO_3

line "e" = " " " " " lines of Na_2SiO_3.

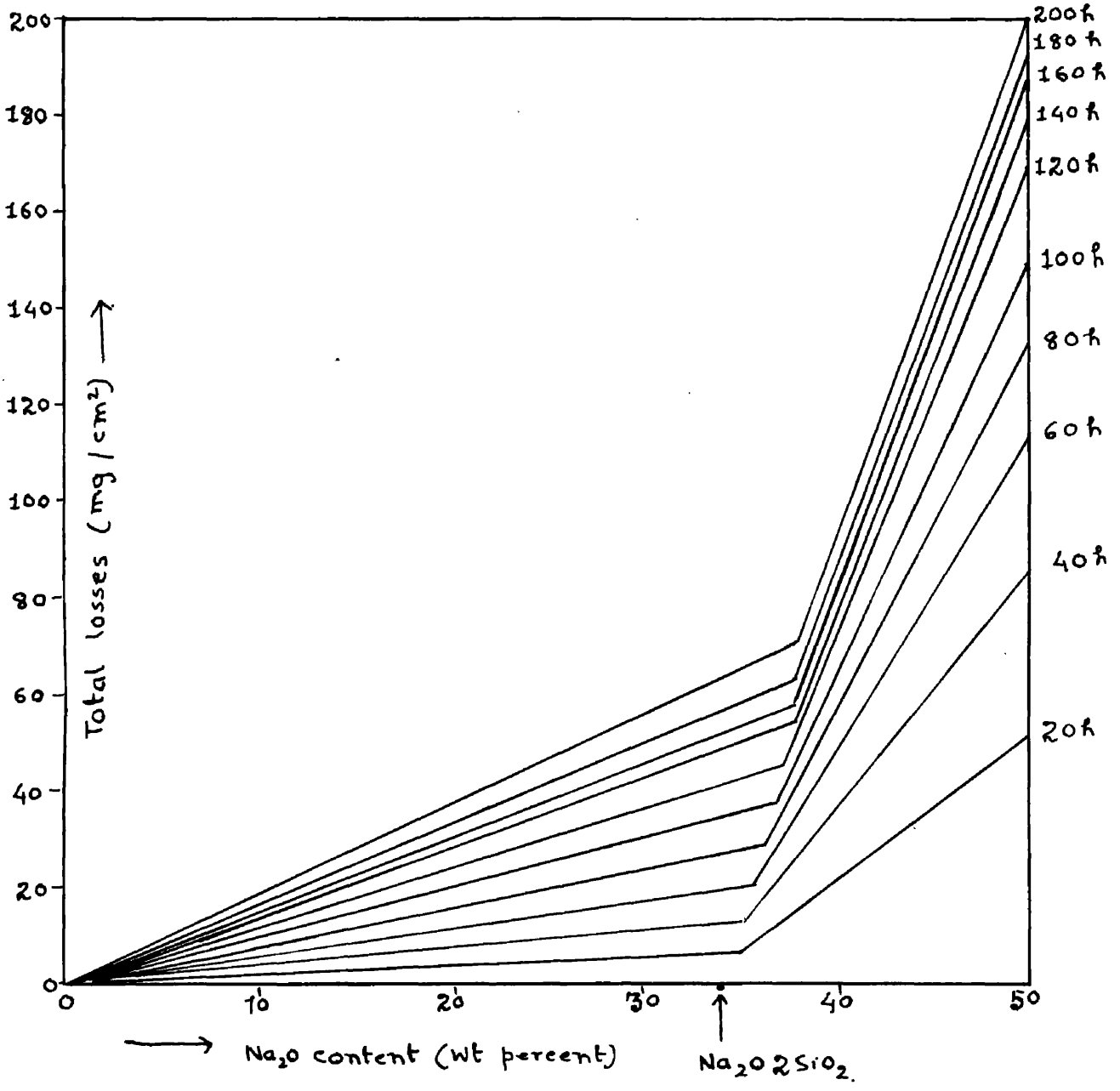

Volatilization losses of Sodium Silicate glasses at 1400°c.
as a function of the composition (Turner)

Fig 9

Analar sodium carbonate and purified silica, in a proportion corresponding to sodium metasilicate were mixed thoroughly and melted in a platinum basin in a muffle (> 1200°C). It was crushed and remelted. The procedure gave sodium silicate whose sodium oxide content was about 2 to 3 per cent lower than that corresponding to sodium metasilicate. This sodium silicate was used to make ternary slags on the $2MnO.SiO_2$ - $Na_2O.SiO_2$, $2MnO.SiO_2$-$Na_2O.SiO_2$, $MnO.SiO_2$ - $Na_2O.SiO_2$ joins. For the slags on the join MnO - $Na_2O.SiO_2$ sodium silicate was prepared which contained a slightly higher per cent of sodium oxide (1 to 2 per cent) than that corresponding to sodium metasilicate. For an X-ray standard of sodium metasilicate and sodium disilicate only one sample of each compound was made corresponding to the exact compositions, $Na_2O.SiO_2$ and $Na_2O.2SiO_2$.

Preparation of ternary Slags.

These were prepared by mixing thoroughly the required amounts of sodium and manganese silicates. Allowance for the non-stoichiometry of the former was made by the addition of calculated amounts of MnO or SiO_2 as required. The mixture was melted in an Armco iron crucible in an atmosphere of purified nitrogen, using a platinum resistance furnace for high melting slags and a Kanthal resistance furnace for those with low melting points. Slags with high MnO or SiO_2 contents were kept about 100°C above the temperature at which they

became fluid for about half an hour, whereas those of high Na_2O content were raised only 50°C above the corresponding temperatures. The slags were observed through the window shown in Fig.10. These were later analysed to check whether the required composition had been obtained.

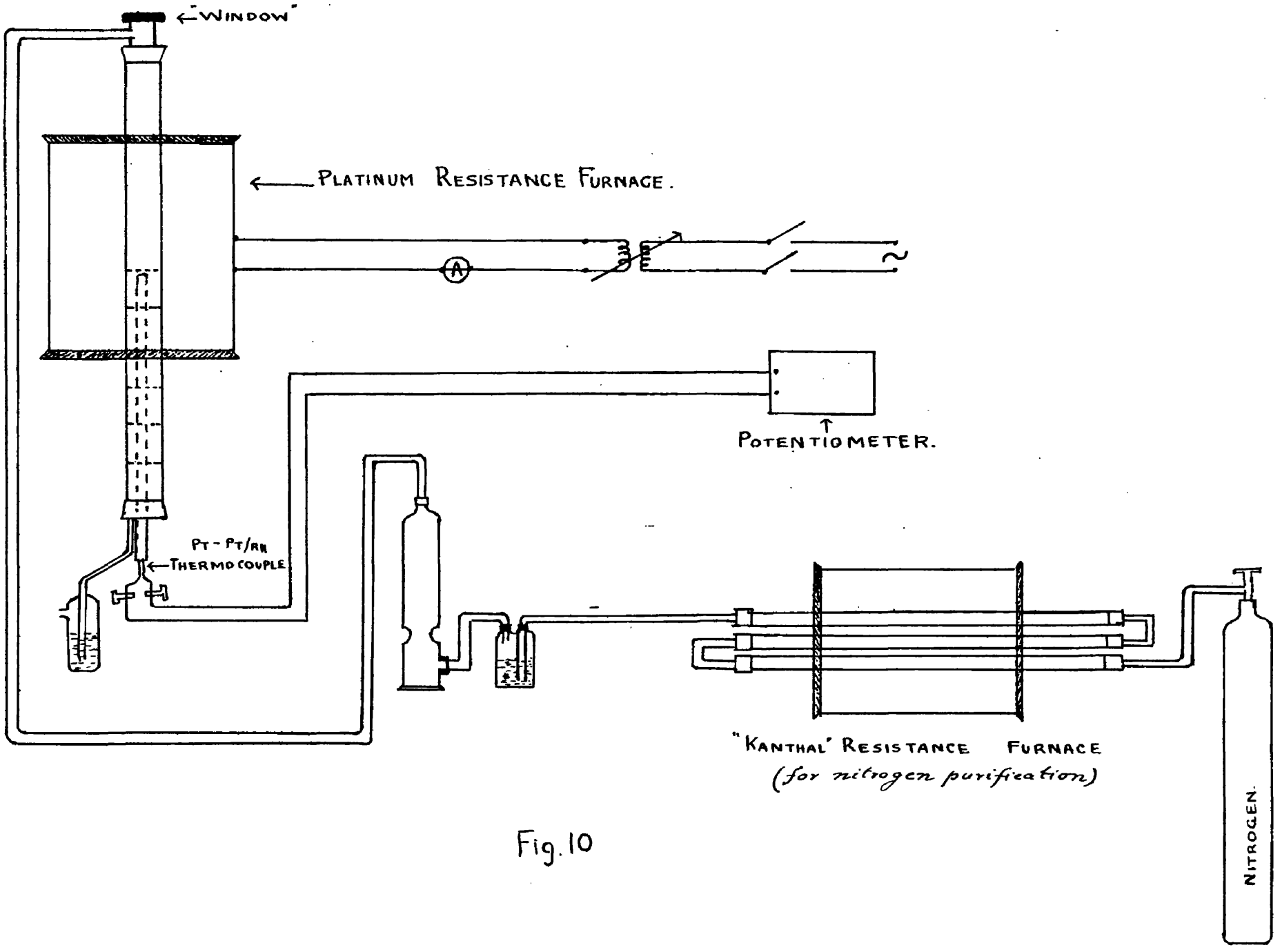
"WINDOW"
PLATINUM RESISTANCE FURNACE.
A
POTENTIOMETER.
PT - PT/RH
THERMO COUPLE
"KANTHAL" RESISTANCE FURNACE
(for nitrogen purification)
NITROGEN.

Fig. 10

CHAPTER 5.

IDENTIFICATION OF SLAG CONSTITUENTS.

IDENTIFICATION OF SLAG CONSTITUENTS.

The identification of the crystalline constituents of the slags was carried out by four methods, viz.,

(1) Microscopic examination using reflected light.

(2) Examination of thin sections using transmitted light.

(3) The determination of refractive indices by the immersion method.

(4) X-ray diffraction photography.

The first method gave direct information on the mode of crystallisation of the slags. It was usually possible to identify with certainty the primary crystalline phase by this method and sometimes the phases which separated during binary precipitation, particularly the binary precipitation of $2MnO.SiO_2$ and MnO.

The other methods were used to confirm the results obtained by microscopic examination of the polished sections and to identify finely divided crystalline phases which had been formed during binary and ternary crystallisation. Identification of crystals by refractive index measurement was extremely useful in the case of high soda slags where, due to the etching effect of the polishing fluid, good micro-sections were extremely difficult to obtain.

Micro-examination of slags.

The slags were polished for micro-examination using the usual polishing procedure. This method did not present any difficulty with slags containing high percentages of silica or manganous oxide but those containing high percentages of Na_2O were extremely difficult to polish. Water was found to have an etching action on the slags. Organic reagents like carbon tetrachloride, alcohol or paraffin oil stained the surface. Slags nearer the sodium metasilicate composition etched even on exposure to the atmosphere within five to ten minutes. Moreover the glassy matrix of the quenched slags tended to be etched and cracks developed during polishing. This effect can be expected. Since in the first place, these slags contained larger amounts of Na_2O, and secondly, the quenching process induced certain mechanical strains in the glass, both these factors will accentuate etching. The quench strain induced a certain amount of anisotropy to the glassy matrix which could be observed in polarized light in a Vickers Projection microscope. Dry polishing, using no water, gave a matte surface unsuitable for examination under microscope. However, these slags were softer. They were polished as lightly as possible to the 4/0 paper stage, dipped in water for a few seconds and quickly dried. These specimens were then polished on a dry "selvyt" without any polishing powder and finally polished on nylon. A difficulty encountered with slags of high Na_2O content was that they were soft and had a tendency to flow. This

obscured the grain boundaries and so slight etching was necessary. It was found that about 0.1 to 0.2 per cent of nitric acid in a mixture of water and alcohol was suitable for etching. In each case the duration of etching had to be found by trial and error. Every specimen had to be dried quickly by cotton wool and then dried in warm air. If the preliminary drying by cotton wool was omitted the slags had a tendency to stain. Specimens were preserved in a desiccator with P_2O_5 as a dehydrant.

Determination of Refractive Index.

When crystalline particles are immersed in a liquid and examined by transmitted light their appearance depends on the relative refractive indices of the crystal and the immersion medium. The observation of "relief" of the particle is a very sensitive test for determination of refractive indices of the crystalline particle relative to the liquid in which the crystal is immersed. Relief is absent when the refractive index of the crystal is equal to that of the surrounding liquid because the light is not reflected or refracted at the interface. The observation of relief is facilitated by the use of the "Becke line" effect.

The "Becke line"effect refers to an optical phenomenon associated with the vertical interface of the two phases of different refractive indices. It is best observed with a high power objective. With a low power objective a reduction in illumination increases the

sensitivity of the test. Fig.11 represents this effect where N_2 is the higher refractive index and N_1 the lower. The resultant effect is a concentration of light above the interface on the side towards the medium of higher refractive index. The concentration of light becomes apparent when the microscope is slightly raised.

Crystal fragments are generally crudely lenticular in cross section, and immersed in a liquid of known refractive index, behave like bi-convex lenses. Their behaviour is diagrammatically represented in Fig.11 (B and C). The effect of slightly raising the objective is shown in 11 (D,E,F). The arrows show the movement of the "Becke line". This movement becomes less apparent as N_F approaches N_L. When $N_F = N_L$ the fragment vanishes. The various effects of oblique illumination are shown in Fig.12.

The above criteria are strictly applicable only when fragments are examined with monochromatic light. In the determination of refractive indices, white light was used. Liquid media generally disperse light more than the solids placed in them. In the case of oblique illumination when the refractive index of the crystal for yellow light matched that of the immersion liquid, colour fringes appeared around the edges of the fragment, red on one edge and blue on the other.

The birefringence of sodium silicates and other new compounds was not high. In no case was the interference colour higher than yellow. Because of the low birefringence only the average refractive

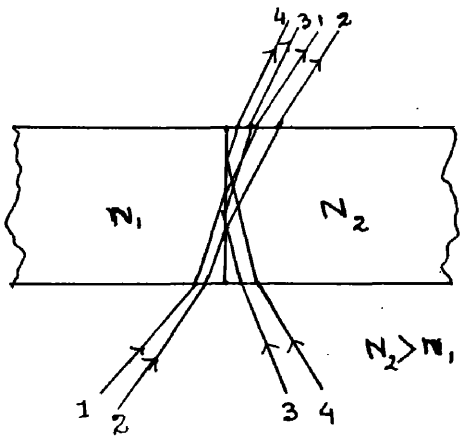

ORIGIN OF THE BECKE LINE

N_i = INDEX OF REFRACTION.

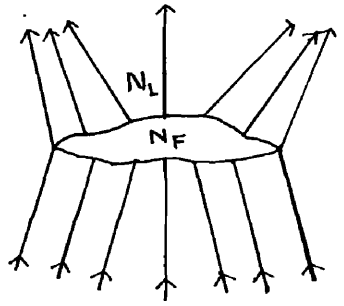

B $N_F < N_L$

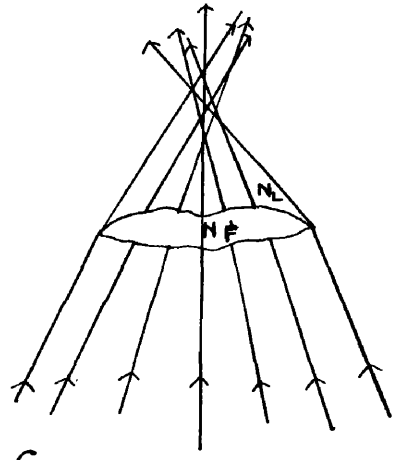

C $N_F > N_L$

REFRACTION OF LIGHT BY LENTICULAR FRAGMENTS.

N_L = INDEX OF REFRACTION OF SURROUNDING LIQUID.

N_F = " " " " FRAGMENT.

Fig 11

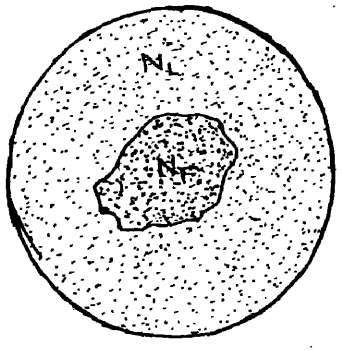

D

MICROSCOPE FOCUSSED ON GRAIN.

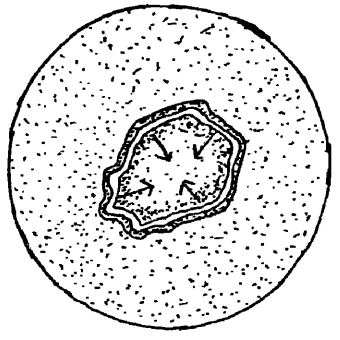

E

MICROSCOPE TUBE SLIGHTLY RAISED

$N_F > N_L$

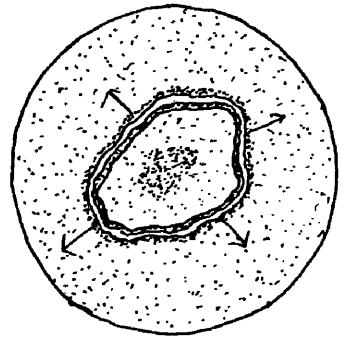

F

MICROSCOPE TUBE SLIGHTLY RAISED

$N_F < N_L$

CENTRAL ILLUMINATION AND BECKE LINE.

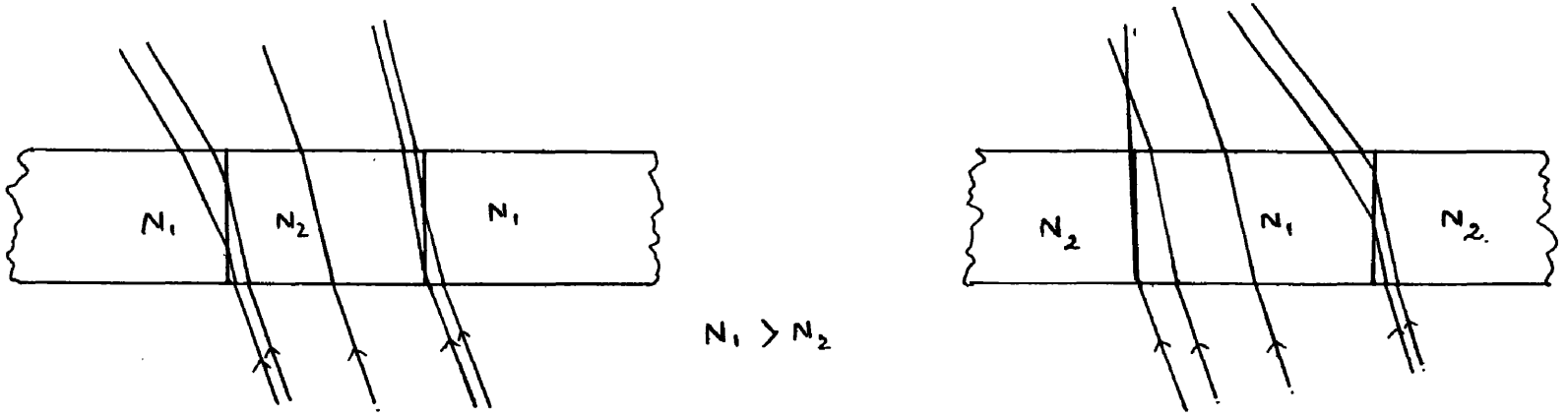

OBLIQUE ILLUMINATION WITH VERTICAL CONTACTS.

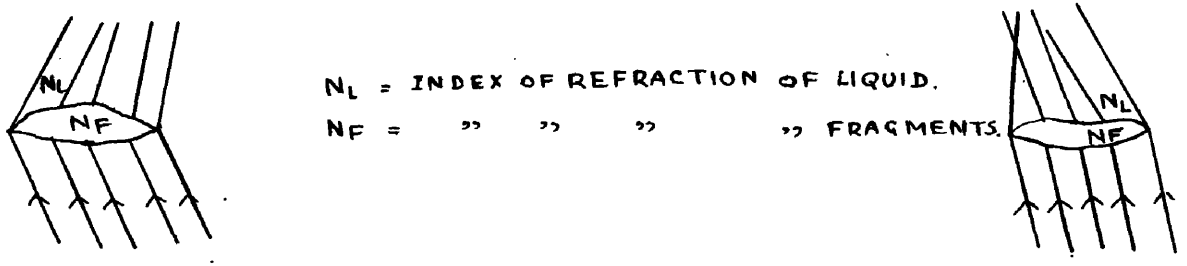

Fig 12

OBLIQUE ILLUMINATION OF LENTICULAR FRAGMENTS.

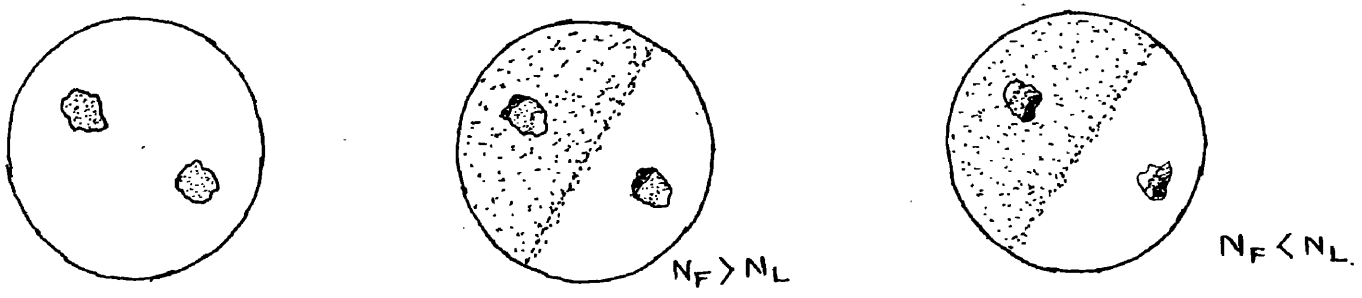

ENTIRE FIELD ILLUMINATED FIELD HALF DARKENED FIELD HALF DARKENED

OBLIQUE ILLUMINATION IN PLAN.

index was determined. Compounds like manganous oxide, tephroite and rhodonite were easily distinguished because of their high refractive indices and high birefringence. These compounds were also easily distinguishable in the micro-examination of polished slags.

The following liquids were used as immersion media(32).

Mixtures of Ethyl Oxalate and Medicinal paraffin

= 1.41 to 1.47

Mixtures of Medicinal paraffin and α-chloronaphalene

= 1.47 to 1.63

Mixtures of α-chloronaphthalene and Methylene Iodide

= 1.63 to 1.74

Mixtures of Methylene iodide and Merwin's Solution

= 1.74 to 1.86

Merwin's Solution was prepared by dissolving 35 grammes of Iodoform, 10 grammes of Sulphur, 31 grammes of Stannic iodide, 16 grammes of arsenic tri-iodide and 8 grammes of antimony tri-iodide in 100 grammes of methylene iodide with periodical shaking and gentle warming.

Other liquids used were:-

Monobromo-benzene	1.554
Bromoform	1.598
α-Bromo naphthalene	1.658

Examination of thin sections using transmitted light.

Thin sections were prepared in a few cases by the normal procedure of grinding with successively finer grades of carborundum powder immersed in water. It was possible to gain information on the mode of crystallisation and optical properties of certain of the crystalline constituents present, but the method was of limited applicability on account of the action of the water used during grinding on the constituents of high sodium oxide slags. Unfortunately it was not possible to modify the procedure to use a non-aqueous suspension medium for carborundum.

X-ray Examination.

X-ray diffraction photographs were taken of all the slags using Cu-K_α radiation from a Raymax rotating anode X-ray unit and a 9 cm. diameter Van Arkel camera. Copper radiation gave considerable darkening of the X-ray picture due to incoherent scattering of the X-ray beam but had to be used, as a more suitable rotating anode was not available.

CHAPTER 6.

THE DETERMINATION OF THE TEMPERATURE OF THERMAL CHANGES.

THE DETERMINATION OF THE TEMPERATURE OF THERMAL CHANGES.

The temperature of the phase changes which occur during the crystallisation of a liquid slag may be determined by a number of methods each of which has certain advantages and disadvantages. The well known method of differential thermal analyses used in physical metallurgy is of little use in the determination of arrest points of certain slags during cooling, due to the tendency to super-cooling and glass formation in silicate systems. The method can be used during heating provided the slag is initially in the completely crystalline state. The differential curves so obtained give a clear indication of thermal arrests occurring during heating but usually additional information is required to enable the changes occurring at each arrest to be identified with certainty. This is particularly true when the possibility of polymorphic changes in the solid state exists. Visual observation of the beginning and end of melting, as described by White, Howat and Hay(33) and used in the investigation of the Na_2O-FeO-SiO_2 system by Carter and Ibrahim(34), furnishes reasonably accurate values for the solidus and liquidus temperatures when the slag is completely or almost completely crystalline. It also provides a useful means of identifying these two arrests on differential curves. The temperatures determined by visual observation are probably accurate to within $\pm$ 5°C, although the error may be slightly greater for the liquidus determination. For greater accuracy and also when difficulty is experienced in crystallizing

the slags completely, the quenching method, used extensively by the Geophysical Laboratory, Washington, D.C., in their numerous investigations of slag systems of interest in geology, may be used. Its main disadvantage is the multiplicity of apparatus required to carry out the method expeditiously. A modification of it was used in the present work along with the other two methods mentioned above. The experimental procedure used in each method will now be described.

Differential Thermal Analysis.

The experimental arrangement is shown in Fig.13A and 13B. One of the Pt/13% Rh.Pt. thermocouples protected by an Armco iron sheath and a gland, was inserted in the slag, the other was placed in magnesia in the second hole in the crucible, which served as a neutral body. The readings on the potentiometer corresponding to the slag temperature and differential were taken every 30 seconds. The galvanometer was normally connected to the differential except for the few seconds required to measure the slag or neutral body temperature. If there was any change in the differential reading, as revealed by the galvanometer during the intermediate periods, the corresponding readings on the potentiometer were noted together with the time.

The temperature of the slag and the differential reading were plotted on the same graph with time as abscissa and both slag temperature and differential reading as the ordinate. The temperature corresponding to a change point can be easily found from the graph.

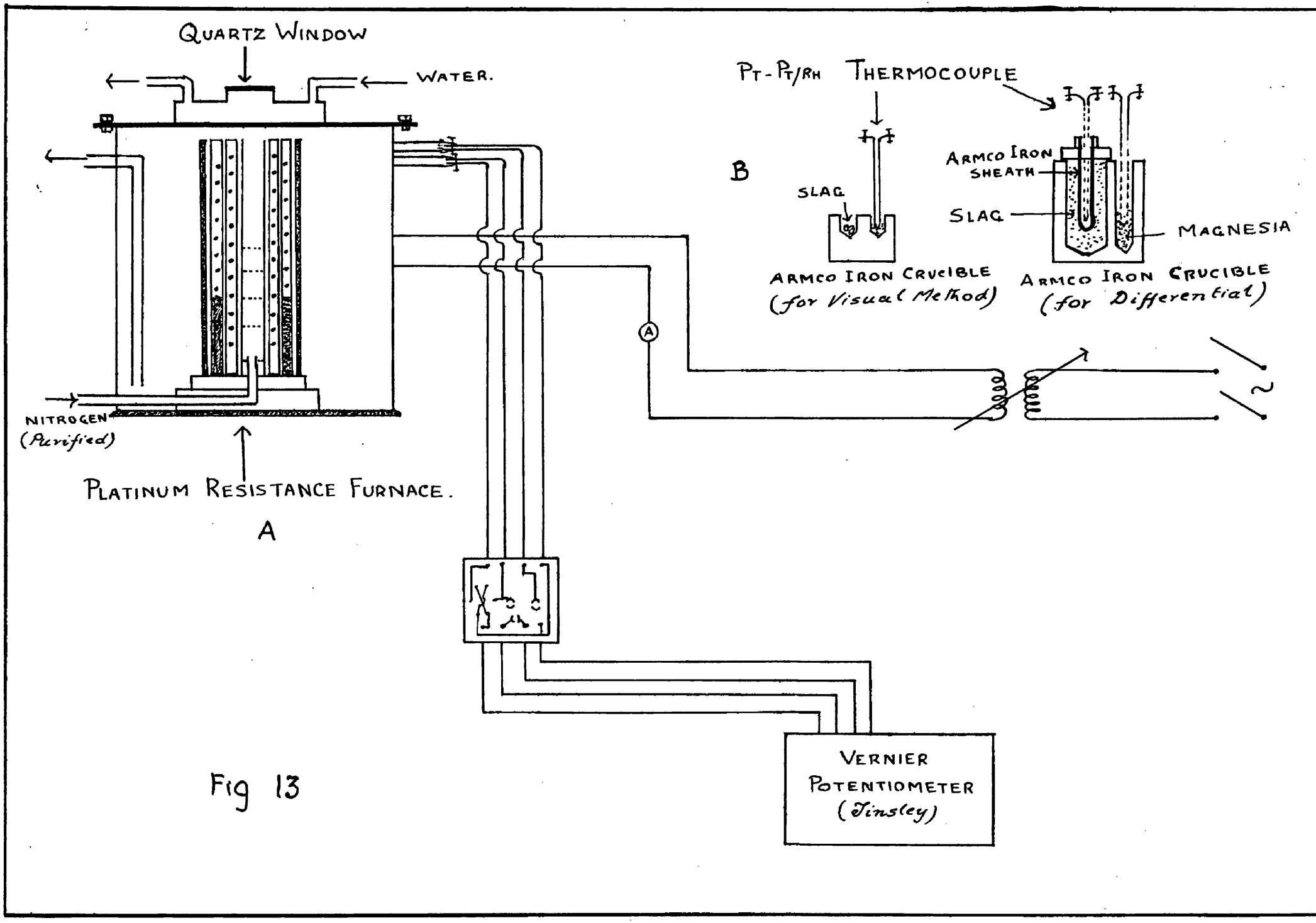
QUARTZ WINDOW
WATER.
NITROGEN
(Purified)
PLATINUM RESISTANCE FURNACE.
A
PT-PT/RH THERMOCOUPLE
B
SLAG
ARMCO IRON CRUCIBLE
(for Visual Method)
ARMCO IRON
SHEATH
SLAG
MAGNESIA
ARMCO IRON CRUCIBLE
(for Differential)
A
VERNIER
POTENTIOMETER
(Tinsley)

Fig 13

The furnace was heated at the rate of one to one and a half degrees centigrade per minute.

Visual Observation of Melting.

The furnace used was the same as that used for differential thermal analysis. The arrangement of the crucible was slightly different as shown in Fig.13. The crucibles were made from Armco iron. Two vertical holes, as close together as possible were drilled in the crucibles to the same depth (~ ½ cm.). One or two fragments of slags were placed in the larger hole and the thermocouple junction inserted in the other. Heating was carried out at about one degree centigrade per minute in an atmosphere of purified nitrogen. The course of melting was observed through the quartz window in the water cooled lid of the furnace, a small lens being used for magnification.

Quenching Method.

For most of the slags examined it was possible to obtain a completely glassy structure by sufficiently rapid cooling and in many cases even furnace cooling was enough to give glass only. If a glass of composition X, Fig.14, is annealed for a sufficiently long period at temperature T_2 and then quenched, crystals of primary phase separating should be distinguishable by refractive index measurements or microscopic examination. If the quenching temperature had been T_1, only glass would have been obtained. By repeated quenching experiments over a narrowing temperature range, the liquidus temperature can be obtained

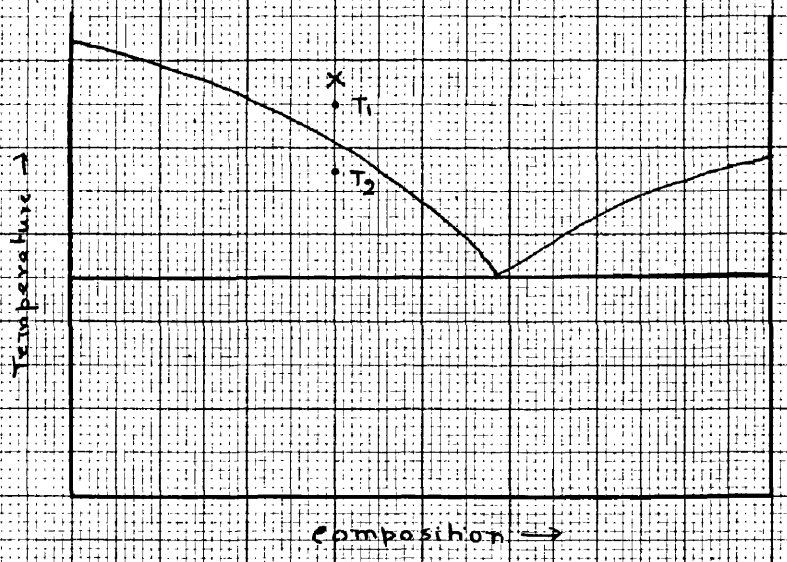

Fig. 14

to within the accuracy of the temperature measuring equipment. The same procedure can be used to determine the temperatures of binary and ternary crystallisation. The crucibles containing the slag were therefore placed in an iron cage and held at given temperatures in an inert atmosphere for a suitable length of time. The cage was then withdrawn on the end of a long iron hook and quenched immediately in water. For the slags which required exceptionally long annealing periods to induce crystallisation, it was found necessary to adopt a different procedure. In the first arrangement used, 0.25 in. diameter, 0.25 in. deep holes containing the slags, were drilled in a strip of Armco iron 12" x 1" x 0.25" as shown in Fig.15A. The holes were 0.5 in. apart. The strip was placed on top of a rectangular bar of Armco iron and inserted into a horizontal Kanthal wound tube furnace of standard design. The temperature gradient was measured using a chromel alumel thermocouple which could be moved along the groove running along the upper surface of the rectangular bar, Fig.15B. The variation of the temperature along the length of the strip was plotted as shown in Fig.15A. The temperature of each hole thus could be obtained within $\pm 5^{\circ}C$. Two slags were used in each experiment, one in each of the two rows of holes. The temperature was first raised above the expected liquidus temperature, an inert atmosphere being maintained throughout. After cooling, in the furnace, the strip was removed and examined to verify that all were in the glassy condition. The strip was then replaced and reheated to a temperature range which it was anticipated

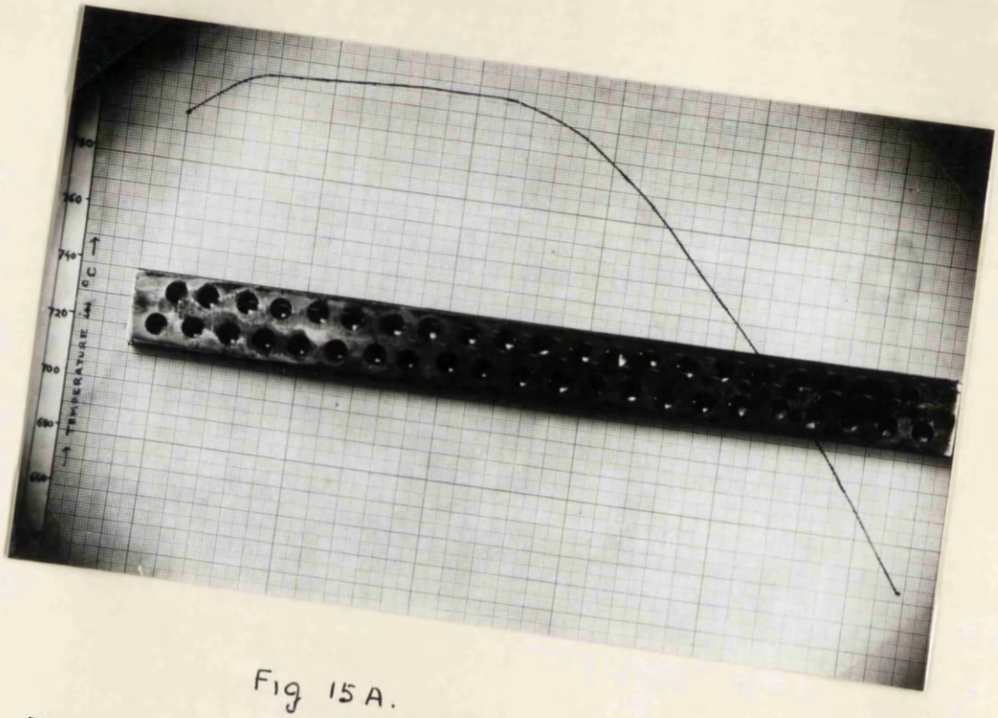

Fig 15 A.

Temperature gradient plotted along the Armco Iron strip containing slags.

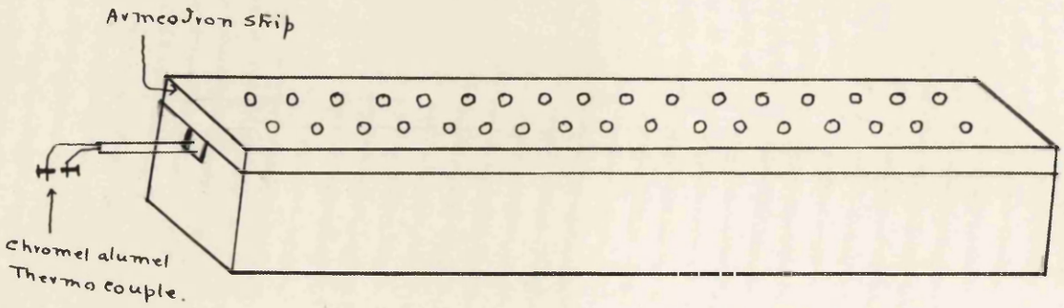

15 B

would include the temperature of the phase change, for approximately one week. After cooling, the bottom layer of the metal strip was buffed off until the slag was exposed. The slags were then examined using transmitted light to detect any sign of crystallisation and the crystals were identified by refractive index measurements. To eliminate the laborious task of buffing the strip, a modified arrangement was used. Instead of placing the slags directly in the holes, the slag was placed in small Armco iron crucibles 0·5 in. diameter, which were inserted in larger holes drilled in the metal strip. As the holes were larger it was only possible to examine one slag at a time. The procedure was essentially the same as before. After quenching, the crucibles were sectioned and examined, and if any crystal were present they were identified by refractive index measurements. A similar procedure was used to determine the temperature of binary and ternary crystallisation. When it was found after sectioning that the contents of a crucible showed a new crystal form, greater accuracy was obtained by quenching over a narrower temperature range using the iron cage method already described.

The slags examined are shown in Fig.16. Compositions, lying on the joins $MnO-Na_2O.SiO_2$, $2MnO.SiO_2-Na_2O.SiO_2$, $2MnO.SiO_2-2Na_2O.SiO_2$, $2MnO.SiO_2-Na_2O.2SiO_2$ and $MnO.SiO_2-Na_2O.SiO_2$, will normally be expressed in terms of the two compounds of which they are composed in weight percentages, and the proportion of MnO, $2MnO.SiO_2$ and $MnO.SiO_2$ will precede that of $2Na_2O.SiO_2$, $Na_2O.SiO_2$ and $Na_2O.2SiO_2$. Compositions of slags not lying in any of the joins will be expressed in the ratio $MnO/Na_2O/SiO_2$. As the slags were made in Armco iron crucibles there was an unavoidable contamination with iron, so most slags were analysed and their analyses are given with iron expressed as FeO.

Most of the slags were subjected to X-ray examination and in certain cases it was necessary to take more than one X-ray diffraction photograph of the same slag in order to identify the phases present at different stages of crystallisation. The X-ray data are given in full in Appendix I. A summary of the optical properties of the compounds is given in Appendix II. The results obtained during the identification of the phases present by X-ray diffraction and refractive index measurement will be presented when discussing various joins.

It will be noted that three new ternary compounds, viz., $Na_2O.MnO.SiO_2$, $Na_2O.MnO.2SiO_2$ and $2Na_2O.3MnO.3SiO_2$ were identified. Evidence in support of these compounds will be given in their respective places.

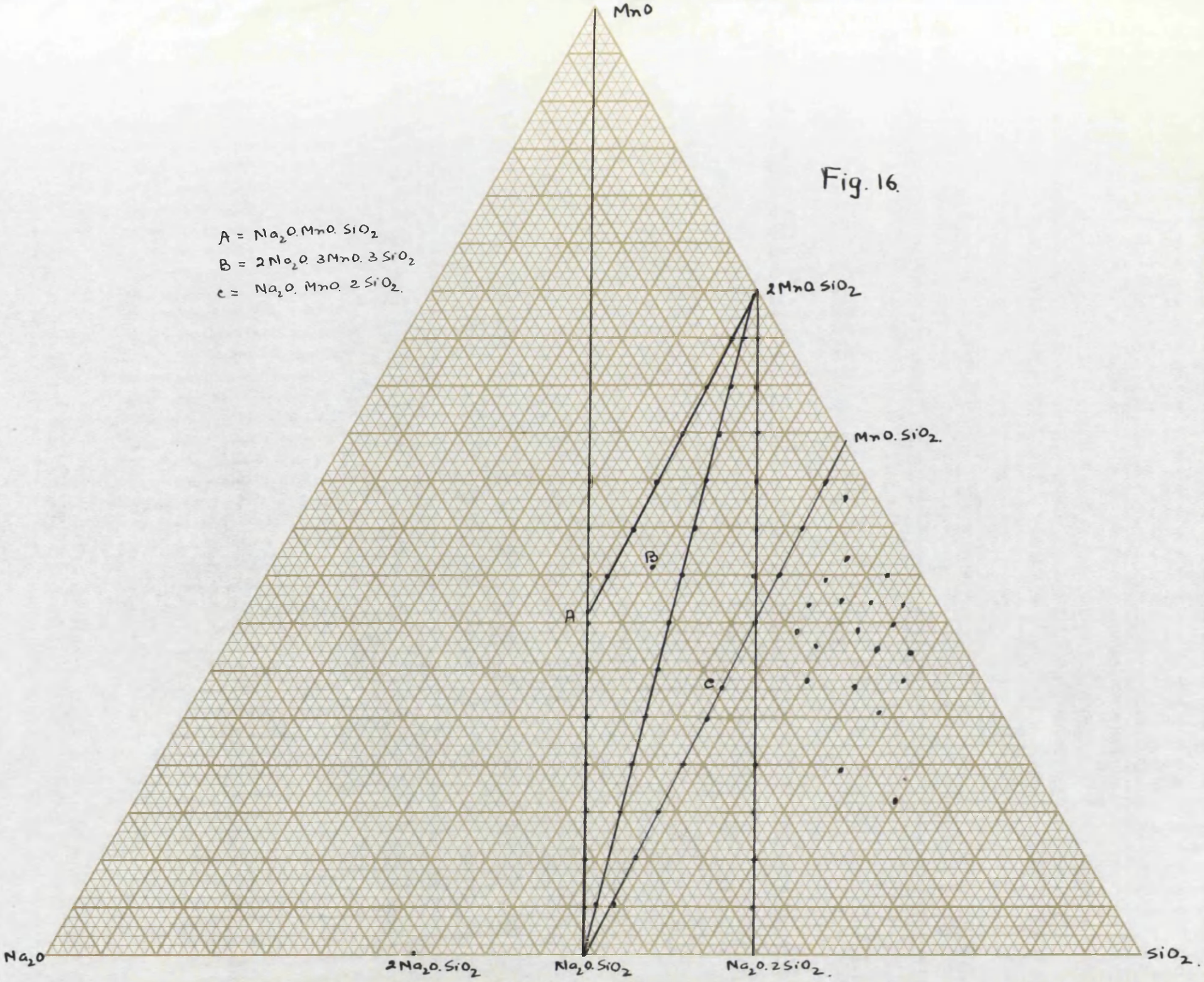
MnO
A = $Na_2O.MnO.SiO_2$
B = $2Na_2O.3MnO.3SiO_2$
C = $Na_2O.MnO.2SiO_2$.
$2MnO.SiO_2$
$MnO.SiO_2$.
B
A
C
Na_2O
$2Na_2O.SiO_2$
$Na_2O.SiO_2$
$Na_2O.2SiO_2$.
SiO_2.

Fig. 16.

PART I.

JOIN $MnO-Na_2O.SiO_2$.

Join $MnO-Na_2O.SiO_2$.

Investigation was limited to slags containing less than 50 per cent of MnO since slags with a higher content had melting points higher than 1500°C and could not be melted with safety in an iron crucible. The composition and analyses of the slags examined are given in Table I. These slags were completely crystalline after cooling in the furnace. It was indeed impossible to quench them to glasses and the quenching method of thermal analysis could not be used. The temperatures of phase changes were determined by visual observation and differential thermal analysis. The phases were identified by X-ray diffraction and petrological examination. A new ternary compound $Na_2O.MnO.SiO_2$ was found to occur at 36.7 per cent MnO and 63.3 per cent $Na_2O.SiO_2$, its average refractive index being 1.653 with very low birefringence (0.006). In thin sections the crystals of the compound looked almost isotropic. The interference colour was never more than first order yellow.

Phase and thermal data for this join are given in Table 2. These data have been used to construct the vertical section shown in Fig.17, from which it may be concluded that $MnO-Na_2O.SiO_2$ is a true binary join.

The 50/50, 45/55 and 40/60 melts showed primary MnO crystals on a background of $Na_2O.MnO.SiO_2$, as shown in Fig.18. The MnO crystals were usually globular although a few star-shaped dendrites were also observed (Fig.19). The 35/65 melt also showed the presence of traces of MnO, although this is contrary to the $MnO-Na_2O.SiO_2$ binary section

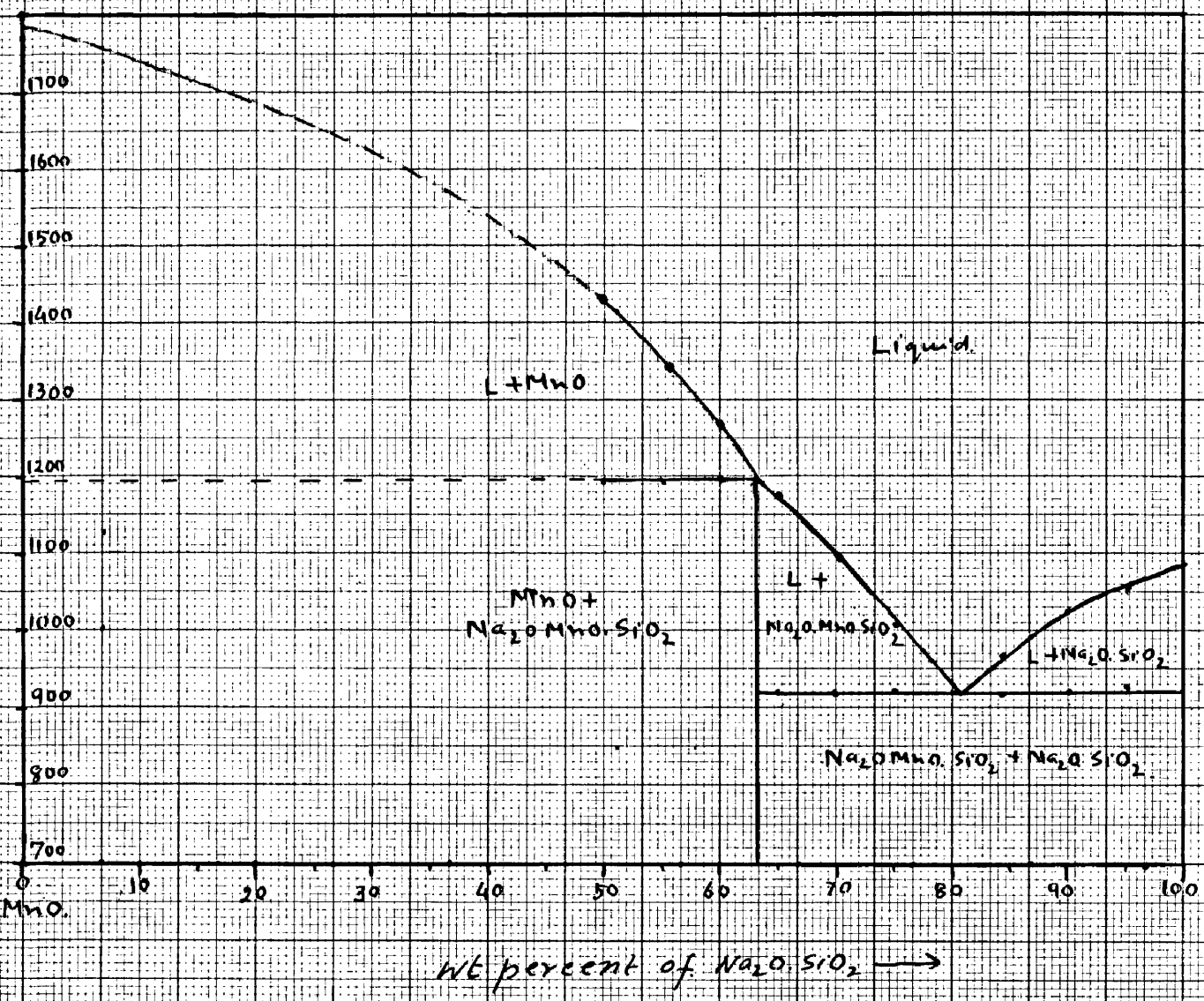
1700
1600
1500
1400
1300
1200
1100
1000
900
800
700
0
MnO.
10
20
30
40
50
60
70
80
90
100
Liquid.
L+MnO
MnO+
$Na_2O.MnO.SiO_2$
L+
$Na_2O.MnO.SiO_2$
$L+Na_2O.SiO_2$
$Na_2O.MnO.SiO_2+Na_2O.SiO_2$
wt percent of $Na_2O.SiO_2$ →

Fig 17

Fig. 18. $MnO : Na_2O.SiO_2$ = 45 : 55
cooled in the Furnace X 150

Fig. 19. $MnO : Na_2O.SiO_2$ = 45 : 55
cooled in the Furnace x 300.

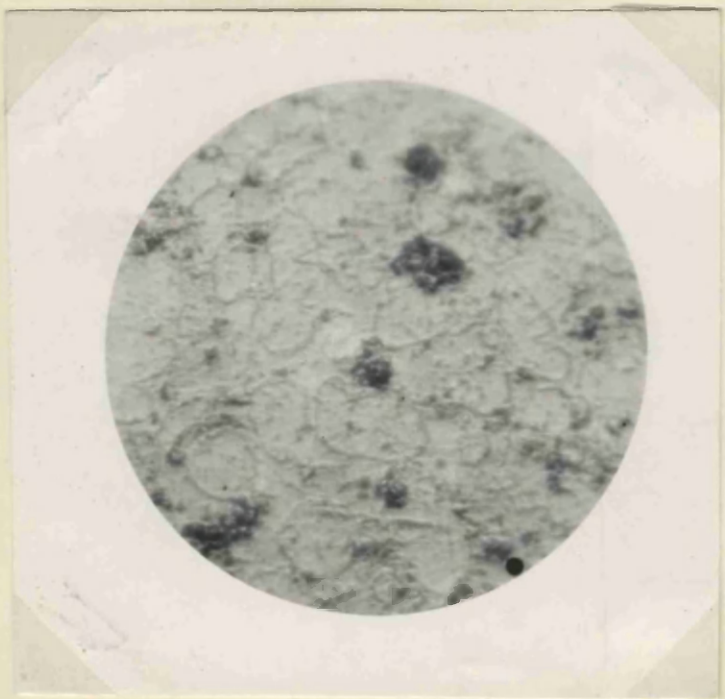

Fig. 20. $MnO : Na_2O.SiO_2$ = 36·7 : 63·3.
Cooled in the furnace.
compound. $Na_2O.MnO.SiO_2$ X 150.

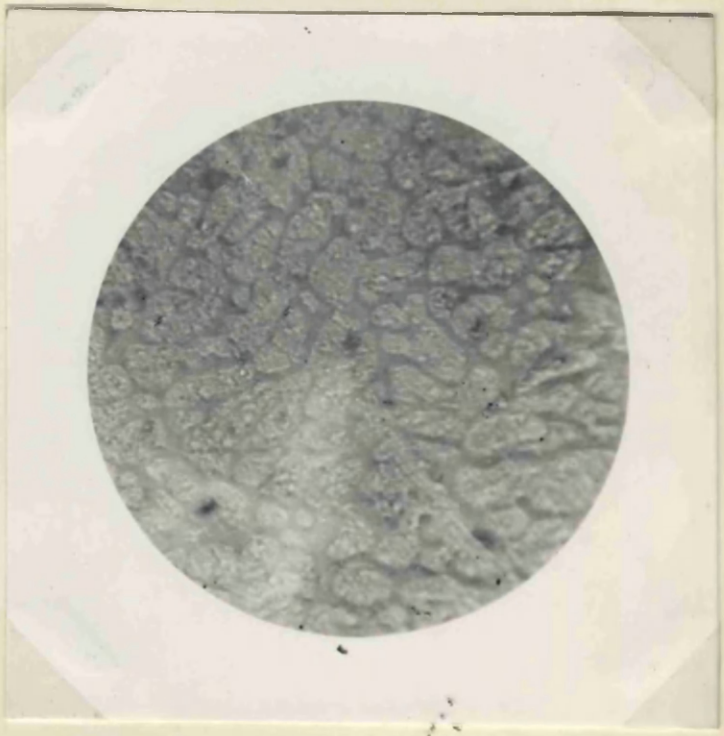

Fig. 21. $MnO : Na_2O.SiO_2$ = 30 : 70
cooled in the Furnace x 150.

TABLE I.

Composition of Slags Examined in Join "$MnO-Na_2O.SiO_2$"

$MnO/Na_2O.SiO_2$	Composition before melting(wt.percent)			Composition after melting(wt.percent)			
	MnO	Na_2O	SiO_2	MnO	Na_2O	SiO_2	FeO
50/50	50	25.2	24.8	49.8	24.5	25.1	0.25
45/55	45	28	27	44.7	27.2	27.1	0.3
40/60	40	30.5	29.5	39.6	29.7	29.8	0.36
35/65	35	33	32	34.6	32.0	32.2	0.44
30/70	30	35.5	34.5	29.9	34.8	34.7	0.49
25/75	25	38	37	24.7	37.4	37.3	0.45
20/80	20	40.5	39.5	19.8	39.9	39.7	0.39
15/85	15	43	42	14.7	42	42.2	0.51
10/90	10	46	44	9.6	45.3	44.2	0.54
5/95	5	48	47	Not analysed.			

TABLE II.

Phases at Room Temperature and Thermal Data on $MnO-Na_2O.SiO_2$ Join.

Composition $MnO/Na_2O.SiO_2$	Phases Identified by X-ray and R.I.	Visual Method: Beginning of melting	Visual Method: End of Melting.	Differential Method: 1st Arrest.	Differential Method: 2nd Arrest.
60/40		Did not melt at 1500°C			
55/45					
50/50	MnO $Na_2O.MnO.SiO_2$	1192°	1430	1193	1435
45/55	MnO $Na_2O.MnO.SiO_2$	1195°	1339	1192	1346
40/60	MnO $Na_2O.MnO.SiO_2$	1193°	1265	1195	1272
36.7/63.3	$Na_2O.MnO.SiO_2$	1195°	1195°	-	-
35/65	$Na_2O.MnO.SiO_2$ $Na_2O.SiO_2$	920°	1175°	921	1179
30/70	$Na_2O.MnO.SiO_2$ $Na_2O.SiO_2$	924	1100	918	1095
25/75	$Na_2O.MnO.SiO_2$ $Na_2O.SiO_2$	920	1005	-	-
20/80	$Na_2O.MnO.SiO_2$ $Na_2O.SiO_2$	920	930	917	935
15/85	$Na_2O.MnO.SiO_2$ $Na_2O.SiO_2$	918	965	919	960
10/90	$Na_2O.MnO.SiO_2$ $Na_2O.SiO_2$	920	1022	922	1025
5/95	$Na_2O.MnO.SiO_2$ $Na_2O.SiO_2$	924	1052	-	-

derived from thermal data shown in Fig.17. It is probable that this is due to a supercooling effect in which separation of MnO occurs along the metastable extension of the MnO liquidus curve. Fig.17 shows that the slope of the MnO liquidus curve does not differ appreciably from that of $Na_2O.MnO.SiO_2$. The super-cooling effect is very slight and would not be expected to affect the result of either the visual or the differential method of determination of the temperature of phase changes, especially as the slow heating rate (1.5 to 2°C per minute) should facilitate the attainment of equilibrium before the start of melting.

The microstructure of a composition corresponding to $Na_2O.MnO.SiO_2$ (36.3 MnO/63.7 $Na_2O.SiO_2$) after slow cooling in the furnace showed only one phase, as can be seen in Fig.20. The compound melted completely at 1195°C.

Slag compositions intermediate between those of $Na_2O.MnO.SiO_2$ and the $Na_2O.MnO.SiO_2$-$Na_2O.SiO_2$ eutectic (18/82) showed primary crystals of $Na_2O.MnO.SiO_2$ surrounded by eutectic (Fig.21). It was not possible to obtain a true representation of the microstructures of the slags 20/80 or 15/85 as even five or ten minutes exposure to the atmosphere completely etched the specimen. The etching effect is represented by the two figures 22 and23 . Fig.22 was taken as soon as possible (within 2 to 3 minutes). Fig.23 represents the microstructure of the same slag (20/80) after allowing it to stand for five to six minutes in the atmosphere.

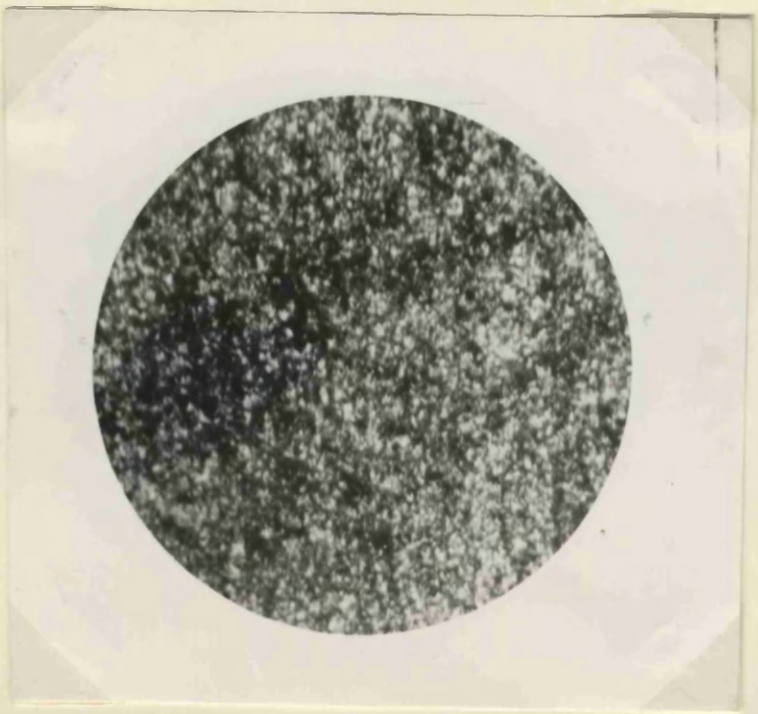

Fig. 22.

Fig 22. $MnO : Na_2O . SiO_2 = 20 : 80$ cooled in the furnace.
Photomicrograph of Polished Section exposed to atmosphere for 2 minutes.
Eutectic ($MnO . Na_2O . SiO_2$ - $Na_2O . SiO_2$) composition.
X 150.

Fig 23. $MnO : Na_2O . SiO_2 = 20 : 80$.
Structure of the polished section (fig 22) after being exposed to atmosphere for 6 minutes.
X 150

Fig. 23.

PART 2.

JOIN 2 $MnO.SiO_2$-$Na_2O.2SiO_2$.

Join $2MnO.SiO_2$-$Na_2O.2SiO_2$.

The compositions examined and their analyses are given in Table 3. All the slags were at first cooled in the furnace. Those containing 50 per cent or more of $Na_2O.2SiO_2$ were completely glassy. These slags were extremely difficult to crystallise. Another new compound $Na_2O.MnO.2SiO_2$ was encountered in this join, having an incongruent melting point and lying within the primary field of separation of $2MnO.SiO_2$.

Slags Cooled in Furnace.

The compositions of the slags are expressed in the ratio $2MnO.SiO_2/Na_2O.2SiO_2$. The slags 92.9/7.1, 85.8/14.2 and 78.5/21.5 when cooled in the furnace, showed lathlike crystals (Fig.24) which were identified by refractive index measurement as $2MnO.SiO_2$ in a glassy matrix. In certain parts of the glassy matrix of these slags not only primary $2MnO.SiO_2$ was seen but also a needle-like structure was visible as shown in Fig.25. This was, at first thought to be an etching effect but it was found that neither the characteristics of the microstructure changed on repolishing nor was it present in all parts of tl glassy matrix. Closer examination (by refractive index measurement) revealed the presence of $MnO.SiO_2$ and of a third unknown phase later identified as $Na_2O.MnO.2SiO_2$, in glassy matrix.

Fig. 24. $2MnO.SiO_2 : Na_2O.2SiO_2 = 92.9 : 7.1$
Lath-like crystals of $2MnO.SiO_2$.
X 100.

Fig 25. $2MnOSiO_2 : Na_2O.2SiO_2 = 85.8 : 14.2$.
cooled in the furnace. X 300.

Fig. 26. $2MnO.SiO_2 : Na_2O.2SiO_2 = 71.5 : 28.5$
cooled in the furnace.

TABLE III.

Analysis. **Join $2MnO.SiO_2$-$Na_2O.2SiO_2$.**

Ratio $2MnO.SiO_2$ / $Na_2O.2SiO_2$	Before Melting.			After Melting.			
	MnO	Na_2O	SiO_2	MnO	Na_2O	SiO_2	FeO
92.9/7.1	65	3	32	65.2	2.8	31.9	0.15
85.7/14.3	60	5	35	60.1	4.7	35.2	0.2
78.5/21.5	55	7.5	37.5	54.9	7.3	37.6	0.16
71.5/28.5	50	10	40	49.8	9.4	40.1	0.13
64.3/35.7	45	12.5	42.5	44.8	12.3	42.9	0.17
57.2/42.8	40	15	45	39.7	14.7	45.2	0.19
50/50	35	17	47.	35.8	16.8	47.3	0.12
42.9/57.1	30	20	50	29.9	19.7	50.1	0.14
35.7/64.3	25	22	53	24.7	21.7	53.2	0.11
28.6/71.4	20	25	55	19.8	24.8	55.1	0.2
21.5/78.5	15	27	58	14.6	26.6	58.2	0.3
14.3/85.7	10	30	60	9.8	29.5	60.3	0.31
7.1/92.9	5	32	63	4.7	31.5	63.3	0.35

The slag 71.5 : 28.5 cooled in the furnace from 1300°C and 1250°C showed a localised region rich in $MnO.SiO_2$ surrounded by an area containing $MnO.SiO_2$, $2MnO.SiO_2$ and glass. In Fig.26, which shows the sectioned crucible containing the 71.5/28.5 composition, the area containing $MnO.SiO_2$ is encircled. Fig.27 shows the structure of the $MnO.SiO_2$ rich area and its neighbourhood. The surrounding area was distinctly green in contrast to the pink $MnO.SiO_2$-rich area. The amount of typical lathlike crystals of $2MnO.SiO_2$ increased towards the top of the crucible (Fig.28). No $Na_2O.MnO.2SiO_2$ crystals could be identified in the slags by refractive index measurements. The peculiarities of the structure of the slag 71.5/28.5 persisted when it was crushed, remelted and cooled in the furnace from 1300°C and 1250°C. But when quenched from 1300°C, this slag was uniformly glassy.

Two slags 64.3/33.7 and 57.2/42.8 showed the usual lathlike $2MnO.SiO_2$ crystals and glass. The rest of the slags with higher $Na_2O.2SiO_2$ were completely glassy.

Differential Thermal Analyses.

It is obvious that differential thermal analyses could not be used with these slags in the join $2MnO.SiO_2$-$Na_2O.2SiO_2$ with accuracy because of the presence of large amounts of glass. The ideal method for these slags is the static (quenching and annealing) method. But it was thought that the slags with high $2MnO.SiO_2$ content might crystallise easily if slowly cooled in the furnace and annealed at low temperature, although the optimum crystallising temperatures of the slags were

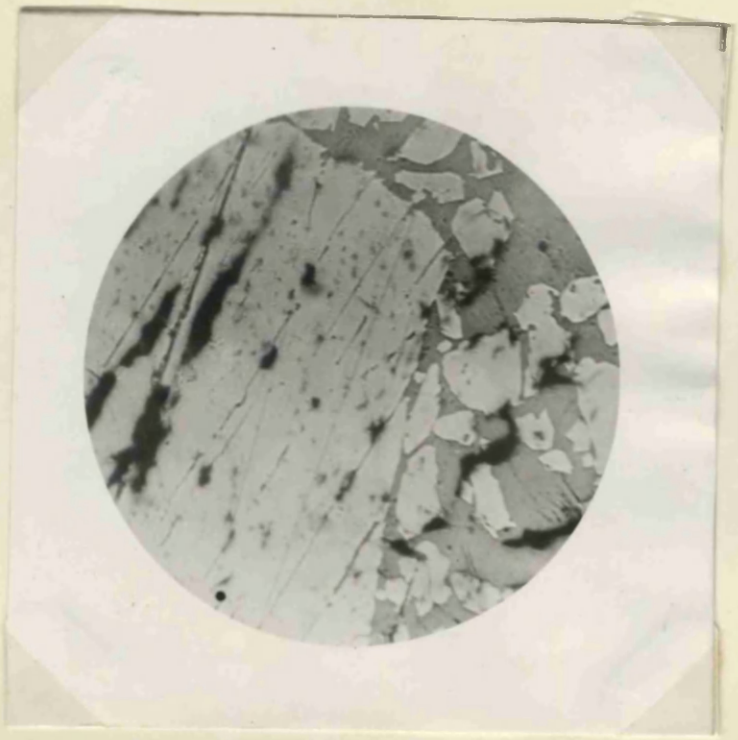

Structure of encircled ($MnO.SiO_2$ rich) area in Fig 26 and its neighbourhood. X100.

Fig 27

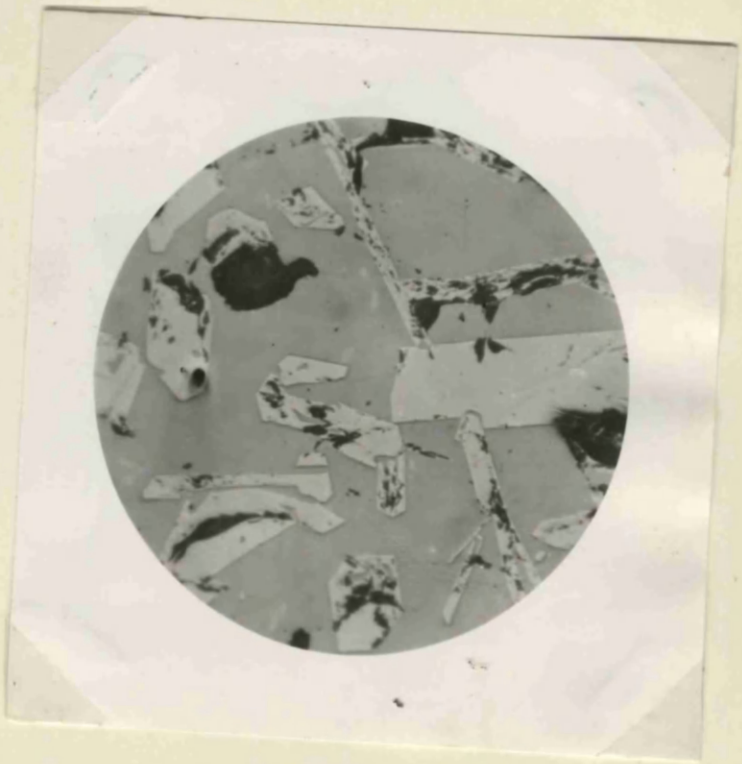

Structure of upper area of the slag in fig 26. Lathlike crystals of $2MnO.SiO_2$. X100.

Fig 28

not known. Then this slag could be used to determine the thermal differential curves on heating. The object of this determination was twofold. Firstly, to determine the probable temperature of the phase changes and secondly, to obtain an indication of whether or not the join $2MnO.SiO_2$ - $Na_2O.2SiO_2$, like the $2FeO.SiO_2$ - $Na_2O.2SiO_2$ join in the Na_2O-FeO-SiO_2 ternary system, is a true binary join. So only three slags 92.7/7.1, 85.8/14.2 and 78.5/21.5 were slowly cooled and annealed at an arbitrary low temperature.

These slags were melted and allowed to cool in the furnace to 1000°C. They were held there for one hour, allowed to cool slowly in the furnace to 500°C and annealed at that temperature for 60 hours These slags were completely crystalline. One of the thermal differential curves obtained using such a slag is shown in Fig.29. It shows three endothermic arrests at 730°C, 750°C and 1265°C., the first two being more pronounced. These represent the probable temperatures of phase changes. X-rays showed the presence of $2MnO.SiO_2$, $MnO.SiO_2$ and $Na_2O.MnO.2SiO_2$. The three change points shown by the differential curve and the presence of three phases at room temperature indicated that the join $2MnO.SiO_2$-$Na_2O.2SiO_2$ is probably not a simple binary join as $2FeO.SiO_2$-$Na_2O.2SiO_2$ is in the Na_2O-FeO-SiO_2 system.

Quenching and Annealing Methods.

All the slags in the join $Na_2O.2SiO_2$-$2MnO.SiO_2$ were annealed and quenched from different temperatures. The results of these

experiments are given in Table IV. Although many more experiments were carried out only relevant data fixing the change points are given in Table. IV.

TABLE IV.

Abbreviations: $2MnO.SiO_2$ = M_2S $Na_2O.MnO.2SiO_2$ = NMS_2
$MnO.SiO_2$ = MS $Na_2O.2SiO_2$ = NS_2
SiO_2 = S glass = L

Slag Composition	Quenched after annealing at - °C.	Time of Annealing	Phases.	Method of Identification.
	1330°	2 hours	L	
$M_2S:NS_2$	1320°	2 hours	$L+M_2S$	R.I.
= 92.9:7.1	765°	2 hours	$L+M_2S$	R.I.
	755°	10 hours	$L+M_2S+NMS_2$	R.I.
$MnO:Na_2O:SiO_2$	730°	10 hours	$L+M_2S+NMS_2$	R.I.
= 63:3:32	720°	60 hours	M_2S+NMS_2+MS	R.I. and X-ray
$M_2S:NS_2$	1280°C	2 hours	L	
=85.8:14.2	1270°C	2 hours	$L+M_2S$	R.I.
	765°C	2 hours	$L+M_2S$	R.I.
$MnO:Na_2O:SiO_2$	755°C	10 hours	$L+M_2S+NMS_2$	R.I.
= 60:5:35	730°C	10 hours	$L+M_2S+NMS_2$	R.I.
	720°C	60 hours	M_2S+NMS_2+MS	R.I. and X-ray.
$M_2S:NS_2$	1230°	2 hours	L	
= 78.5:21.5	1220°C	2 hours	$L+M_2S$	R.I.
	765°	2 hours	$L+M_2S$	R.I.
$MnO:Na_2O:SiO_2$	755°	12 hours	$L+M_2S+NMS_2$	R.I.
=55:7.5:37.5	730°	12 hours	$L+M_2S+NMS_2$	R.I.
	720°	72 hours	M_2S+NMS_2+MS	R.I. and X-ray.
$M_2S:NS_2$	1160°	2 hours	2L	
= 71.5:28.5	1140°C	1 hour	$L+M_2S+MS$	R.I.
	1110°C	1 hour	$L+M_2S+MS$	R.I.
$MnO:Na_2O:SiO_2$	1100°C	2 hours	$L+M_2S$	R.I.
= 50:10:40	765°C	2 hours	$L+M_2S$	R.I.
	755°C	12 hours	$L+M_2S+NMS_2$	R.I.
	730°C	12 hours	$L+M_2S+NMS_2$	R.I.
	720°C	72 hours	M_2S+NMS_2+MS	R.I. and X-ray.

TABLE IV (cont'd).

Slag Composition.	Quenched after annealing at - °C.	Time of Annealing	Phases.	Method of Identification.
$M_2S:NS_2$	1105°C	2 hours	L	
=64.3:35.7	1095°C	1 hour	$L+M_2S$	R.I.
	765°C	2 hours	$L+M_2S$	R.I.
$MnO:Na_2O:SiO_2$	755°C	12 hours	$L+M_2S+NMS_2$	R.I.
=45:12.5:42.5	730°C	14 hours	$L+M_2S+NMS_2$	R.I.
	720°C	72 hours	M_2S+NMS_2+MS	R.I. and X-ray.
$M_2S:NS_2$	1035°C	2 hours	L	
= 57.2/42.8	1025°C	1 hour	$L+M_2S$	R.I.
	765°C	1 hour	$L+M_2S$	R.I.
$MnO:Na_2O:SiO_2$	755°C	14 hours	$L+M_2S+NMS_2$	R.I.
= 40:15:45	730°C	14 hours	$L+M_2S+NMS_2$	R.I.
	720°C	84 hours	M_2S+NMS_2+MS	R.I. and X-ray.
$M_2S:NS_2$	960°C	2 hours.	L	
= 50:50	950°C	2 hours	$L+M_2S$	R.I.
	765°C	2 hours	$L+M_2S$	R.I.
$MnO:Na_2O:SiO_2$	755°C	72 hours	$L+M_2S+NMS_2$	R.I.
= 35:18:47	730°C	72 hours	$L+M_2S+NMS_2$	R.I.
	720°C	15 days	$MS+NMS_2$	R.I. and X-ray.
$M_2S:NS_2$	860°C		L	
= 42.9:57.1	850°C	2 hours	$L+M_2S$	R.I.
	765°C	3 hours	$L+M_2S$	R.I.
$MnO.Na_2O.SiO_2$	755°C	72 hours	$L+M_2S+NMS_2$	R.I.
= 30:20:50	740°C	72 hours	$L+M_2S+NMS_2$	R.I.
	730°C	72 hours	$L+NMS_2$	R.I.
	690°C	72 hours	$L+NMS_2$	R.I.
	680°C	15 days	$NMS_2+MS+SiO_2$	R.I. and X-ray.

TABLE IV (cont'd).

Slag Composition	Quenched after annealing at - °C.	Time of Annealing	Phases.	Method of Identification.
$M_2S:NS_2$	765°C		L	
= 35.7:64.3	750°C	4 hours	$L+NMS_2$	R.I.
	730°C	24 hours	$L+NMS_2$	R.I.
$MnO:Na_2O:SiO_2$	720°C	72 hours	$L+NMS_2+SiO_2$	R.I.
= 25:22:53	710°C	15 days	NMS_2+SiO_2	R.I. and X-ray.
$M_2S:NS_2$	755°C		L	
= 28.6:71.4	745°C	2 hours	$L+NMS_2$	R.I.
	730°	2 hours	$L+NMS_2$	R.I.
$MnO:Na_2O:SiO_2$	720°	10 hours	$L+NMS_2+NS_2$	R.I.
= 20:25:55	700°	7 days	$NMS_2+NS_2+SiO_2$	R.I. and X-ray.
$M_2S:NS_2$	775°C		L	
=21.5:78.5	765°	1 hour	$L+NS_2$	R.I.
	745°	2 hours	$L+NS_2$	R.I.
$MnO:Na_2O:SiO_2$	735°	10 hours	$L+NS_2+NMS_2$	R.I.
= 15:27:58	700°	7 days	$NS_2+NMS_2+SiO_2$	R.I. and X-ray.
$M_2S:NS_2$	815°C		L	
= 14.3:85.7	805°	1 hour	$L+NS_2$	R.I.
	745°	2 hours	$L+NS_2$	R.I.
	735°	6 hours	$L+NS_2+NMS_2$	R.I.
	710°	6 hours	$L+NS_2+NMS_2$	R.I.
	700°	4 days	$NS_2+NMS_2+SiO_2$	R.I. and X-ray.
$M_2S:NS_2$	850		L	
= 7.1:92.9	840	2 hours	$L+NS_2$	R.I.
	700	4 days	$NS_2+NMS_2+SiO_2$	R.I. and X-ray.

TABLE V.

Summary of Thermal data of Slags in Join $2MnO.SiO_2$-$Na_2O.2SiO_2$.

Slag Composition	Primary phase separation.		Secondary phase separation.		End of Freezing Phases at Room temp.	
92:9:7·1	1325		760		725	
85:8:14·2	1275	M_2S	760		725	
78.5:21.5	1225		760		725	M_2S+MS
71.5:28.5	1155	MS (2-Liquid formation)	760	M_2S + NMS_2	725	+ NMS_2
64.3:35.7	1100		760		725	
57.2:42.8	1030	M_2S	760		725	
50:50	955		760		725	MS+NMS_2
42.9:57.1	855		760		685	NMS_2+MS+SiO_2
35.7:64.3	760	NMS_2	725	NMS_2+SiO_2	715	NMS_2+SiO_2
28.6:71.4	750		725		710	
21.5:78.5	760		740	NMS_2+NS_2	715	NMS_2+NS_2
14.3:85.7	810	NS_2	740		705	+ SiO_2
7.1:92.9	845		-		-	

The Compound $Na_2O.MnO.2SiO_2$ and Microstructure of Slags.

The identification of the new compound $Na_2O.MnO.2SiO_2$ was facilitated by three facts arising from the experimental results given in Tables IV and V.

(1) The $2MnO.SiO_2$-$Na_2O.2SiO_2$ is not a true binary join.

(2) This join intersects three three-phase triangles in the solid state.

(i) $2MnO.SiO_2$-$MnO.SiO_2$-$Na_2O.MnO.2SiO_2$.

(ii) $Na_2O.MnO.2SiO_2$-$MnO.SiO_2$-SiO_2.

(iii) $Na_2O.MnO.2SiO_2$-SiO_2-$Na_2O.2SiO_2$.

(3) It also intersects two binary joins $MnO.SiO_2$-$Na_2O.MnO.2SiO_2$ and $Na_2O.MnO.2SiO_2$-SiO_2 at the compositions 50/50 and 35.7/64.3 (Fig. 30 A and B respectively).

The unknown compound must lie at the intersection of two lines originating from $MnO.SiO_2$ and SiO_2 (Fig.30). The compound $Na_2O.MnO.SiO_2$ was already identified and it appeared probable that the unknown compound ($Na_2O.MnO.2SiO_2$) would lie at the intersection of the lines joining $MnO.SiO_2$ to $Na_2O.SiO_2$ and $Na_2O.MnO.SiO_2$ to SiO_2 (Fig.30, point C). The required mixture MnO, $Na_2O.2SiO_2$ and SiO_2 corresponding to the composition $Na_2O.MnO.2SiO_2$ was melted and cooled in the furnace. The microstructure (Fig.31) showed white crystals of $2MnO.SiO_2$ which appear to have taken part in a peritectic reaction. The slag was crushed, remelted, slowly cooled to 600°C and maintained at that temperature for one hour. The microstructure (Fig.32) showed only $Na_2O.MnO.2SiO_2$ and glass as determined

Fig. 30

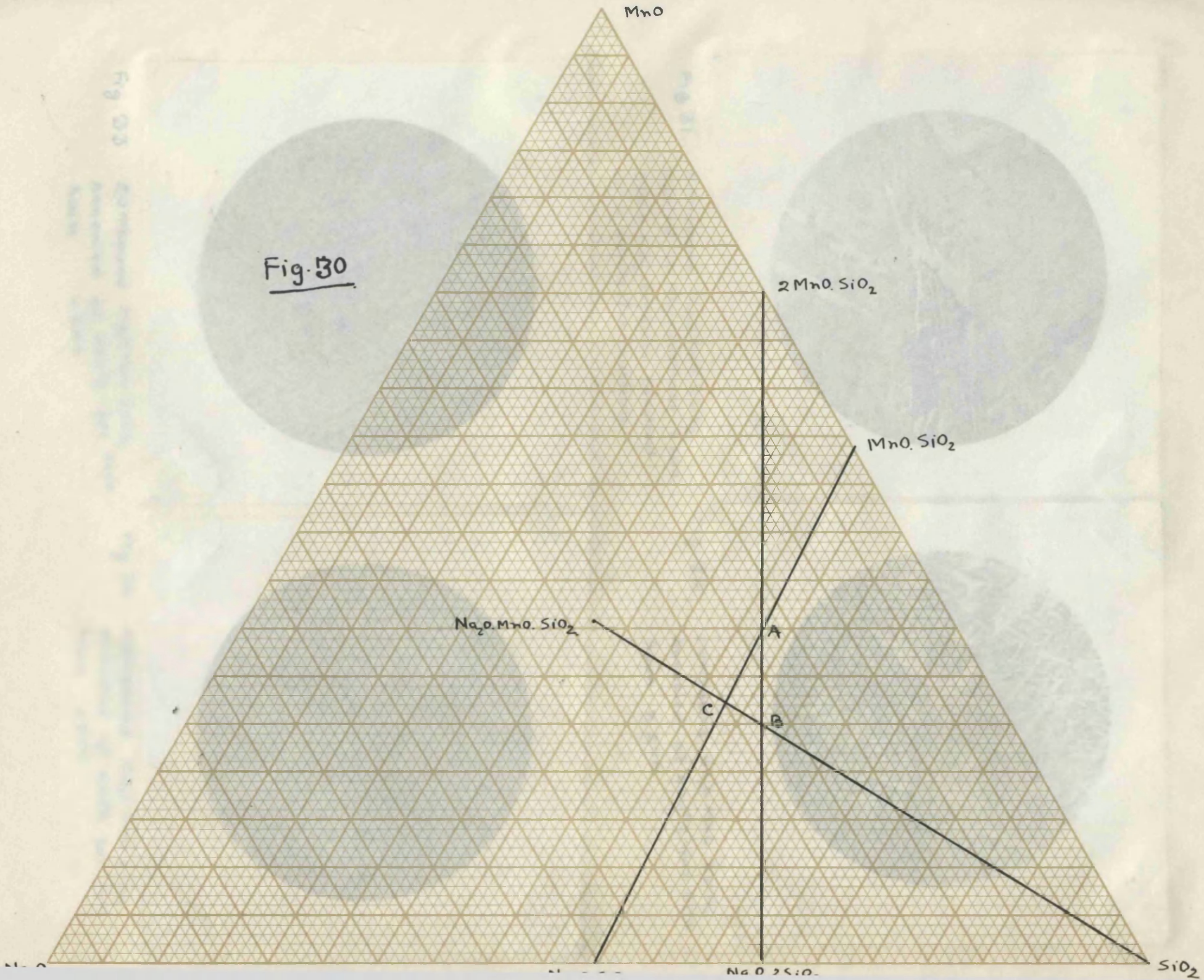

Fig 31. compound $Na_2O\,MnO.\,2SiO_2$. cooled in the furnace x 200. $2MnO.\,SiO_2$ crystals involved in a peritectic reaction.

Fig. 32. compound $Na_2O\,MnO.\,2SiO_2$ Annealed at 600°c for one hour x 200.

Fig. 33 compound $Na_2O\,MnO\,2SiO_2$ Annealed at 600°c for two hours. x 200.

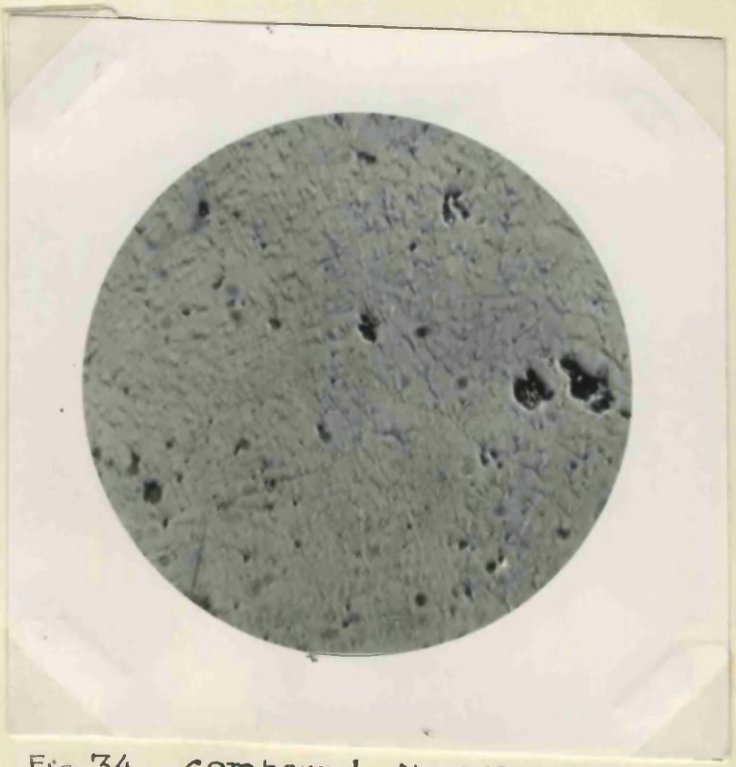

Fig 34. compound $Na_2O\,MnO\,2SiO_2$ Annealed at 600°c for five hours x 200

by X-ray and refractive index measurement. It was further annealed at 600°C for one hour, the corresponding microstructure being shown in Fig.33. On further annealing for three hours at 600°C the microstructure revealed a single phase (Fig.34). Petrological and X-ray examination confirmed that a single phase was present. The compound melted incongruently at 820°C. From the characteristic structure developed during annealing it appeared probable that growth twins were formed during the process of crystallisation. However, no conclusive proof was obtained.

In the microstructures of the slags in this join ($2MnO.SiO_2$-$Na_2O.2SiO_2$) crystals of $2MnO.SiO_2$ could be easily distinguished under the microscope. They were always lathlike, even in quenched slags, although the crystallites were smaller (Fig.35). Crystals of $Na_2O.MnO.2SiO_2$ and $MnO.SiO_2$ could not be distinguished from each other. Fig.36 and 37 show the microstructures after binary and ternary crystallisation.

It was found that the ternary peritectic reaction

$$\text{Liquid} + 2MnO.SiO_2 = MnO.SiO_2 + Na_2O.MnO.2SiO_2$$

was extremely sluggish. This was clearly shown during the stages of annealing of the slag 50/50. The structure at 755°C is shown in Fig.38. The needle shaped $2MnO.SiO_2$ crystals are clearly seen, also some rectangular $2MnO.SiO_2$ crystals which appear to have partially undergone peritectic reaction. Because of this suggestiveness of the peritectic reaction, two slags of the composition 50/50 were annealed at lower temperatures. One of which showed the structure shown in Fig.38 and the other completely glassy. After annealing for 84 hours at

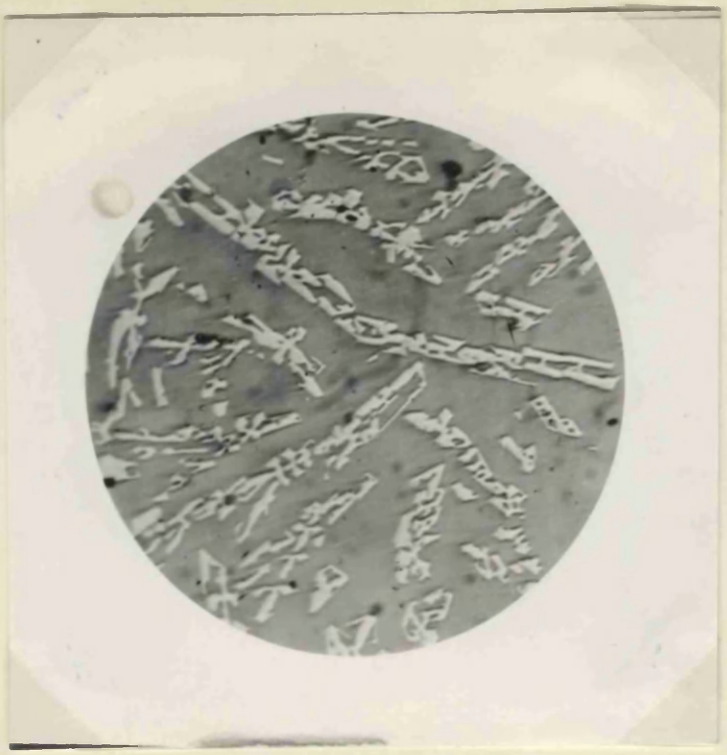

Fig. 35. $2MnO.SiO_2 : Na_2O.2SiO_2 = 92{\cdot}9 : 7{\cdot}1$
Quenched from 1320°c × 100.

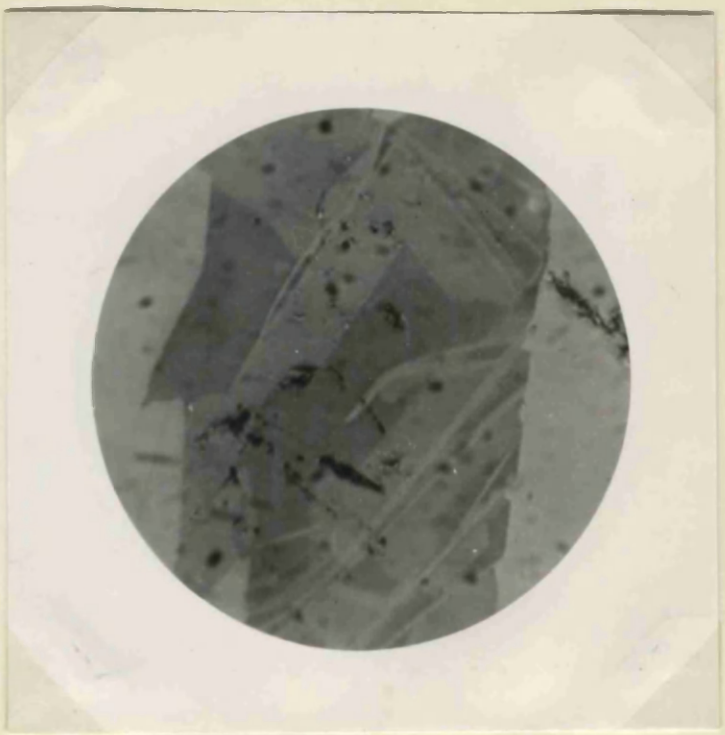

Fig. 36. $2MnO.SiO_2 : Na_2O.2SiO_2 = 92{\cdot}9 : 7{\cdot}1$
Quenched from 755°c × 350

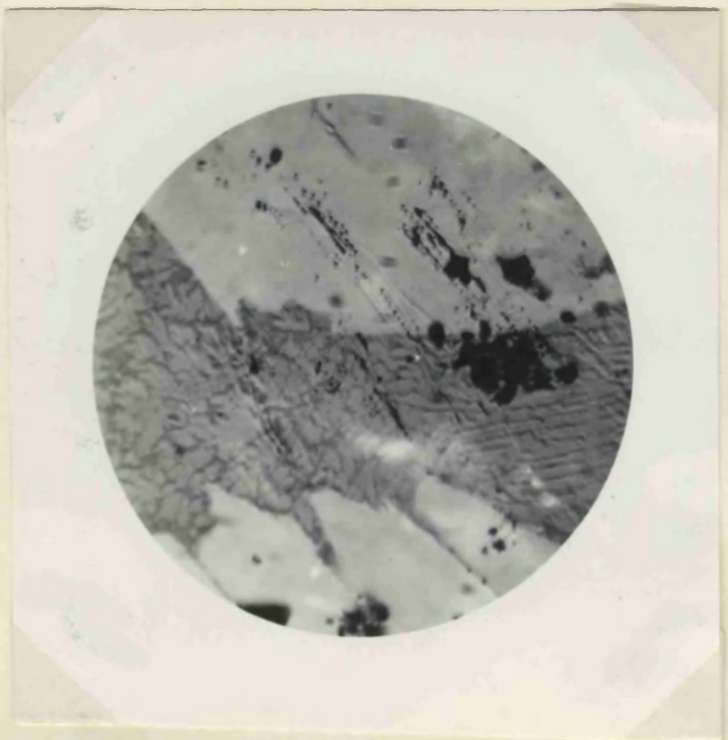

Fig. 37. $2MnO.SiO_2 : Na_2O.2SiO_2 = 92{\cdot}9 : 7{\cdot}1$
Quenched from 720°c × 300.

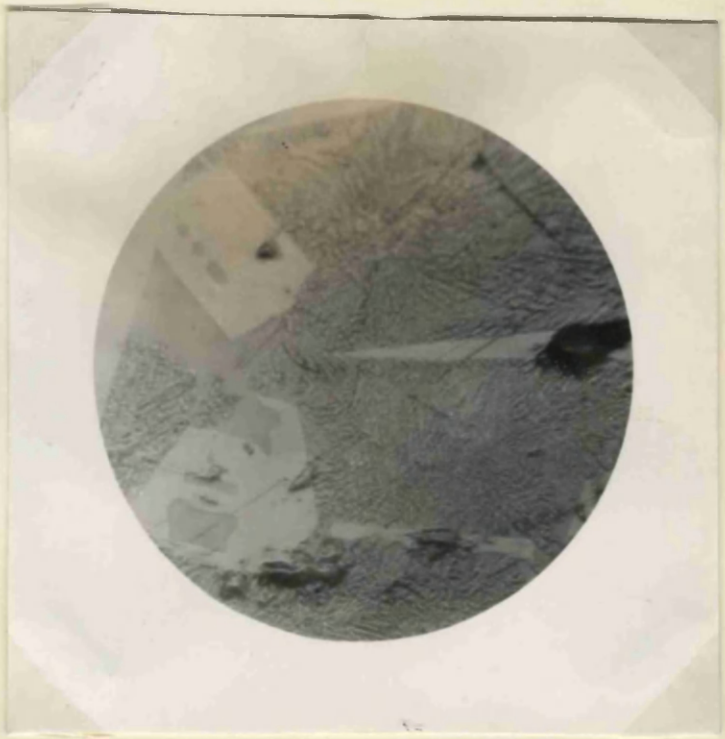

Fig. 38. $2MnO.SiO_2 : Na_2O.2SiO_2 = 50 : 50$
Annealed at 755°c for 72 hours.
× 200.

720°C the first showed the structure given in Fig.39. The part encircled in Fig.39 showed the contours of a parent rectangular $2MnO.SiO_2$ crystal. Under higher magnification the structure showed the remnant of $2MnO.SiO_2$ crystals, (Fig.40). The completely glassy slag annealed for 15 days at 720°C showed no $2MnO.SiO_2$ crystals. The structure is shown in Fig.41. X-ray and refractive index measurement revealed the presence of $MnO.SiO_2$ and $Na_2O.MnO.2SiO_2$ only.

As has already been mentioned the slags with higher $Na_2O.2SiO_2$ contents were extremely difficult to crystallise. Moreover as the $Na_2O.2SiO_2$ content of the slags was increased polishing became difficult. When completely glassy slags were annealed, the ternary precipitate was extremely fine and could only be identified by X-ray diffraction and refractive index measurements. Primary crystals of $Na_2O.MnO.2SiO_2$ could be easily obtained, (Fig.42). Primary $Na_2O.2SiO_2$ crystals were very heavily etched (Fig.43). These slags were not soft enough to polish on dry "selvyt" without polishing powder and reproduction of the microstructure was extremely difficult.

From the examination of the slags on the join $2MnO.SiO_2$-$Na_2O.2SiO_2$ it is seen that it is not a tieline and intersects three three-phase triangles. The results of the quenching and annealing experiments show that $MnO.SiO_2$ only occurs in slags containing up to 50 per cent $Na_2O.SiO_2$, forming as a result of a peritectic reaction

$$L + 2MnO.SiO_2 = MnO.SiO_2 + Na_2O.MnO.2SiO_2$$

in which $2MnO.SiO_2$ is consumed. This reaction, as has been shown, is

Fig. 39. $2MnO.SiO_2 : Na_2O.2SiO_2 = 50:50$
Quenched from 720°c X 200 for 84 hours. (The slag used in this case was that showing the structure shown in Fig 38.)

Fig. 40. $2MnO.SiO_2 : Na_2O.2SiO_2 = 50:50$.
The encircled part in Fig 39 under higher magnification X 500. showing remnants of $2MnO.SiO_2$ crystals undergoing peritectic reaction.

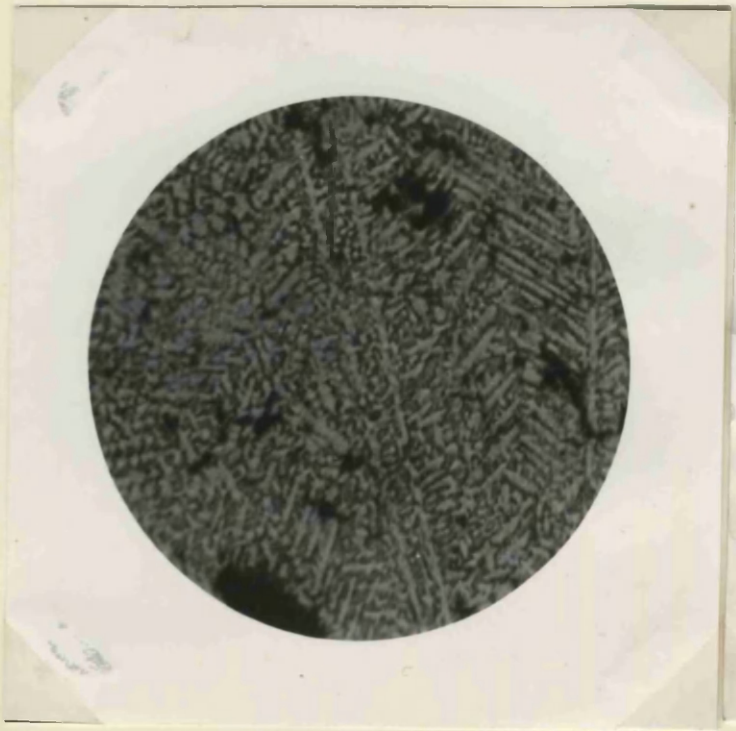

Fig. 41. $2MnO.SiO_2 : Na_2O.2SiO_2 = 50:50$.
Quenched from 720°c after annealing for 15 days. X 200. (completely glassy slag being used for annealing) contains $MnO.SiO_2$ and $Na_2O.MnO.2SiO_2$.

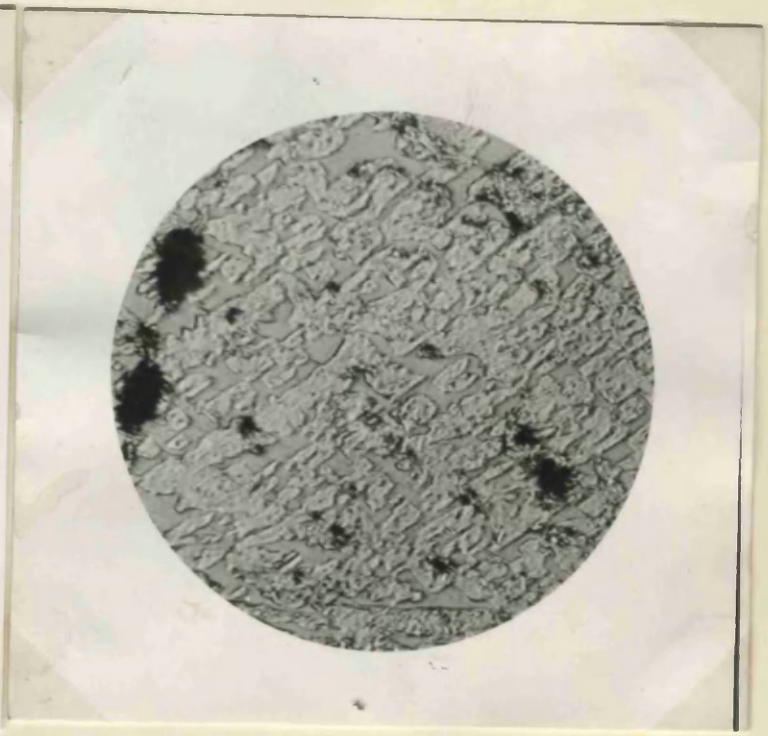

Fig. 42. $2MnO.SiO_2 : Na_2O.2SiO_2 = 35.7 : 64.3$.
Annealed and Quenched from 730°c X 200.
Primary crystals of $Na_2O.MnO.2SiO_2$.

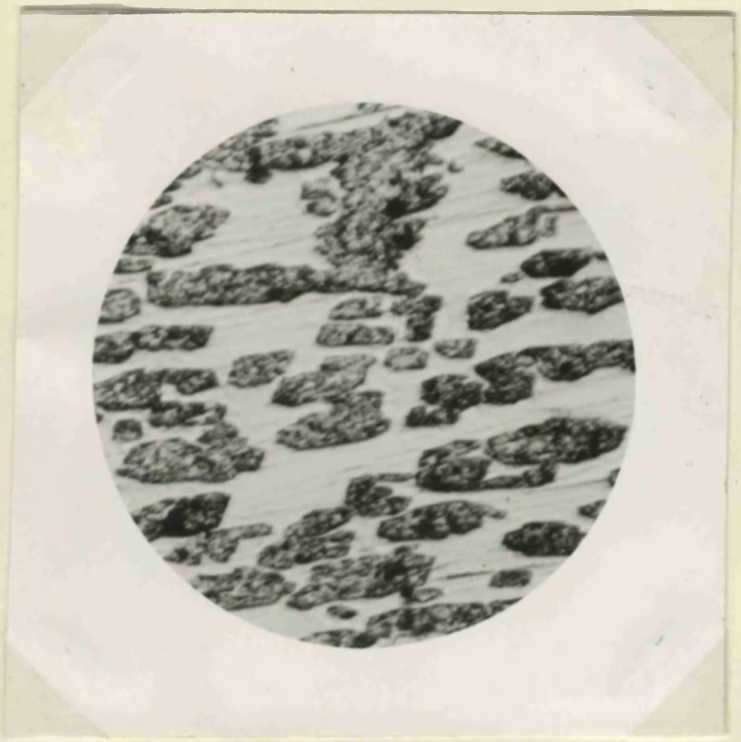

Fig. 43. $2MnO.SiO_2 : Na_2O.2SiO_2 = 14{\cdot}3 : 85{\cdot}7$.

Annealed and Quenched from

745°C x200.

Primary crystals of $Na_2O.2SiO_2$.

Heavily etched. in polishing process.

slag too hard to polish on dry "selvyt"

very sluggish. Under these conditions it is difficult to visualise how $MnO.SiO_2$ can crystallise in furnace cooled slags especially when these slags give glass so easily. But $MnO.SiO_2$ does crystallise in furnace cooled slags of composition 92.9/7.1, 85.8/14.2 and 78.5/21.5. Also, $2MnO.SiO_2$ and $MnO.SiO_2$ crystallise from the slag 71.5/28.5, between 1140° to 1110°C. The structure of this slag and the apparent anomaly will be discussed after the liquid immiscibility gap in the Na_2O-MnO-SiO_2 system has been discussed.

PART 3.

JOIN $2MnO.SiO_2$-$Na_2O.SiO_2$.

Join $2MnO.SiO_2$-$Na_2O.SiO_2$.

Composition and analyses of the slags examined are given in Table VI. The slags were first melted and cooled in the furnace. Some slags showed segregation and had to be crushed and remelted. All the slags in this join were completely crystalline after cooling in the furnace. The beginning and the end of melting were determined by the visual method. The differential thermal analyses curves showed definite heat effects and changes of slope. Some showed as many as five changes. This is illustrated in Fig.44. To interpret these points the quenching and annealing method had to be undertaken. Another new compound $2Na_2O.3MnO.3SiO_2$ was encountered. The arguments leading to the location of this compound will be postponed till the join $2MnO.SiO_2$-$2Na_2O.SiO_2$ has been described as the results of the two joins $2MnO.SiO_2$-$Na_2O.SiO_2$ and $2MnO.SiO_2$-$2Na_2O.SiO_2$ are necessary for its identification.

The results obtained by the visual and differential methods are given in Table VII, which also indicates the phases present at room temperature. From these thermal data the liquidus is drawn and is presented in Fig.45. To substantiate this diagram the slags marked were annealed and quenched from different temperatures. The results of the quenching and annealing experiments are given in Table VIII.

TABLE VI.

Analyses of the Slags on the Join $2MnO.SiO_2$-$Na_2O.SiO_2$.

Ratio $2MnO.SiO_2$ / $Na_2O.SiO_2$	Composition before melting.			Composition after melting.			
	MnO.	Na_2O	SiO_2	MnO	Na_2O	SiO_2	FeO
92.9/7.1	65	4	31	64.8	3.7	31.06	0.12
85.8/14.2	60	7.5	32.5	59.8	7.2	32.5	0.16
78.5/21.5	55	11	34	54.6	10.8	34.2	0.17
71.5/28.5	50	15	35	49.5	14.6	35.2	0.23
64.3/35.7	45	18.5	36.5	44.7	18.01	36.5	0.21
57.2/42.8	40	22	38	39.7	21.5	38.1	0.20
50/50	35	25.5	39.5	34.7	24.9	39.6	0.22
42.9/57.1	30	29.5	40.5	29.5	29.0	40.6	0.28
35.7/64.3	25	33	42	34.5	32.3	42.1	0.28
28.6/71.4	20	36.5	43.5	19.6	36.0	43.6	0.3
21.5/78.5	15	40	45	14.5	39.2	45.1	0.4
14.3/85.7	10	44	46	9.5	43.0	46.1	0.43
7.1/92.9	5	47.5	47.5	4.6	46.2	47.7	0.5

TABLE VII.

Thermal Data and Phases present at Room Temperature.

$2MnO.SiO_2$ / $Na_2O.SiO_2$	Phases at Room Temp.	Visual Method. Beginning of melting	Visual Method. End of melting	Differential Thermal Analyses. 1st Arrest	2nd Arrest	3rd Arrest	4th Arrest
92.9/7.1	M_2S $N_2M_6S_3$ NMS_2	723°	1320°	720°	830°	1192°	1318°
85.8/14.2	M_2S $N_2M_6S_3$ NMS_2	730°	1260°	722°	828°	1200°	1255°
78.6/21.4	M_2S $N_2M_6S_3$ NMS_2	730°	1190°	725°	830°	1108°	1185°
71.5/28.5	M_2S $N_2M_6S_3$ NMS_2	732°	1160°	727°	825°	-	1150°
64.3/35.7	M_2S $N_2M_6S_3$ NMS_2	730°	1095°	720°	800°	910°	1006, 1100
57.2/42.8	M_2S $N_2M_6S_3$ NMS_2	725°	1030°	729°	772°	-	1022°
50/50	$N_2M_6S_3$ NMS NMS_2	790°	925°	783°	930°	-	-
42.9/57.1	NMS NMS_2 NS	732°	950°	740°	-	-	955°
35.7/64.3	NMS NMS_2 NS	740	923	N.D.	N.D.	N.D.	N.D.

TABLE VII (cont'd).

$2MnO.SiO_2$ / $Na_2O.SiO_2$	Phases Present at Room Temp.	Visual Method. Beginning of melting	Visual Method. End of melting	Differential Thermal Analyses 1st Arrest	2nd Arrest	3rd Arrest	4th Arrest
28.6/71.4	NMS NMS_2 NS	743°	910°	740°	920°	-	-
21.5/78.5	NMS NMS_2 NS	742°	995°	745°	910°	985°	-
14.3/85.7	NMS NMS_2 NS	740°	1020°	745°	910°	1030°	-
7.1/92.9	NMS NMS_2 NS	745°	1070	N.D.	N.D.	N.D.	N.D.

TABLE VIII.

Join $2MnO.SiO_2$-$Na_2O.SiO_2$

Results of Annealing and Quenching Experiments.

Composition $2MnO.SiO_2/Na_2O.SiO_2$	Phases present	Temp. of Annealing	Method of Identification.
92.9/7.1	Liquid + M_2S	1200°C	Micro and R.I.
	Liquid + M_2S + MnO	1190°C	"
	Liquid + M_2S + MnO	830°C	"
	Liquid + M_2S + $N_2M_6S_3$	820°C	"
	Liquid + M_2S + $N_2M_6S_3$	730°C	"
	M_2S + $N_2M_6S_3$ + NMS	720°C	R.I.and X-ray
85.8/14.2	Liquid + M_2S	1200°C	Micro and R.I.
	Liquid + M_2S + MnO	1190°C	"
	Liquid + M_2S + MnO	830°C	"
	Liquid + M_2S + $N_2M_6S_3$	820°C	"
	Liquid + M_2S + $N_2M_6S_3$	730°C	"
	M_2S + $N_2M_6S_3$ + NMS	720°C	R.I.and X-ray
78.5/21.5	Liquid	1190°C	
	Liquid + MnO	1180°C	R.I.and micro.
	Liquid + MnO	1110°C	"
	Liquid + MnO + M_2S	1100°C	"
	Liquid + MnO + M_2S	830°C	"
	Liquid + M_2S + $N_2M_6S_3$	820°C	"
	Liquid + M_2S + $N_2M_6S_3$	730°C	"
	M_2S + $N_2M_6S_3$ + NMS	720°C	R.I.and X-ray
71.5/28.5	Liquid	1160°	
	Liquid + MnO	1150°	Micro
	Liquid + MnO	830°	"
	Liquid + $N_2M_6S_3$ + M_2S	820°	Micro and R.I
	Liquid + $N_2M_6S_3$ + M_2S	730°	"
	M_2S + $N_2M_6S_3$ + NMS	720°	R.I.and X-ray

TABLE VIII (Cont'd).

Composition $2MnO.SiO_2/Na_2O.SiO_2$	Phases present.	Temp. of Annealing -	Method of Identification.
64.3/35.7	Liquid	1100°	
	Liquid + MnO	1090°	Micro
	Liquid + MnO	1010°	"
	Liquid + MnO + $N_2M_3S_3$	1000°	Micro and R.I.
57.2/42.8	Liquid	1030°	
	Liquid + $N_2M_3S_3$	1020°	Refractive Index
	Liquid + $N_2M_3S_3$	770°	"
	Liquid + $N_2M_3S_3$ + NMS_2	760°	"
	Liquid + $N_2M_3S_3$ + NMS_2	730°	"
	$N_2M_3S_3$ + NMS_2 + M_2S	720°	R.I. and X-ray
42.9/57.1	Liquid	950°	
	Liquid + NMS	940°	R.I.
	Liquid + NMS	750°	R.I.
	NMS + NS + NMS_2	740°	R.I. and X-ray.
35.7/64.3	Liquid	930°	
	Liquid + NMS	920°	R.I.
	Liquid + NMS	870°	"
	Liquid + NMS + NS	860°	"
	Liquid + NMS + NS	750°	"
	NMS + NS + NMS_2	740°	R.I. and X-ray.

Discussion of the quenching and annealing experiments and microstructures.

In this section the identification of phases with slags by refractive index measurements was extremely useful. It was easy to distinguish crystals of $2MnO.SiO_2$ and MnO but impossible to identify $2Na_2O.3MnO.3SiO_2$, $Na_2O.MnO.SiO_2$ and $Na_2O.MnO.2SiO_2$ by examination of microstructures. Moreover, the glassy matrix of the quenched slags tended to be etched and cracks developed during polishing.

The slags 92.9/7.1 and 85.8/14.2 cooled in the furnace showed primary $2MnO.SiO_2$. When quenched, only primary $2MnO.SiO_2$ was present up to 1200°C but when quenched from 1190° MnO was also present. The structures at 1200°C and 1190° are shown in Figures 46 and 47. The MnO globules were always surrounded by crystals of $2MnO.SiO_2$ and were always brighter. Crystallisation of $2MnO.SiO_2$ and MnO continued to 830°C. At 820°C no MnO was observed in the slags. Two crystalline phases were now present, $2MnO.SiO_2$ and $2Na_2O.3MnO.3SiO_2$ (Fig.48). These two continued to be stable crystalline phases up to 730°C. At 720°C the slags were completely crystalline containing three crystalline phases $2MnO.SiO_2$, $2Na_2O.3MnO.3SiO_2$ and $Na_2O.MnO.SiO_2$ (Fig.49).

$2MnO.SiO_2$ was no longer the primary phase in the 78.5/21.5 slag. The primary MnO crystals obtained on quenching from 1180° are shown in Fig.50. These MnO crystals were globular but were arranged in the forms of dendrites. Binary precipitation of MnO and $2MnO.SiO_2$ was observed at 1110°C. In this case the MnO crystals were not

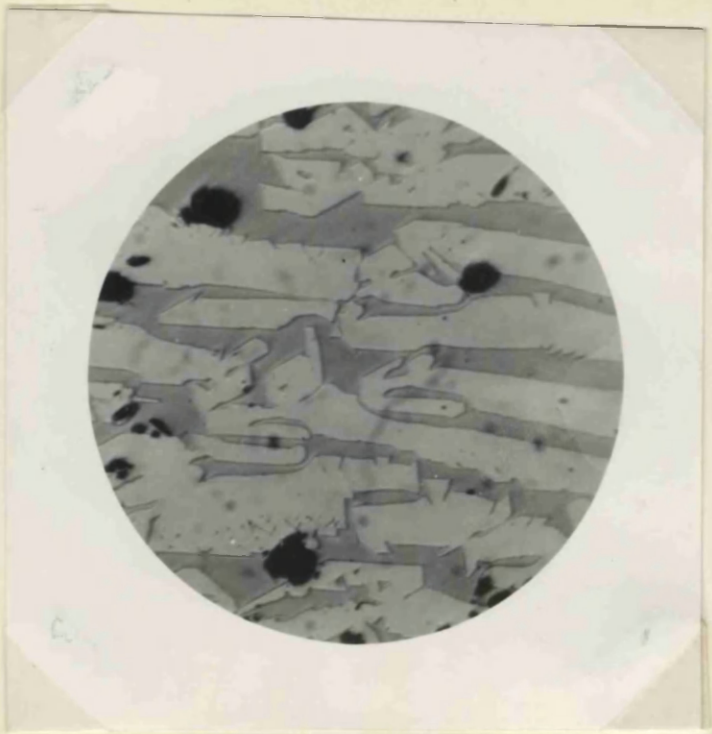

Fig 46. $2MnO.SiO_2 : Na_2O.SiO_2 = 92{\cdot}9 : 7{\cdot}1$
Quenched from 1200° x 100
(Primary $2MnO.SiO_2$ and glass)

Fig. 47. $2MnO.SiO_2 : Na_2O.SiO_2 = 92{\cdot}9 : 7{\cdot}1$
Quenched from 1190°c x 200
($2MnO.SiO_2$ and bright crystal of MnO)

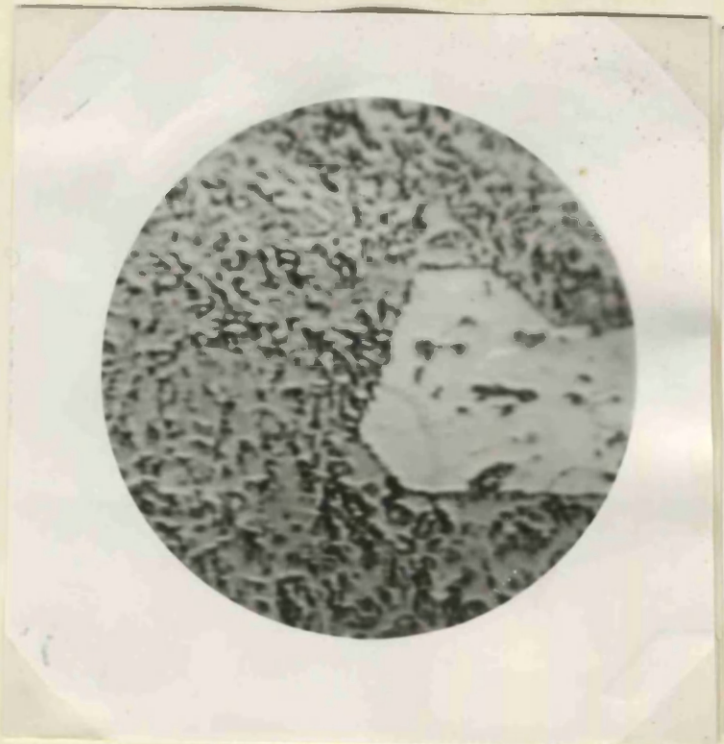

Fig 48. $2MnO.SiO_2 : Na_2O.2SiO_2 = 92{\cdot}9 : 7{\cdot}1$
Quenched from 820°c x 450
(White crystals of $2MnO.SiO_2$ and $2Na_2O.3MnO.3SiO_2$)

Fig. 49. $2MnO.SiO_2 : Na_2O.SiO_2 = 92{\cdot}9 : 7{\cdot}1$
Quenched from 720°c x 450
(White crystal of $2MnO.SiO_2$, $2Na_2O.3MnO.3SiO_2$ and $Na_2O.MnO.2SiO_2$ in the matrix)

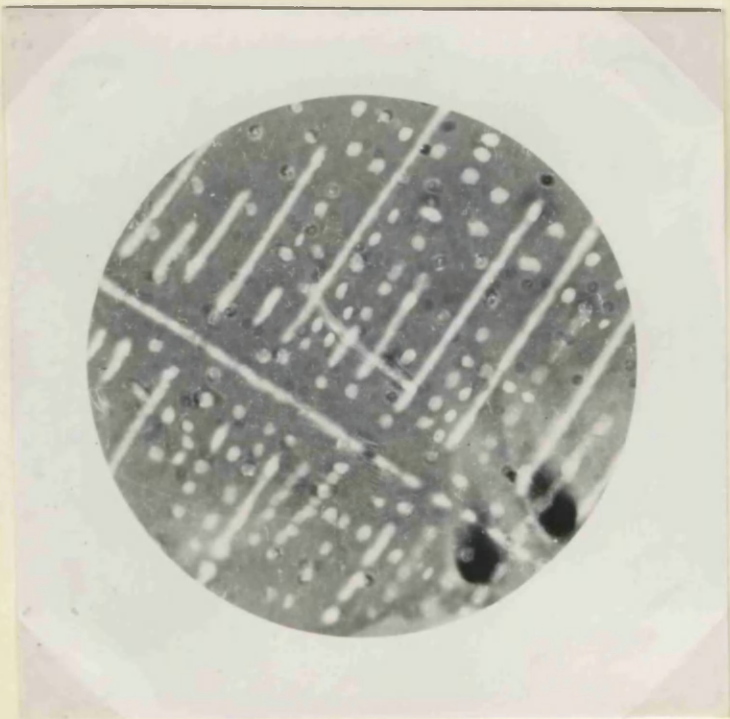

Fig. 50. $2MnO.SiO_2 : Na_2O.SiO_2 = 78.5 : 21.5$
Quenched from 1180°c × 150
(Bright crystals of MnO)

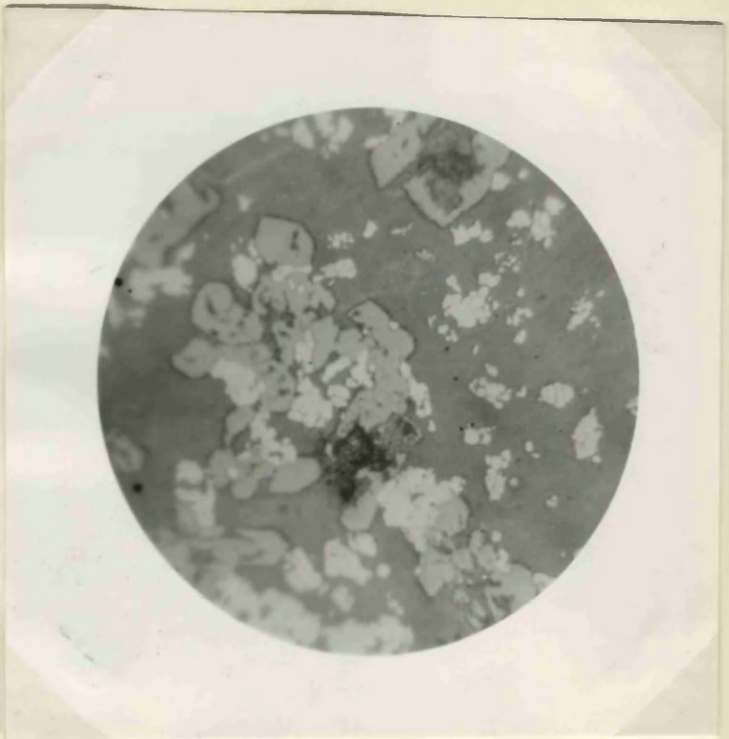

Fig. 51. $2MnO.SiO_2 : Na_2O.SiO_2 = 78.5 : 21.5$
Quenched from 1100°c × 150
(White crystals of $2MnO.SiO_2$ and brighter crystals of MnO)

Fig 52. $2MnO.SiO_2 : Na_2O.SiO_2 = 78.5 : 21.5$
Quenched from 820°c × 150
(White crystals of $2MnO.SiO_2$. $2Na_2O.3MnO.3SiO_2$ in the matrix)

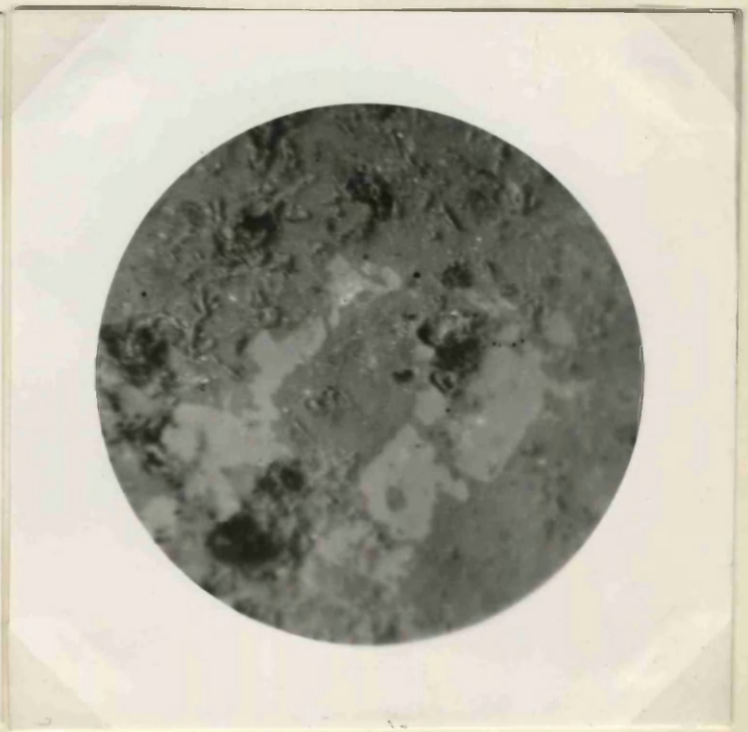

Fig 53. $2MnO.SiO_2 : Na_2O.SiO_2 = 78.5 : 21.5$
Quenched from 720°c × 250
(White crystals of $2MnO.SiO_2$. Matrix containing $2Na_2O.3MnO.3SiO_2$ and $Na_2O.MnO.2SiO_2$)

dendritic. Again the MnO and $2MnO.SiO_2$ crystals were superimposed on one another (Fig.51). This is probably because MnO and $2MnO.SiO_2$ nucleate each other. The crystals of MnO vanished at 820°C and fine crystals of $2Na_2O.3MnO.3SiO_2$ were observed in a glassy matrix along with large white crystals of $2MnO.SiO_2$ (Fig.52). Ternary crystallisation is shown in Fig.53. It is worth noticing that the typical large lathlike crystals of $2MnO.SiO_2$ were not present.

The 71.5/28.5 slag showed primary crystallisation of MnO but no binary precipitation of $2MnO.SiO_2$ and MnO was observed. At 820°C $2MnO.SiO_2$ and $2Na_2O.3MnO.3SiO_2$ crystallised out and MnO redissolved. Ternary crystallisation of $2Na_2O.3MnO.3SiO_2$, $2MnO.SiO_2$ and $Na_2O.MnO.SiO_2$ occurred at 720-730°C. (Fig.54).

MnO was still the primary phase in the 64.3/35.7 slag but the primary phase in the 57.2/42.8 slag was $2Na_2O.3MnO.3SiO_2$. Fig.55 shows the structure of this slag quenched from 1020°, containing $2Na_2O.3MnO.3SiO_2$ and glass. The structure obtained after ternary crystallisation at 720° is shown in Fig.56. Crystals of $2MnO.SiO_2$ could be easily distinguished even in ternary mixtures. The microstructure showed large holes especially around the crystals of $2MnO.SiO_2$. It was noticed that although $2MnO.SiO_2$ crystallised at the ternary stage the crystals were fairly large. This is probably due to the higher stability of $2MnO.SiO_2$. The stability of $2MnO.SiO_2$ was also observed in discussing the join $2MnO.SiO_2$-$Na_2O.2SiO_2$.

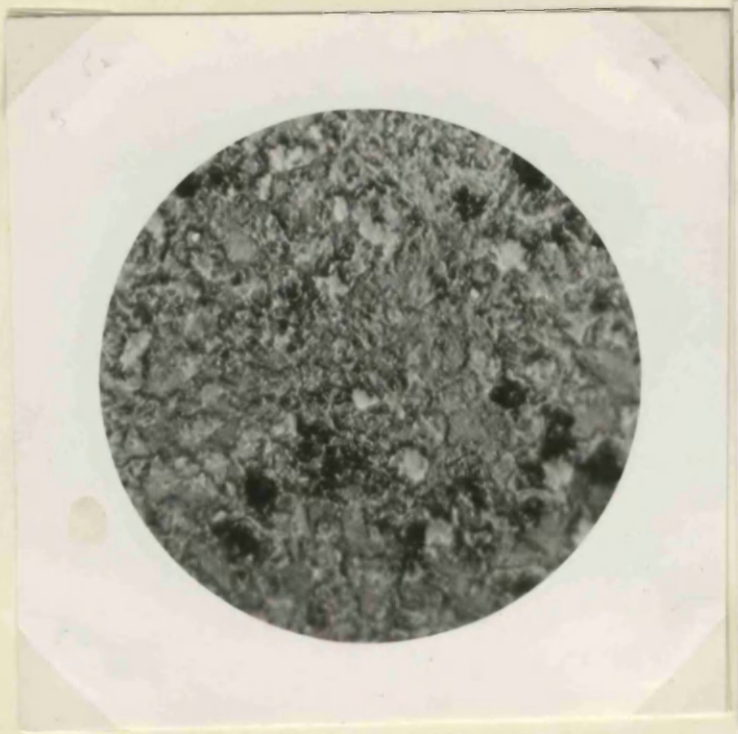

Fig. 54. $2MnO.SiO_2 : Na_2O.SiO_2 = 71.5 : 28.5$
Quenched from 720°c X 150.
globular crystals of $2MnO.SiO_2$.
Matrix containing $2Na_2O.3MnO.3SiO_2$
and $Na_2O.MnO.2SiO_2$.

Fig. 55. $2MnO.SiO_2 : Na_2O.SiO_2 = 57.2 : 42.8$.
Quenched from 1020°c X 150.
White crystals of $2Na_2O.3MnO.3SiO_2$.
The matrix containing glass is etched.

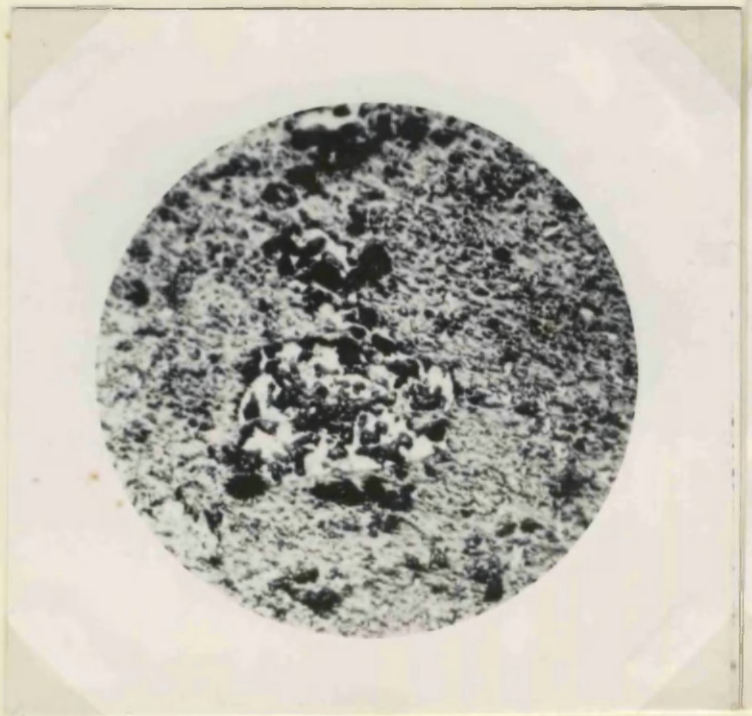

Fig. 56. $2MnO.SiO_2 : Na_2O.SiO_2 = 57.2 : 42.8$
Quenched from 720°c X 150.
Ternary precipitation of $2MnO.SiO_2$,
$2Na_2O.3MnO.3SiO_2$ and $Na_2O.MnO.2SiO_2$.
Hole around $2MnO.SiO_2$ crystals.

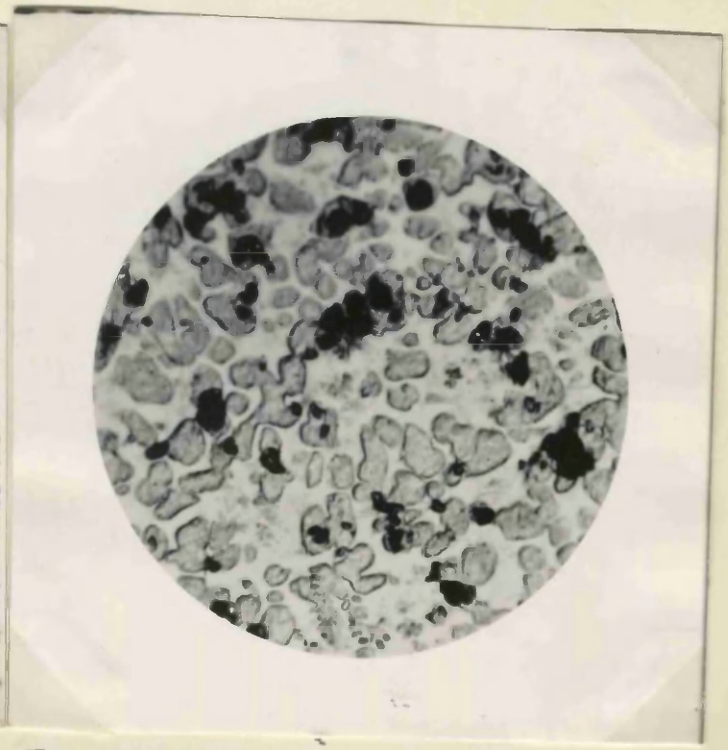

Fig. 57. $2MnO.SiO_2 : Na_2O.SiO_2 = 42.9 : 57.1$
Quenched from 940°c X 150
Primary crystals of $Na_2O.MnO.2SiO_2$.

The 42.9/57.1 slag showed primary crystals of $Na_2O.MnO.SiO_2$ in glass (Fig.57) when quenched from 940°C. No range of secondary crystallisation was observed. The 35.7/64.3 slag also showed primary crystals of $Na_2O.MnO.SiO_2$ when quenched from temperature 930° and 860°C. This was followed by binary crystallisation of $Na_2O.MnO.SiO_2$ and $Na_2O.SiO_2$ as shown in Fig.58, which illustrates the structure of the slag quenched from 860°C.

Fig. 58. $2MnO.SiO_2 : Na_2O.SiO_2 = 35{\cdot}7 : 64{\cdot}3$.
Quenched from 860°C × 300.
Primary lenticular $Na_2O.MnO.SiO_2$ crystals. Matrix shows needle shaped $Na_2O.SiO_2$.

PART 4.

JOIN $2MnO.SiO_2$-$2Na_2O.SiO_2$.

Join $2MnO.SiO_2$ - $2Na_2O.SiO_2$.

Eight slags were prepared on this join. As it was difficult to prepare and keep $2Na_2O.SiO_2$, all the slags were prepared from $Na_2O.SiO_2$, MnO and SiO_2. The slags were analysed and their analyses are given in Table IX. It was difficult to prepare and examine slags of higher Na_2O content on account of loss of Na_2O by volatilisation. Thermal data were obtained by the visual method and also by differential thermal analyses. The interpretation of the microstructures of the furnace-cooled slags was relatively simple. The identification of the unknown compound $2Na_2O.3MnO.3SiO_2$ was greatly facilitated by the results of the examination of the slags on this join. The thermal data obtained from both methods are given in Table X, which also indicates the phases present at room temperature as identified by X-ray diffraction and refractive index measurements.

Discussion of the Join $2MnO.SiO_2$-$2Na_2O.SiO_2$ and Microstructures.

In the microstructure of the slag 96/4 containing $2MnO.SiO_2$, MnO and $2Na_2O.3MnO.3SiO_2$ the large primary crystals were clearly seen (Fig.59). The binary precipitation of MnO is also seen. No such large crystals of $2MnO.SiO_2$ were in the microstructure of the slag 93.7. The $2MnO.SiO_2$ crystals had the typical form obtained in secondary crystallisation. Again all the crystals were superimposed on MnO crystals (Fig.60). Beyond this composition primary dendrites

TABLE IX.

Composition and Analyses of the Join

$2MnO.SiO_2$ - $Na_2O.MnO.SiO_2$ - $2Na_2O.SiO_2$.

Ratio $\frac{2MnO.SiO_2}{2Na_2O.SiO_2}$	Before Melting.			After Melting.			
	MnO	Na_2O	SiO_2	MnO	Na_2O	SiO_2	FeO
96:4				Not Analysed.			
92.9:7.1	65	5	30	64.8	4.8	30.1	0.16
85.8:14.2	60	10	30	59.7	9.6	30.2	0.21
78.5:21.5	55	15.0	30.0	54.6	14.1	30.7	0.3
71.5:28.5	50	20	30	49.5	19.5	30.2	0.31
64.3:35.7	45	24	31.0	44.6	23.3	31.3	0.33
57.2:42.8	40	29	31	39.5	28.2	31.8	0.4
50:50	33	32	35	32.4	31	35.4	0.59

TABLE X.

Thermal Data and Phases at Room Temperature the Join $2MnO.SiO_2$ - $Na_2O.MnO.SiO_2$.

Composition $2MnO.SiO_2$ / $2Na_2O.SiO_2$	Phases present at Room Temp. by R.I. and X-ray	Visual Method. Beginning of melting	Visual Method. End of Melting.	Differential Method. 1st Arrest	Differential Method. 2nd Arrest	Differential Method. 3rd Arrest
92.9/7.1	M_2S MnO $N_2M_6S_3$	830°	1330°	825°	1325°	
85.8/14.2	MnO M_2S	826°	1310°	822°	1060°	1305°
78.5/21.5	MnO M_2S $N_2M_6S_3$	830°	1295°	825°	950°	1300°
71.5/28.5	MnO $N_2M_6S_3$	1120°	1270°	1125°	1280°	
64.3/35.7	MnO $N_2M_6S_3$ NMS	870°	1255°	880°	1265°	
57.2/42.8	MnO $N_2M_6S_3$ NMS	875°	1210°	879	1105	1205°

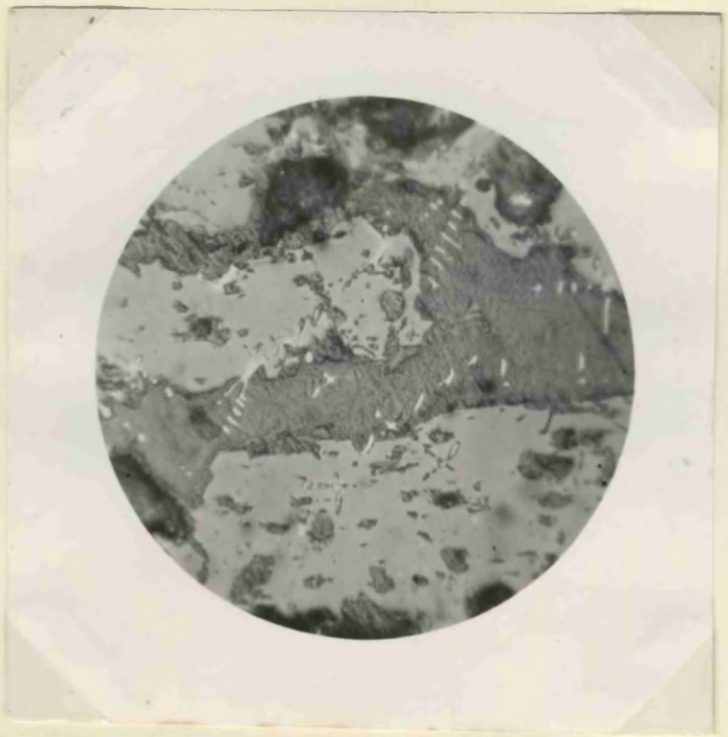

Fig. 59 X 150

Fig. 59.

$2MnO.SiO_2 : 2Na_2O.SiO_2 = 96:4.$
Cooled in the furnace
Large primary crystals of
$2MnO.SiO_2$. Binary precipitation
of MnO (bright, small crystals)

Fig. 60.

$2MnO.SiO_2 : 2Na_2O.SiO_2 = 92.9 : 7.1$
cooled in the furnace
Binary crystallisation of
$2MnO.SiO_2$ and MnO. The two
types of crystals are superimposed.
No lathlike $2MnO.SiO_2$ crystals
was visible.

Fig. 60 X 150.

of MnO were observed and the secondary $2MnO.SiO_2$ (Fig.61). In this microstructure, again, the characteristic lathlike crystals of primary $2MnO.SiO_2$ were not present. MnO separated as the primary phase in all the remaining slags examined. The 71.5/28.5 slag is of interest in that it contained only MnO and $2Na_2O.3MnO.3SiO_2$ (Fig.62). Neither the slag 71.5/28.5 nor 64.3/35.7 slag showed any $2MnO.SiO_2$. The latter showed only MnO, $Na_2O.MnO.SiO_2$ and $2Na_2O.3MnO.3SiO_2$ (Fig.63).

The identification of the compound was greatly facilitated from the nature of the slag $2MnO.SiO_2:2Na_2O.SiO_2$ = 71.8:28.2. As this slag only shows MnO and the unknown compound ($2Na_2O.3MnO.3SiO_2$) this compound should lie on the line joining MnO and the slag 71.8:28.2. It was found to lie on the intersection of ~~join~~ lines joining $Na_2O.MnO.SiO_2$ and $MnO.SiO_2$, and that joining MnO and the slag 71.8:28.2. The X-ray data and the refractive index are given in the Appendix.

Fig 61 X 200.

Fig 61.

$2MnO.SiO_2 : 2Na_2O.SiO_2 = 85.8 : 14.2$.
cooled in the furnace. Primary bright dendrites of MnO. White crystals of $2MnO.SiO_2$ (Secondary). No lathlike primary $2MnO.SiO_2$ crystals were observed.

Fig. 62.

$2MnO.SiO_2 : 2Na_2O.SiO_2 = 71.5 : 28.5$
MnO and $2Na_2O.3MnO.3SiO_2$.
Bright MnO crystals were globular.
No $2MnO.SiO_2$ was observed.

Fig 62 X 200.

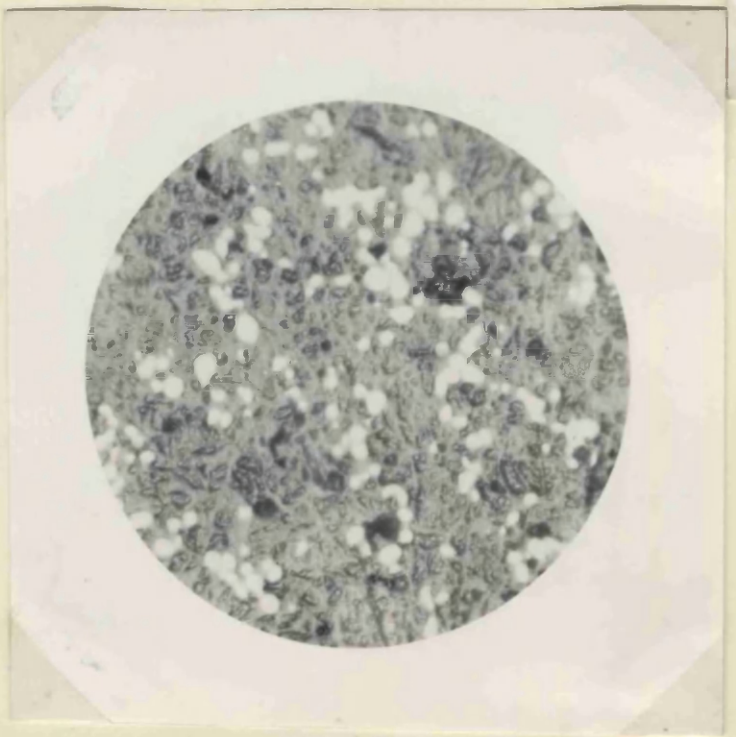

Fig. 63. X 200.

Fig. 63

$2MnO.SiO_2 : 2Na_2O.SiO_2 = 64.3 : 35.7$.
Bright globular primary MnO.
Matrix contains $2Na_2O.3MnO.3SiO_2$ and $Na_2O.MnO.SiO_2$. Again no $2MnO.SiO_2$ crystals were obsered.

PART 5.

JOIN $MnO.SiO_2$ - $Na_2O.SiO_2$.

Join $MnO.SiO_2$-$Na_2O.SiO_2$.

Two major difficulties presented themselves during the interpretation of the join $MnO.SiO_2$-$Na_2O.SiO_2$.

(1) Separation into two immiscible liquids was found to occur with certain slags on this join.

(2) The differential thermal analyses heating curves of these slags showed one exothermic change (Fig.64) at 715°C.

In addition the usual difficulties were encountered during polishing with slags of high $Na_2O.SiO_2$ content, but the constituents could easily be identified by petrological methods.

All slags were melted and cooled in the furnace. The 95/5 slag was completely crystalline and contained $MnO.SiO_2$, $2MnO.SiO_2$ and $Na_2O.MnO.2SiO_2$. The composition 90/10, 85/15, 80/20 and 78/22, on cooling in the furnace distinctly showed two layers. Fig.65 shows the crucible sectioned vertically and polished. The top layer contained $MnO.SiO_2$ and glass and the lower layer $MnO.SiO_2$, $2MnO.SiO_2$ and glass identified by refractive index measurements. The lower layer showed a definite arrangement of the crystals (Fig.66).

A thin section of the lower section of the slag was prepared and examined in transmitted light under crossed nicols. Two types of arrangements were observed as shown schematically in Fig.67.

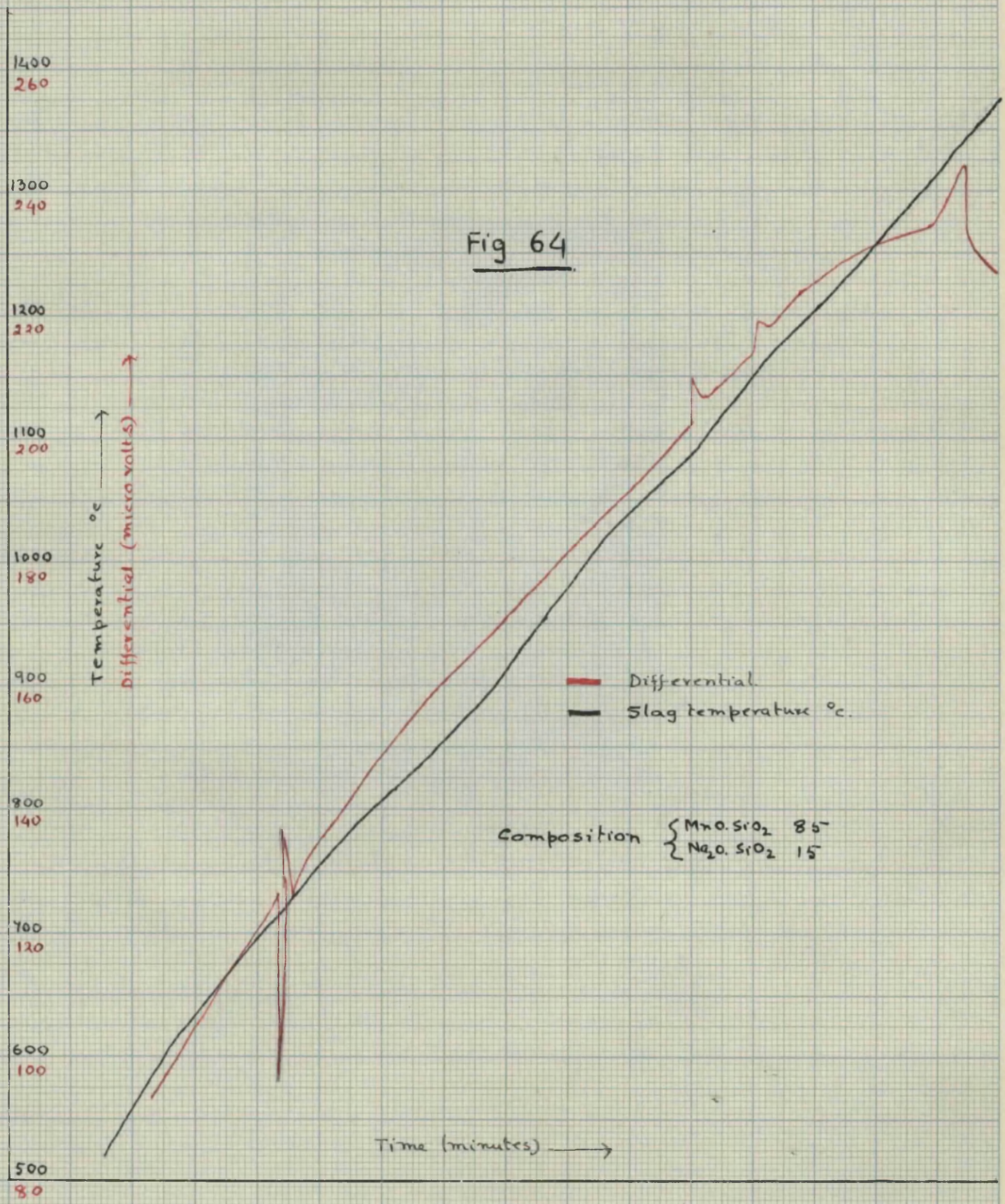
1400
260
1300
240
1200
220
1100
200
1000
180
900
160
800
140
700
120
600
100
500
80
Temperature °c
Differential (micro volts)
Differential
Slag temperature °c.
Composition
MnO. SiO2 85
Na2O. SiO2 15
Time (minutes)

Fig 64

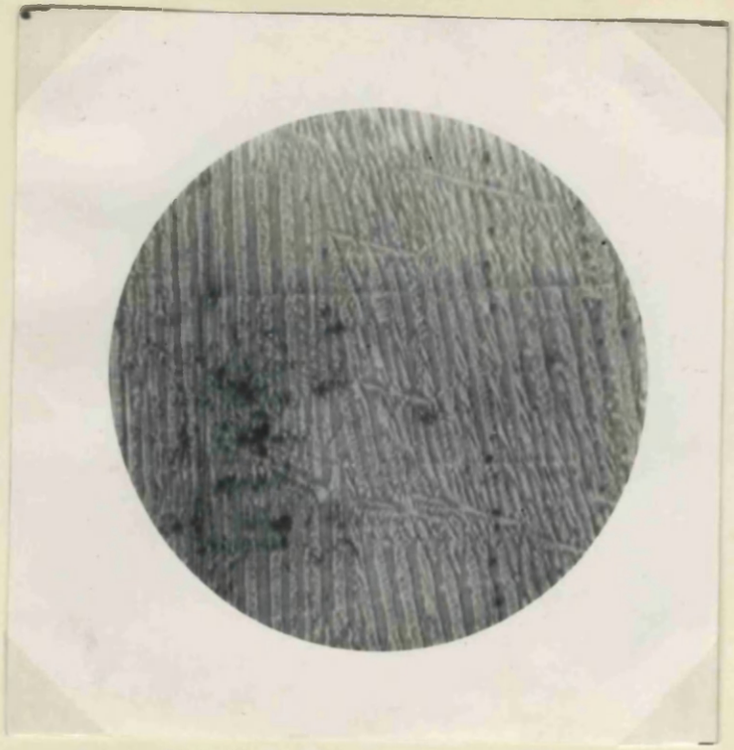

Fig. 66. $MnO.SiO_2 : Na_2O.SiO_2 = 85:15$. cooled in the furnace x200. structure of the lower layer of the two layers in fig 65.

Fig. 66.

Fig. 68: $MnO : SiO_2 = 62:38$ (Murad)

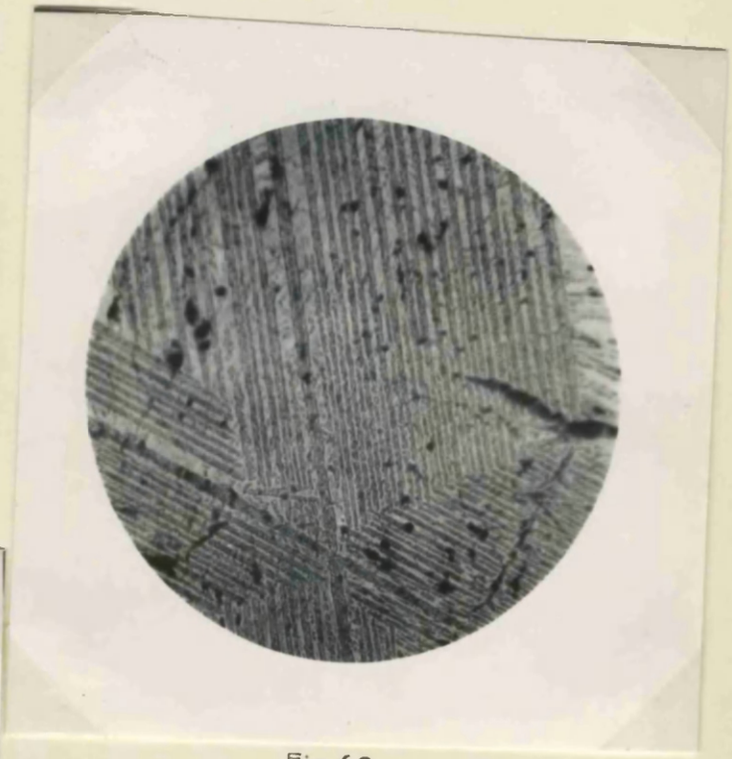

Fig 68

Fig 69 $MnO : SiO_2 = 62:38$ (Murad)

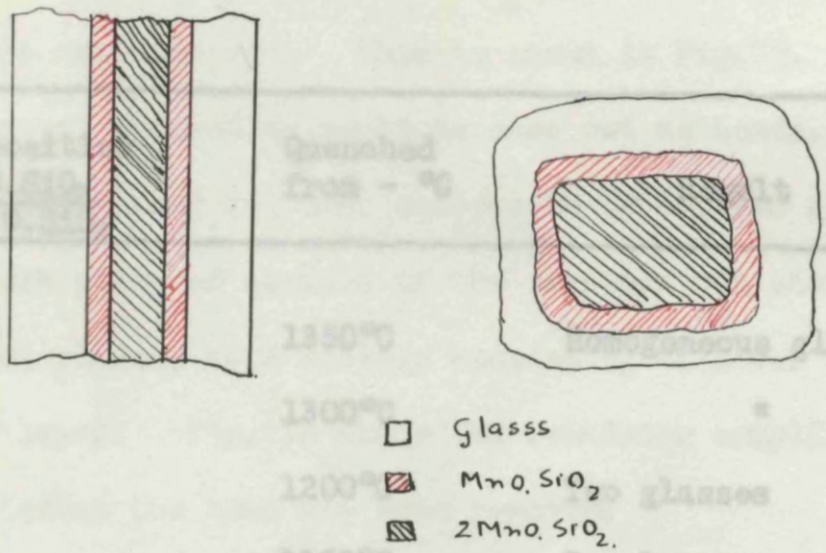

Fig. 67

The crystals seemed to have been etched during the preparation of the thin section. The "etch-lines" had a definite order; this is also represented in Fig.67. The first arrangements were more predominant than the second. A similar arrangement of $2MnO.SiO_2$ and $MnO.SiO_2$ was also observed by Murad in his investigation on the $MnO-SiO_2$ system. In his pure $MnO-SiO_2$ slags no glass was present. Figs.68, 69, show the structure 62/38 = $MnO.SiO_2$. In this etched structure, again, similar arrangements of "etch lines" are observed. This suggests that the structure forms by shear strain.

To decide whether the separation into two layers was due to differentiation during crystallisation or due to separation into two immiscible liquids, a number of slags were quenched from different temperatures. The composition and the results of quenching are given in Table XI.

TABLE XI.

Composition $\frac{MnO.SiO_2}{Na_2O.SiO_2}$	Quenched from - °C	Result	Crystalline Phase present in lower layer.
92/8	1350°C	Homogeneous glass	
	1300°C	"	
	1200°C	Two glasses	-
	1100°C	Two layers.	$MnO.SiO_2$
	1050°C	"	$2MnO.SiO_2$ / $MnO.SiO_2$
90/10	1350°C	Homogeneous glass	
85/15	1300°C	Two glasses	
80/20	1200°C	"	
78/22	1100°C	Two layers.	$MnO.SiO_2$
	1050°C	Two layers	$2MnO.SiO_2$ / $MnO.SiO_2$
75/25	1350°C	Homogeneous glass	
	1300°C	Two glasses	
	1200°C	"	
	1100°C	Homogeneous glass	
	1050°C	Glass + Crystal	$2MnO.SiO_2$

When crucibles containing two glasses were broken a peculiar fracture was observed. This is shown in Fig.70. With slight pressure the central protruding portions came out as beads. The beads were completely glassy and were surrounded by another glassy layer. Fig.71A shows the polished section of the crucible containing the bead. Two distinct glasses were visible consisting of an inner bead and the encircling glassy layer. Fig.71B shows the remaining complimentary concave hemi - sphere after the bead has been removed.

The colour of the inner bead remained pink in all the slags but that of the encircling layer changed from pink to green as the amount of $Na_2O.SiO_2$ was increased. The refractive index of the inner beads also remained virtually constant whereas that of the outer layer changed considerably. Table XII gives the refractive indices of the two layers (quenched from 1200°C).

TABLE XII.

Slags	Outer Layer	Inner Layer.
92/8	1.653	1.658
90/10	1.647	1.656
85/15	1.636	1.657
80/20	1.631	1.655

Fig. 70. $MnO.SiO_2 : Na_2O.SiO_2 = 85:15$
Quenched from 1200°c.
The protruding central bead.
Surrounded by another glassy layer. (shown below).

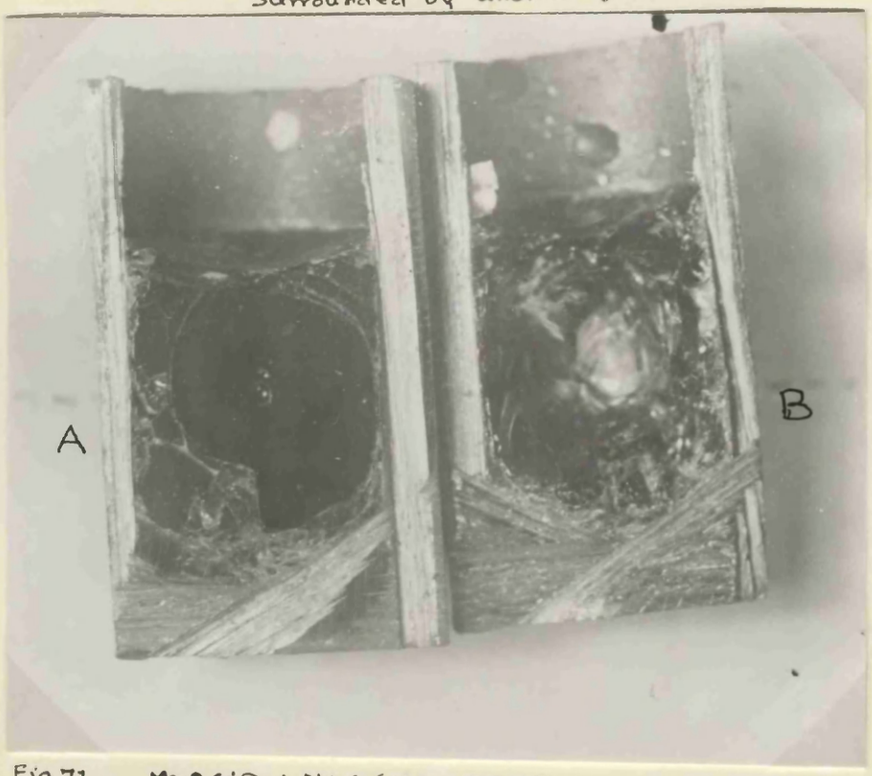

Fig 71. $MnO.SiO_2 : Na_2O.SiO_2 = 85:15$.
A:- Polished section of the crucible shown in Fig 70.
B:- The remaining complimentary part, after the bead has been removed, having a concave hemisphere at the centre.

With slags containing two layers, quenching and annealing experiments could not be carried out satisfactorily, since once the two layers separated, it was not possible to obtain uniform slags by annealing at lower temperatures. It was therefore not possible to find out the equilibrium phase distribution at room temperature.

Table XI shows that with the exception of the 75/25 slag, all the lower layers contained primary $MnO.SiO_2$ and secondary $2MnO.SiO_2$. The upper layer remained completely glassy in all cases, even when quenched from 1050°C after 25 minutes at that temperature (Fig.72). But when the same slag was annealed for two hours at 1050°C $MnO.SiO_2$ crystals crystallised out (Fig.73). These results indicate that these slags lie in the primary field of crystallisation of $MnO.SiO_2$.

It is also seen from Table XI that the 75/25 slag, although showing two layers at 1200°C is a homogeneous glass at 1100°C and two layers are absent. When this slag was annealed at various temperatures and then quenched the following results were obtained. All the constituents were identified by refractive index measurements.

Temp.	Time.	Phase.
1080°C	1 hour	glass
1070°C	"	glass + $2MnO.SiO_2$
750°C	"	glass + $2MnO.SiO_2$
740°C	"	glass + $2MnO.SiO_2$
730°C	84 hours	glass + $2MnO.SiO_2$ + $Na_2O.MnO.2SiO_2$
720°C	15 days.	$MnO.SiO_2$ + $Na_2O.MnO.2SiO_2$.

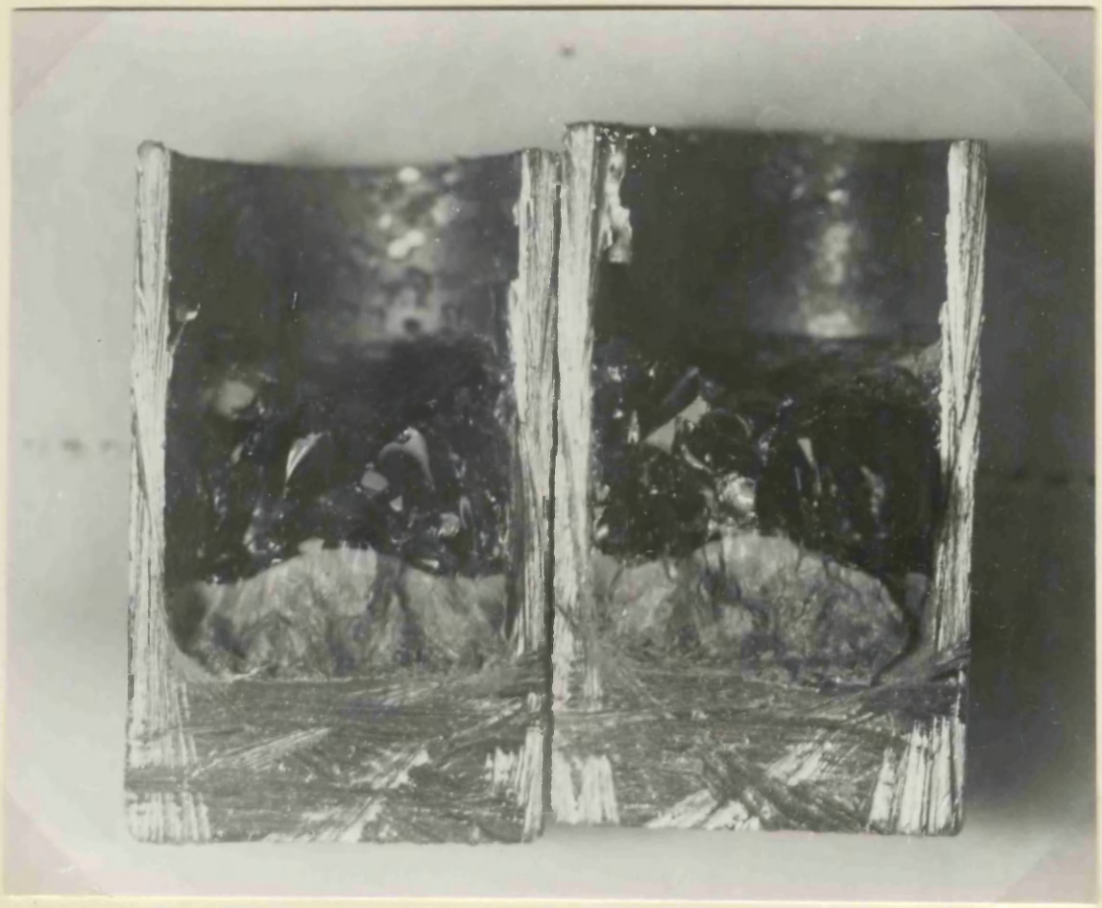

Fig. 72. $MnO.SiO_2 : Na_2O.SiO_2 = 85:15$
Melted at 1300°c cooled to 1050°, held for 25 minutes and quenched. Top layer pink glass. Bottom layer grey showing structure similar to that shown in Fig 66.

Fig 73. composition $MnO.SiO_2 : Na_2O.SiO_2 = 85:15$. Slag shown in Fig 72 annealed at 1050°c for two hours. The upper glassy crystallized to show $MnO.SiO_2$ shown in this fig 73.

Differential Thermal Analyses.

As already mentioned the existence of an exothermic change in the slags showing two layers presented difficulty in interpreting the result of this join. The result of the quenching and annealing experiments and the presence of only two phases at room temperature suggests that the join $MnO.SiO_2$-$Na_2O.MnO.2SiO_2$-$Na_2O.SiO_2$ is a tie line and $2MnO.SiO_2$ is not a stable phase at room temperature. Therefore the slags showing two layers are in the state of non-equilibrium at room temperature. In such a case the presence of an exothermic change is probably due to the tendency of the slag to return to equilibrium. This could not be verified with the slag 90/10, 85/15, 80/20 and 78/22 as once the two liquids separated it was impossible to obtain a uniform slag by annealing at lower temperature. But the slag 75/25 although showing two layers when cooled in the furnace, does not show the same when quenched from 1100°C. The furnace cooled slag shows the differential thermal (heating) curve given in Fig.74 which again shows the exothermic change at about 715°C. The slag (75/25) was quenched from 1100°C and annealed at 720°C. Then this was used to obtain the differential thermal curve. Figure 75 indicates the curve obtained In this curve no exothermic change point is noticed.

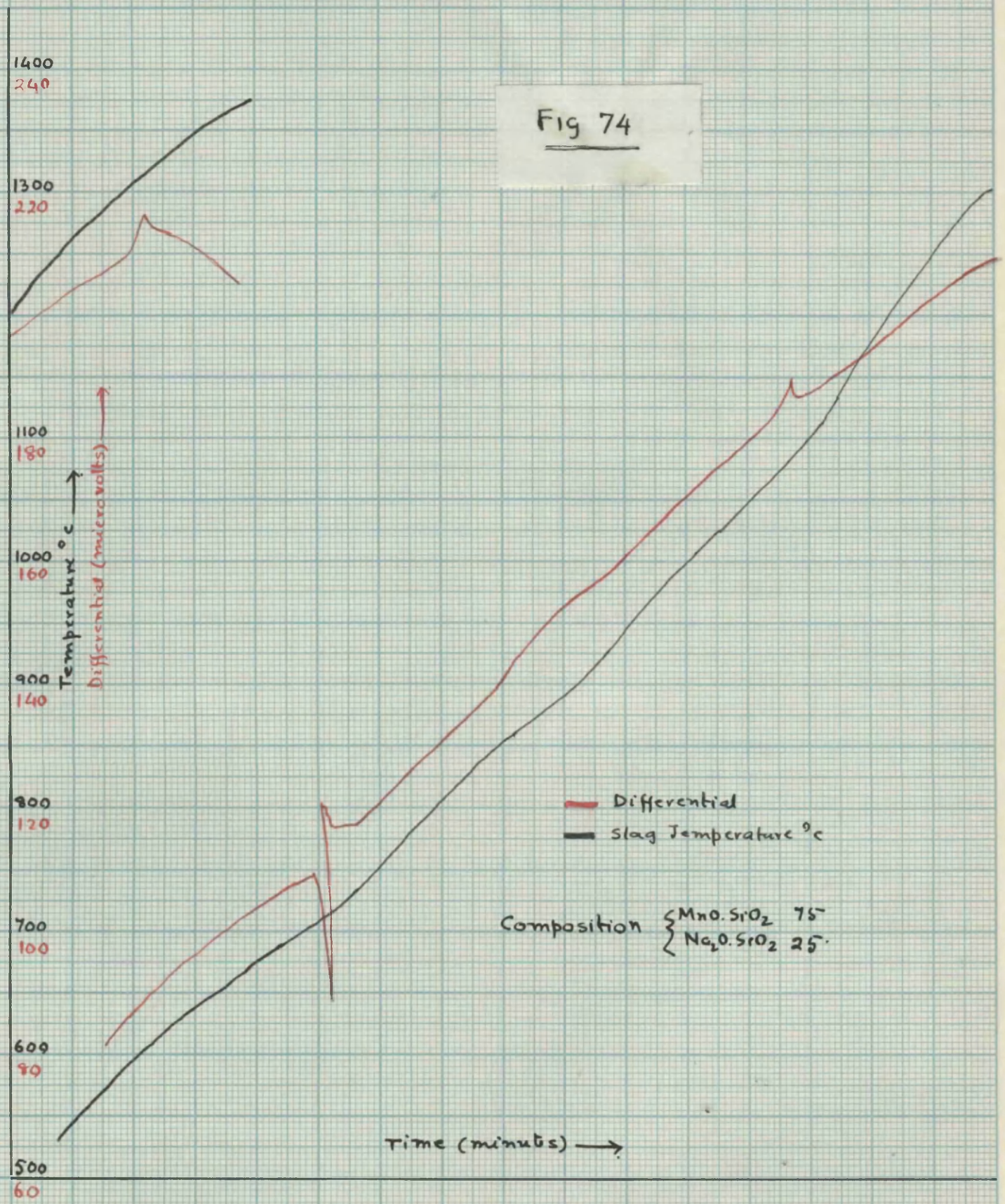
Fig 74
1400
240
1300
220
1100
180
1000
160
900
140
800
120
700
100
600
80
500
60
Temperature °c
Differential (microvolts)
Differential
Slag Temperature °c
Composition
MnO.SiO2 75
Na2O.SiO2 25
Time (minutes)

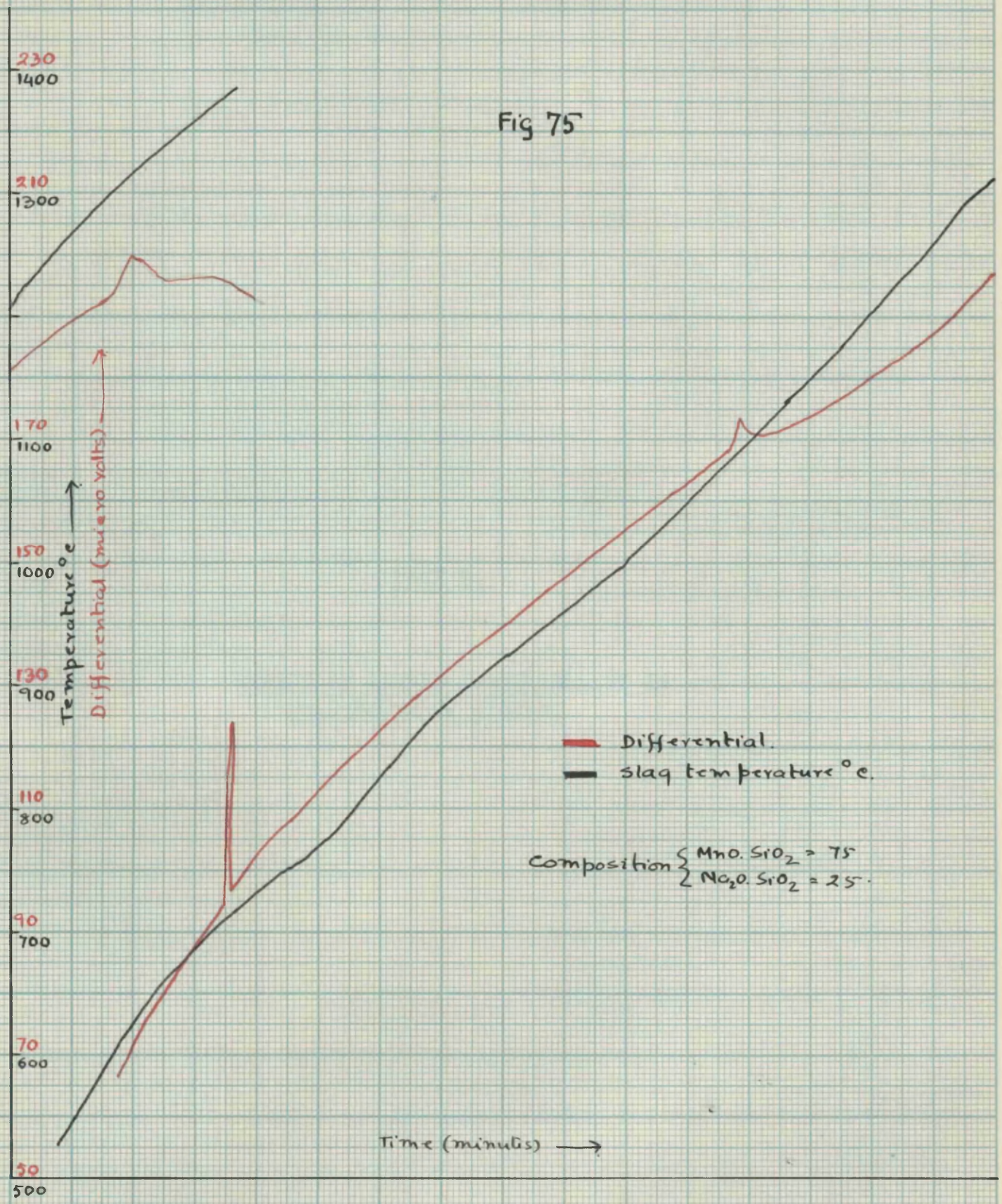
230
1400
210
1300
170
1100
150
1000
130
900
110
800
90
700
70
600
50
500
Temperature °c
Differential (micro volts)
Time (minutes)
Differential.
slag temperature °c.
Composition { MnO. SiO2 = 75
Na2O. SiO2 = 25.

Fig 75

PART 6.

EXTENT OF LIQUID IMMISCIBILITY IN Na_2O-MnO-SiO_2 SYSTEM.

Fig 76

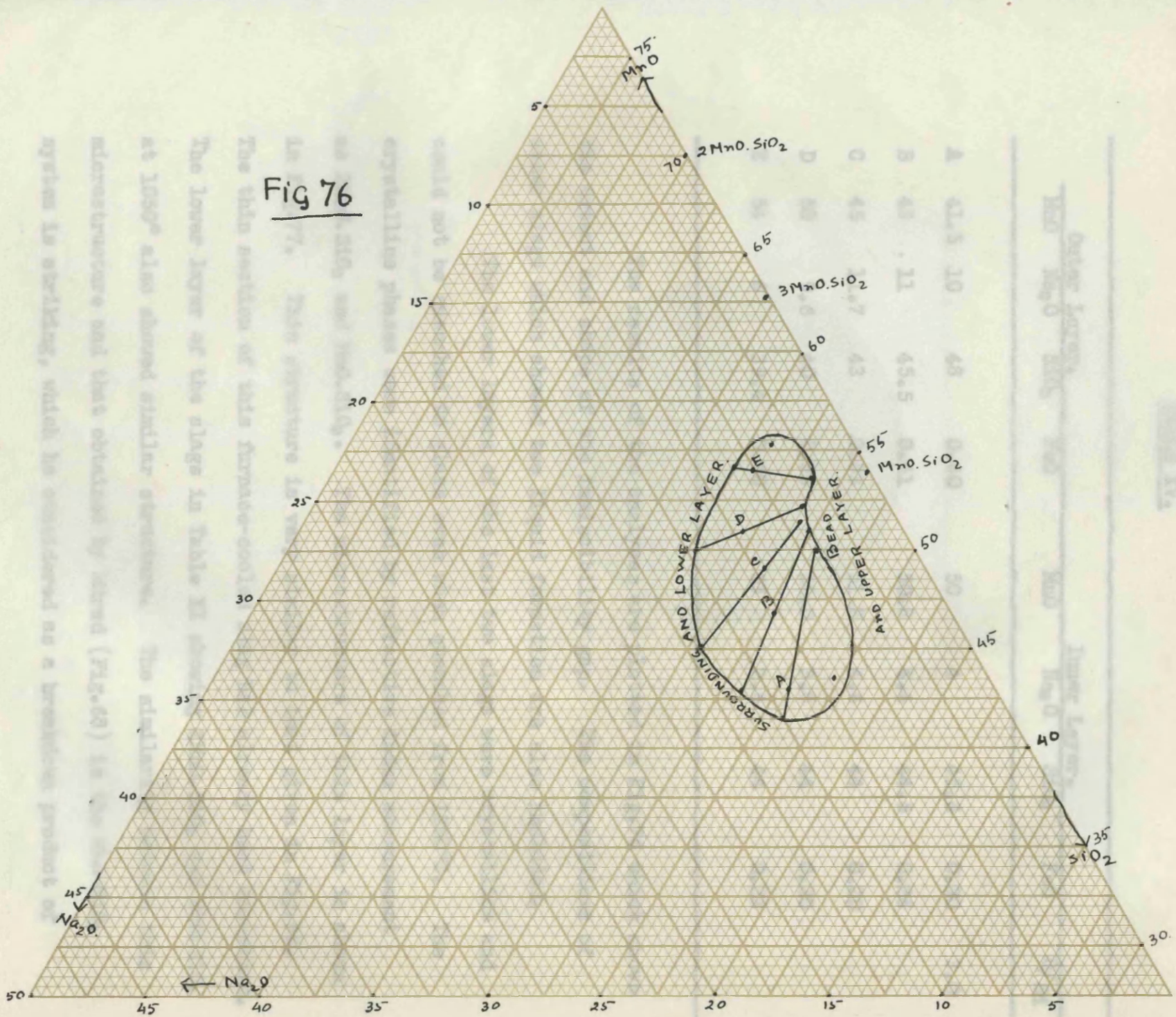
MnO
2MnO.SiO2
3MnO.SiO2
MnO.SiO2
SiO2
Na2O
Na2O
SURROUNDING AND LOWER LAYER.
BEAD LAYER AND UPPER LAYER.
A
B
C
D
E

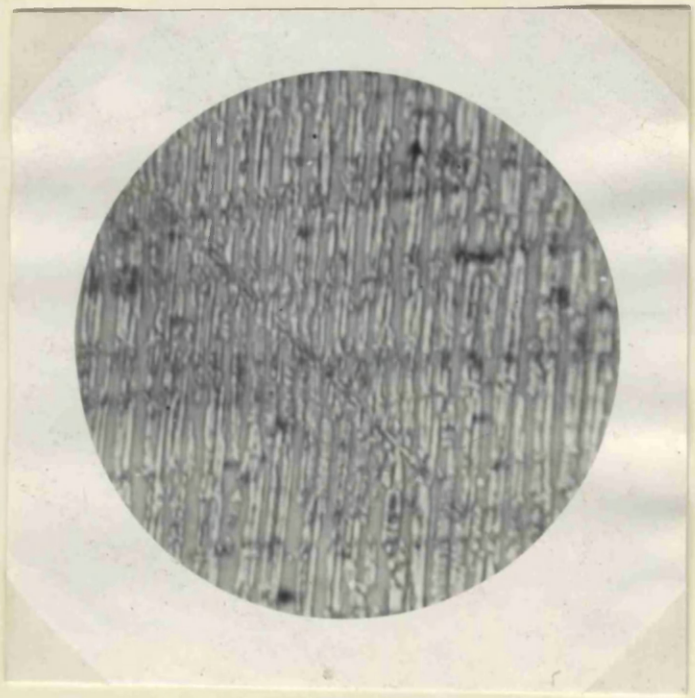

Fig. 77 $MnO : Na_2O : SiO_2 = 51 : 7 : 42$. x 200.

The slag quenched from 1200°c This structure is very similar to the one shown in Fig 66. This lower layer also contain $2MnO.SiO_2$ and $MnO.SiO_2$.

Primary Field of Silica, $MnO.SiO_2$ and $Na_2O.MnO.2SiO_2$.

The following slags were prepared to determine the primary field of crystallisation of silica. These slags were not analysed but were weighed accurately up to the third place of decimal and melted in iron crucibles.

TABLE XVI.

MnO	Na_2O	SiO_2
16	14.5	69.5
19.5	17.5	63
25.5	11	63.5
29	7	64
32	5	63
28	12	60
32	8	60
35	5	60
37	3	60
40	3	57
37.5	6	56.5
34	9	57
37	9	54
32.5	13.5	54
29	16	55
42	6	52
39.5	9	51.5
37	12	51
34	14.5	51.5
58	3	49

These slags were extremely difficult to crystallise. After being melted in iron crucibles they were cooled very slowly in the furnace (8 to 10 hours) and finally annealed at 600°C for 7 days. The slag

Fig. 78. $MnO : Na_2O : SiO_2 = 32 : 8 : 60$
slowly cooled in the furnace and
annealed at 600°c for 7 days. x100.
Needle shaped crystals of silica (Tridymite)

Fig. 79. $MnO : Na_2O : SiO_2 = 32 : 8 : 60$. Same annealing process as in Fig 78. The skeleton structure of silica (Probably cristobalite). Photograph taken with transmitted light, the particle immersed in light whose refractive index was similar to the surrounding glass.

CHAPTER 8.

THE TERNARY DIAGRAM Na_2O-MnO-SiO_2.

The Ternary Diagram Na_2O-MnO-SiO_2.

Three new compounds $Na_2O.MnO.SiO_2$, $Na_2O.MnO.2SiO_2$ and $2Na_2O.3MnO.3SiO_2$ were found to exist in the part of the Na_2O-MnO-SiO_2 system investigated. All these compounds were found to have incongruent melting points. These compounds are represented in Fig.80 which also includes the phases present in the slags examined at room temperature.

Equilibrium Phase Distribution at Room Temperature.

(1) The data given in Chapter 7, Part 5, indicates that when considering the solid state phase distribution in the Na_2O-MnO-SiO_2 system, $MnO.SiO_2$-$Na_2O.MnO.2SiO_2$ and $Na_2O.MnO.2SiO_2$-$Na_2O.SiO_2$ can be regarded as tie lines. It is probable that $Na_2O.MnO.2SiO_2$-SiO_2 is also a tie line because the slag "L" only shows two phases, $Na_2O.MnO.2SiO_2$ and SiO_2 at room temperature. More over at that temperature no $Na_2O.2SiO_2$ is present in the slag "B" which further substantiates that $Na_2O.MnO.2SiO_2$-SiO_2 is a tie line, It would be present if instead $Na_2O.2SiO_2$-$MnO.SiO_2$ were a tie line.

If $MnO.SiO_2$-$Na_2O.MnO.2SiO_2$, $Na_2O.MnO.2SiO_2$-$Na_2O.SiO_2$ and $Na_2O.MnO.2SiO_2$-SiO_2 are tie lines, $Na_2O.MnO.2SiO_2$-$Na_2O.2SiO_2$ must be a tie line. This would give the phase distribution

$Na_2O.SiO_2$ - $Na_2O.MnO.2SiO_2$ - $Na_2O.2SiO_2$.

$Na_2O.2SiO_2$ - $Na_2O.MnO.2SiO_2$ - SiO_2

SiO_2 - $Na_2O.MnO.2SiO_2$ - $MnO.SiO_2$

Phases at Room temperature:—

A = $2MnO.SiO_2 + MnO.SiO_2 + Na_2O.MnO.2SiO_2$

B = $MnO.SiO_2 + Na_2O.MnO.2SiO_2 + SiO_2$

C = $Na_2O.MnO.2SiO_2 + SiO_2 + Na_2O.2SiO_2$.

D = $2MnO.SiO_2 + Na_2O.MnO\,2SiO_2 + 2Na_2O.3MnO.3SiO_2$.

E = $Na_2O.MnO.2SiO_2 + Na_2O.MnO\,SiO_2 + 2Na_2O.3MnO.3SiO_2$.

F = $Na_2O.MnO.2SiO_2 + Na_2O.SiO_2 + Na_2O.MnO.SiO_2$.

G = $MnO + 2MnO.SiO_2 + 2Na_2O.3MnO.3SiO_2$

H = $MnO + 2Na_2O.3MnO.3SiO_2 + Na_2O.MnO.SiO_2$.

Fig 80

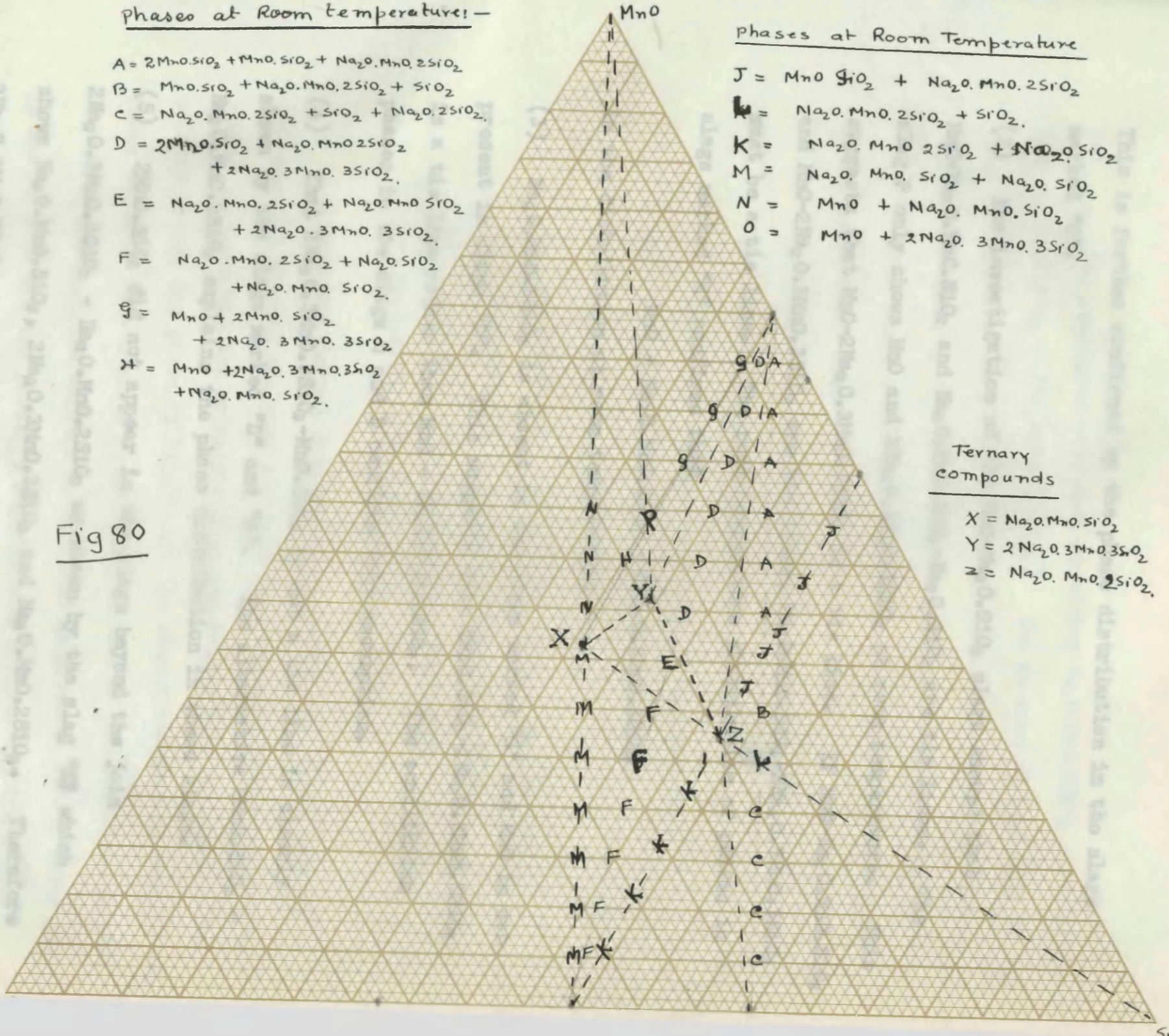

Phases at Room Temperature

J = $MnO\,SiO_2 + Na_2O.MnO.2SiO_2$

L = $Na_2O.MnO.2SiO_2 + SiO_2$.

K = $Na_2O.MnO\,2SiO_2 + Na_2O\,SiO_2$

M = $Na_2O.MnO.SiO_2 + Na_2O.SiO_2$

N = $MnO + Na_2O.MnO.SiO_2$

O = $MnO + 2Na_2O.3MnO.3SiO_2$

Ternary compounds

X = $Na_2O.MnO.SiO_2$

Y = $2Na_2O.3MnO.3SiO_2$

Z = $Na_2O.MnO.2SiO_2$.

This is further confirmed by the phase distribution in the slags marked "C".

(2) The investigation of the $MnO-Na_2O.SiO_2$ slags showed that $MnO-Na_2O.MnO.SiO_2$ and $Na_2O.MnO.SiO_2-Na_2O.SiO_2$ are tie lines. The slag P only shows MnO and $2Na_2O.3MnO.3SiO_2$ at room temperature. This suggests that $MnO-2Na_2O.3MnO.3SiO_2$ is a tie line. If $MnO-Na_2O.MnO.SiO_2$ and $MnO-2Na_2O.3MnO.3SiO_2$ are tie lines, $Na_2O.MnO.SiO_2-2Na_2O.3MnO.3SiO_2$ must be a tie line. The room temperature distribution of phases in slags marked "H" confirms that

$$MnO - Na_2O.MnO.SiO_2 - 2Na_2O.3MnO.3SiO_2$$

is the distribution at room temperature.

(3) $Na_2O.MnO.2SiO_2$ is absent in the slags marked "G" and MnO is not present in slags "D". This suggests that $2MnO.SiO_2-2Na_2O.3MnO.3SiO_2$ is a tie line rather than $MnO - Na_2O.MnO.2SiO_2$. The equilibrium phases in the slags G and D confirms this assumption.

(4) That $2Na_2O.3MnO.3SiO_2-MnO.SiO_2$ is not a tie line is clearly shown by the slags marked "D" and "A". The alternative $2MnO.SiO_2$ - $Na_2O.MnO.2SiO_2$ explains the phase distribution in these slags.

(5) $2MnO.SiO_2$ did not appear in the slags beyond the join $2Na_2O.3MnO.3SiO_2$ - $Na_2O.MnO.2SiO_2$ as shown by the slag "E" which shows $Na_2O.MnO.SiO_2$, $2Na_2O.3MnO.3SiO_2$ and $Na_2O.MnO.2SiO_2$. Therefore $2Na_2O.3MnO.3SiO_2$ - $Na_2O.MnO.2SiO_2$ is a tie line.

(6) The remaining join must be either $Na_2O.MnO.2SiO_2$ - $Na_2O.MnO.SiO_2$ or $Na_2O.SiO_2$ - $2Na_2O.3MnO.3SiO_2$. The absence of $Na_2O.SiO_2$ in the slag E suggests the former as the tie line rather than the latter. This is confirmed by the phase distribution of the slags marked "F".

From these considerations the proposed phase distributions in the solid state are:-

1. MnO - $Na_2O.MnO.SiO_2$ - $2Na_2O.3MnO.3SiO_2$
2. MnO - $2Na_2O.3MnO.3SiO_2$ - $2MnO.SiO_2$
3. $2MnO.SiO_2$ - $2Na_2O.3MnO.3SiO_2$ - $Na_2O.MnO.2SiO_2$
4. $2MnO.SiO_2$ - $Na_2O.MnO.2SiO_2$ - $MnO.SiO_2$
5. $MnO.SiO_2$ - $Na_2O.MnO.2SiO_2$ - SiO_2
6. $Na_2O.MnO.SiO_2$ - $2Na_2O.3MnO.3SiO_2$ - $Na_2O.MnO.2SiO_2$
7. $Na_2O.MnO.SiO_2$ - $Na_2O.SiO_2$ - $Na_2O.MnO.2SiO_2$
8. $Na_2O.SiO_2$ - $Na_2O.MnO.2SiO_2$ - $Na_2O.2SiO_2$
9. $Na_2O.2SiO_2$ - $Na_2O.MnO.2SiO_2$ - SiO_2.

From the thermal data obtained earlier, by visual method, differential thermal analyses and quenching and annealing experiments, binary sections and the primary phases separating were obtained. The primary phases are given in Fig.81 and the binary sections in Figs.82-86. These together were used to obtain the position of the invariant points.

The liquidus surface so obtained is given in Fig.81 which is in accord with all the previous experimental results and the binary sections shown in Figs.82-86.

Fig. 81

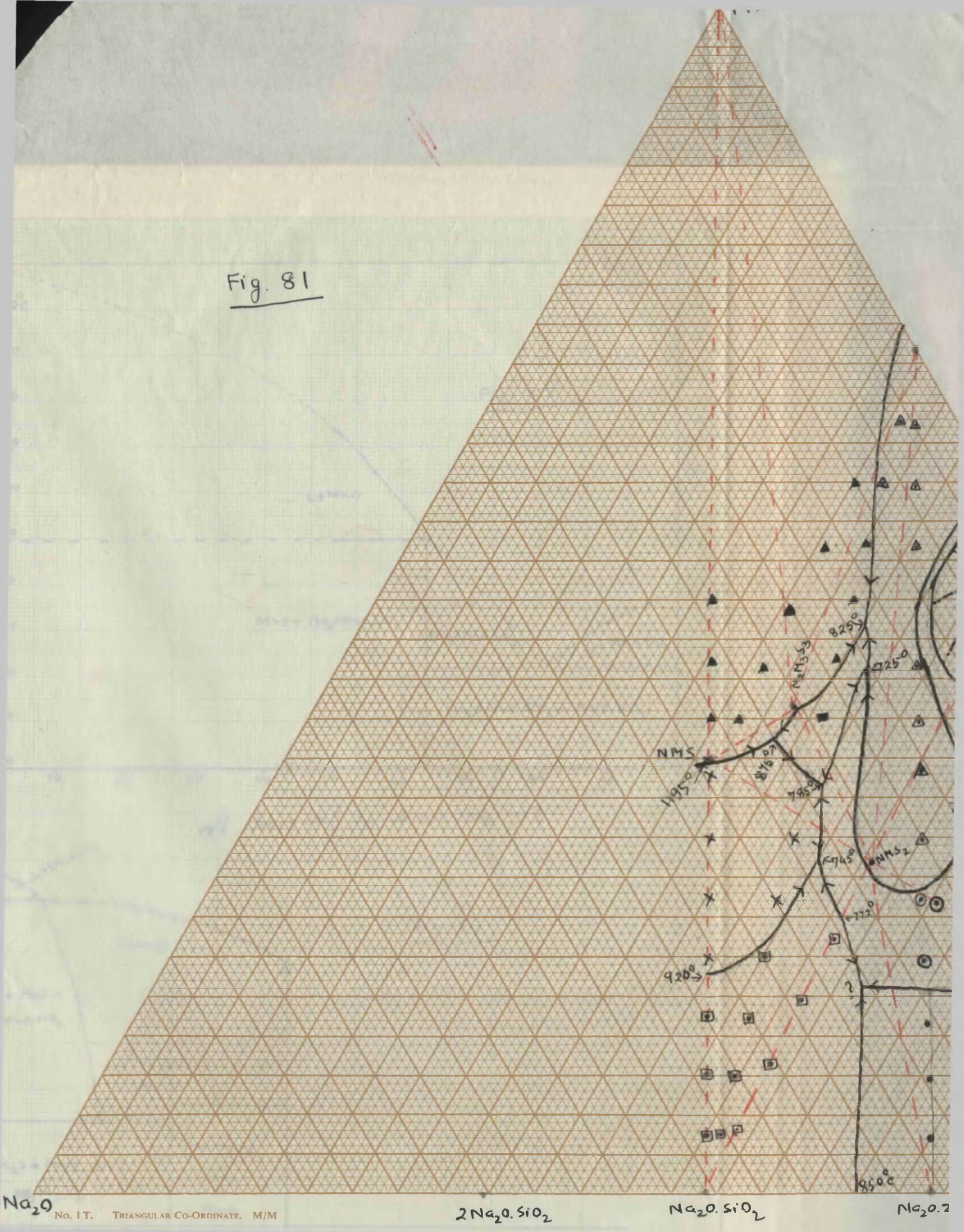

No. 1 T. TRIANGULAR CO-ORDINATE. M/M

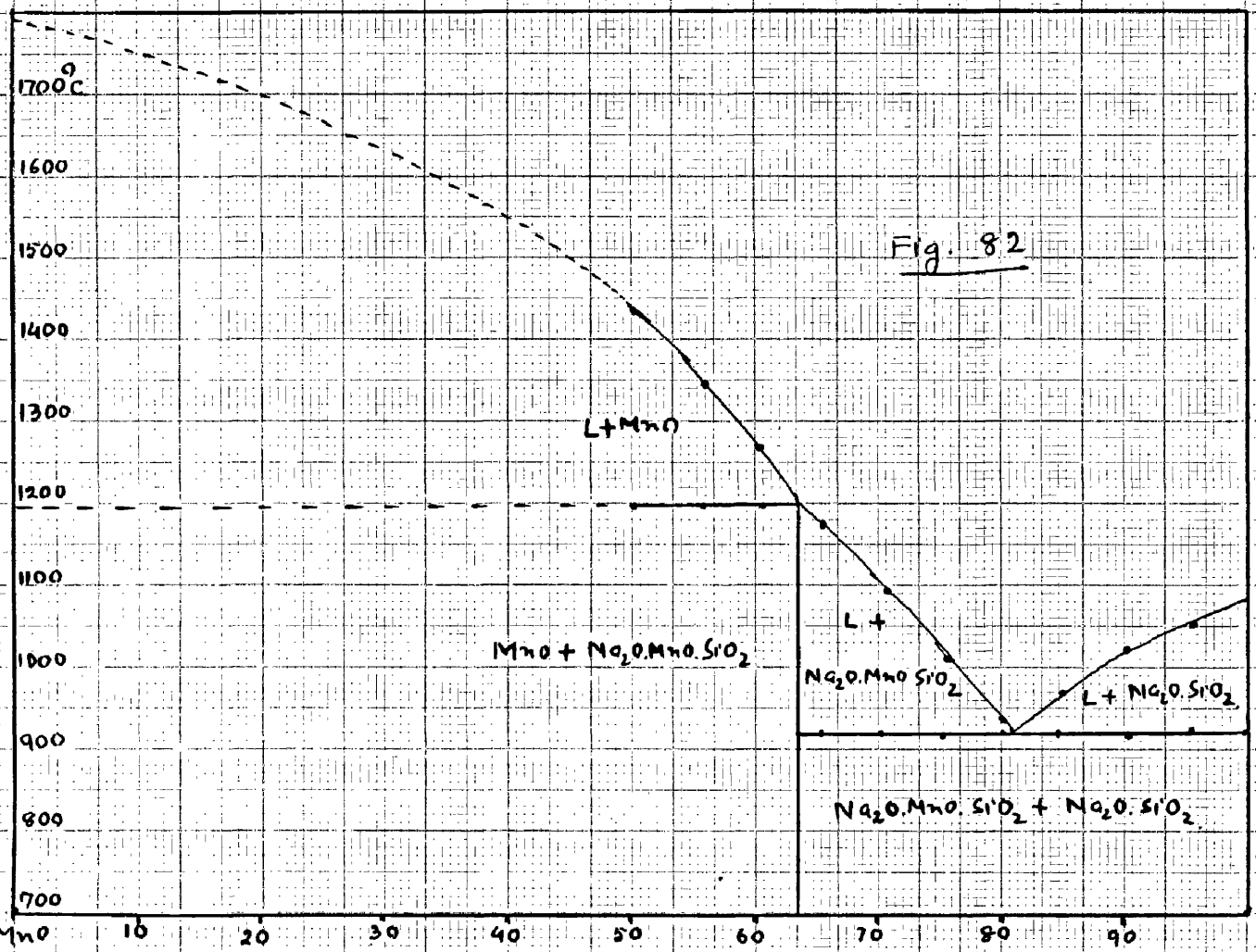
1700°C
1600
1500
1400
1300
1200
1100
1000
900
800
700
L+MnO
MnO + Na2O.MnO.SiO2
L + Na2O.MnO.SiO2
L + Na2O.SiO2
Na2O.MnO.SiO2 + Na2O.SiO2
MnO
10
20
30
40
50
60
70
80
90
Wt percent of Na2O.SiO2 →

Fig. 82

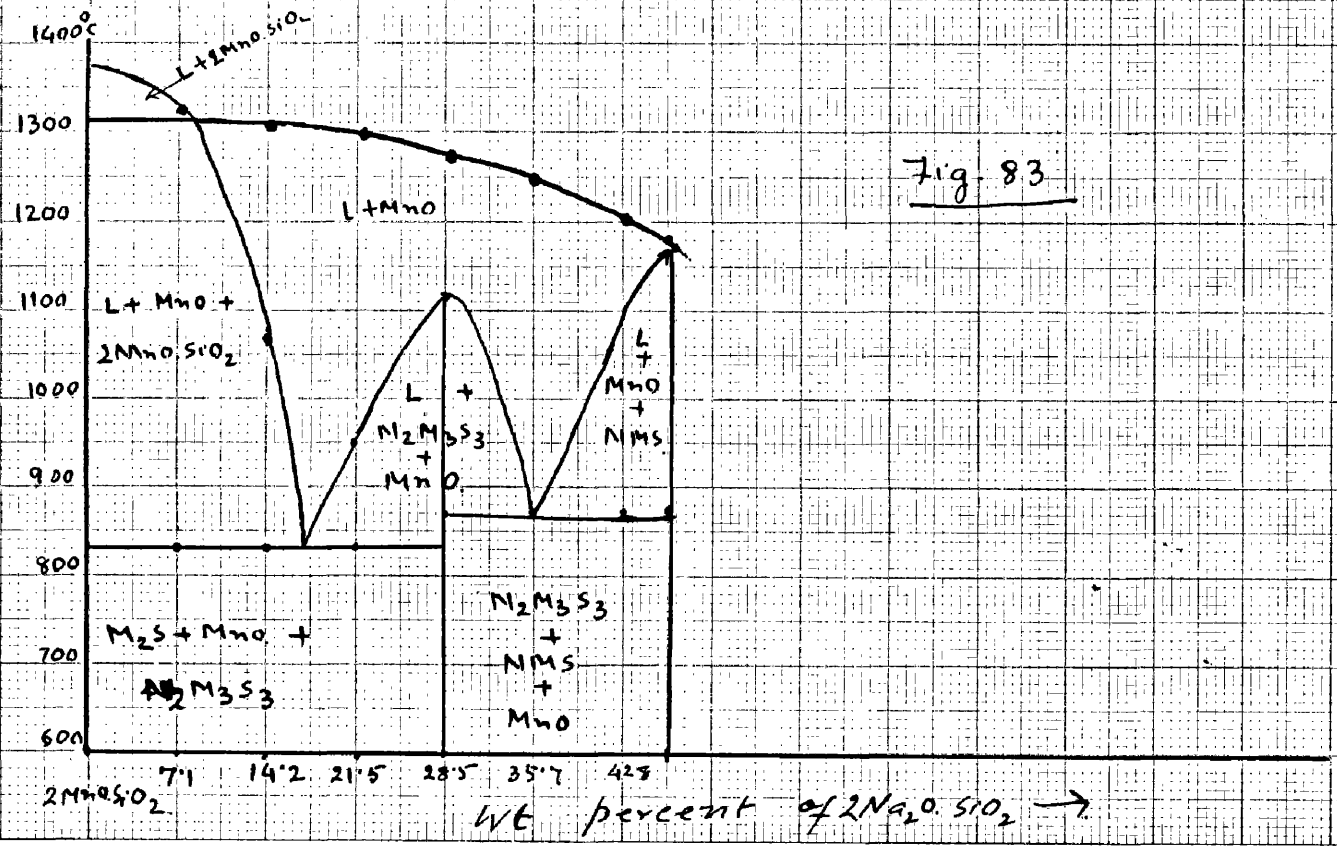
1400°C
1300
1200
1100
1000
900
800
700
600
L+2MnO.SiO2
L+MnO
L+ MnO + 2MnO.SiO2
L + N2M3S3 + MnO
L + MnO + NMS
M2S + MnO + N2M3S3
N2M3S3 + NMS + MnO
2MnO.SiO2
7.1
14.2
21.5
28.5
35.7
42.8
Wt percent of 2Na2O.SiO2 →

Fig. 83

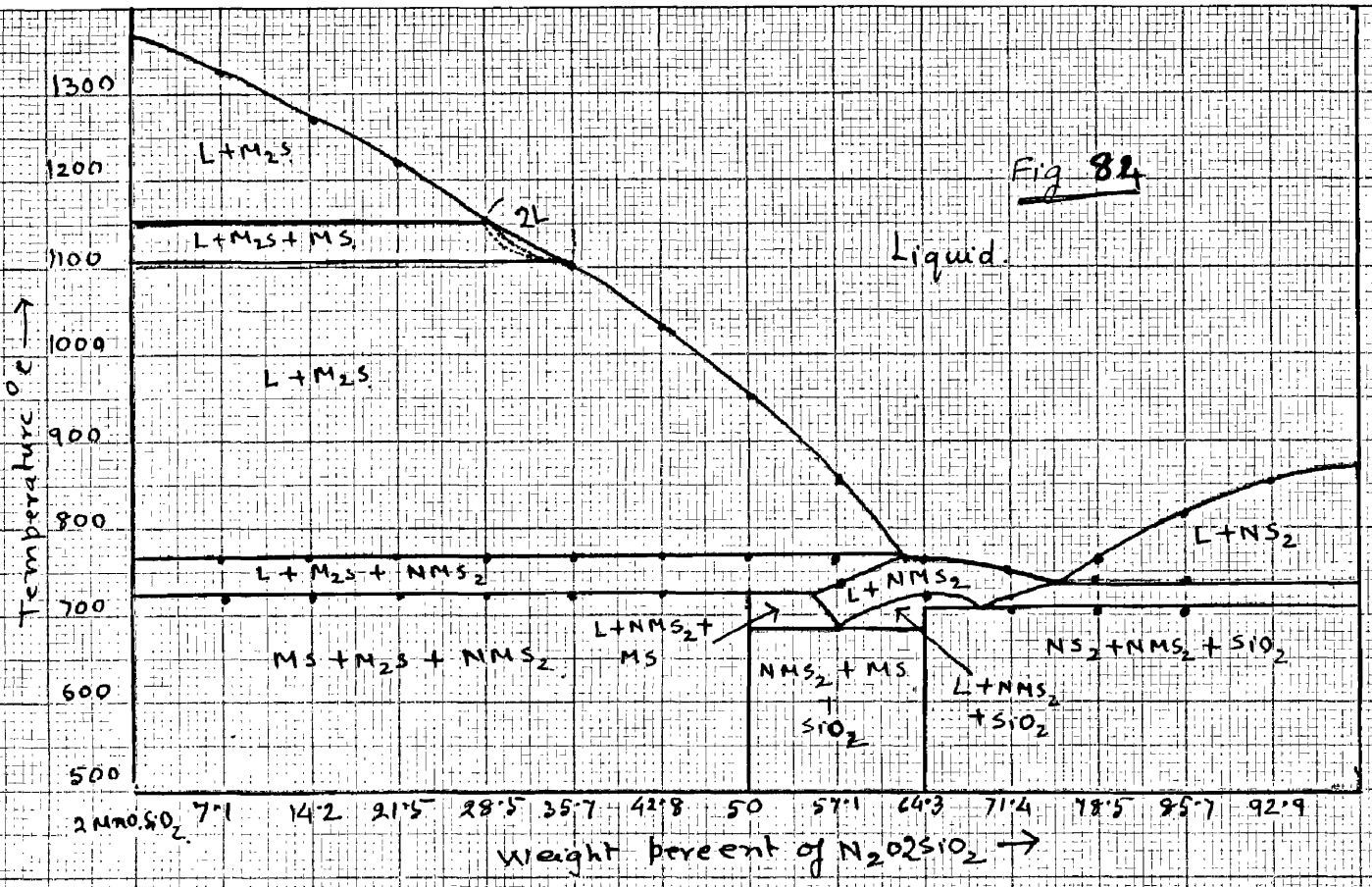
Fig 84
Liquid
L+M2S
2L
L+M2S+MS
L+M2S
L+M2S+NMS2
L+NMS2
L+NS2
L+NMS2+MS
MS+M2S+NMS2
NMS2+MS+SiO2
L+NMS2+SiO2
NS2+NMS2+SiO2
Temperature °C
1300
1200
1100
1000
900
800
700
600
500
2MnO.SiO2
7·1
14·2
21·5
28·5
35·7
42·8
50
57·1
64·3
71·4
78·5
85·7
92·9
Weight percent of Na2O2SiO2

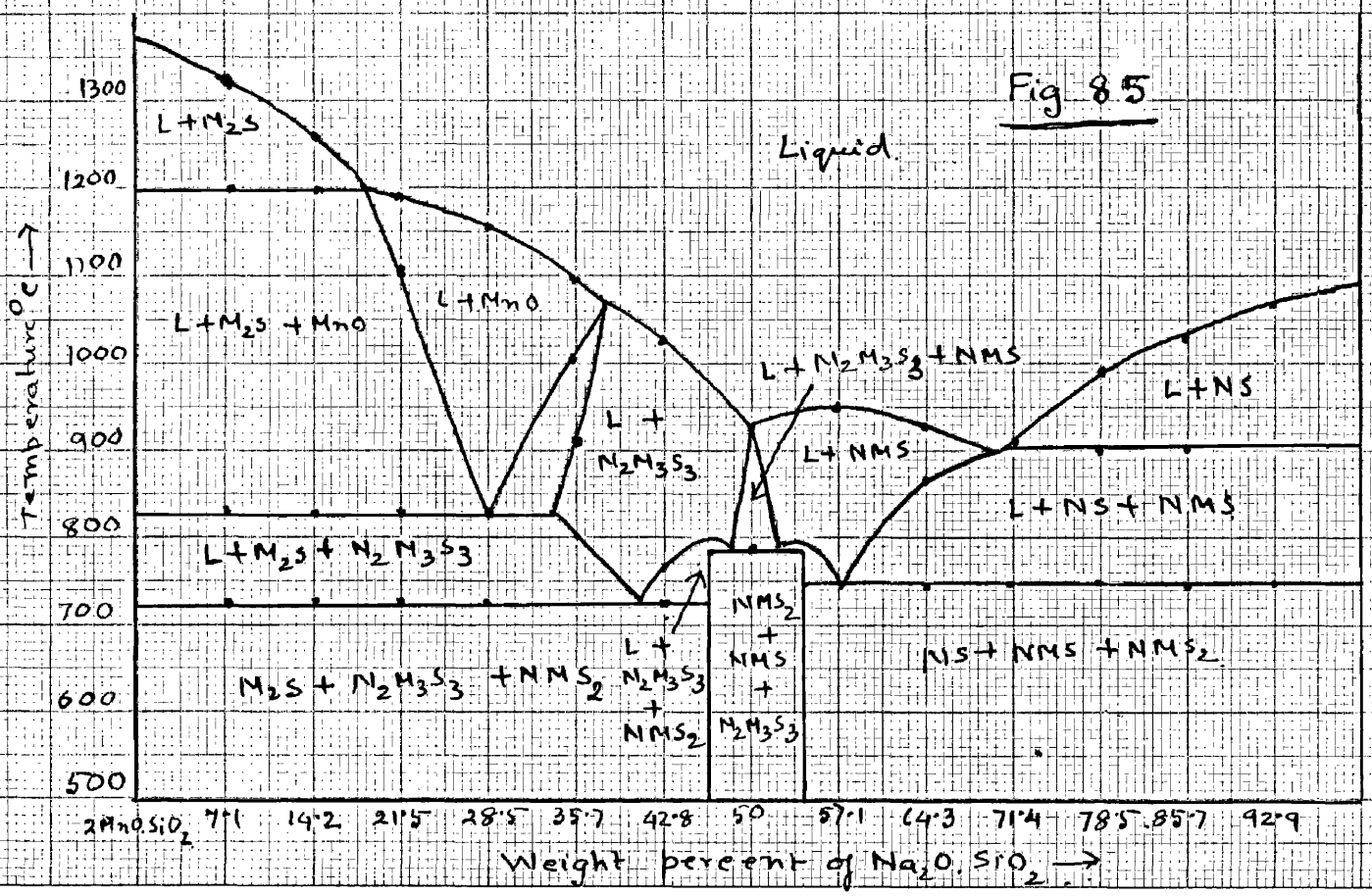
Fig 85
Liquid
L+M2S
L+MnO
L+M2S+MnO
L+N2M3S3+NMS
L+NS
L+N2M3S3
L+NMS
L+NS+NMS
L+M2S+N2M3S3
NMS2+NMS+N2M3S3
L+N2M3S3+NMS2
M2S+N2M3S3+NMS2
NS+NMS+NMS2
Temperature °C
1300
1200
1100
1000
900
800
700
600
500
2MnO.SiO2
7·1
14·2
21·5
28·5
35·7
42·8
50
57·1
64·3
71·4
78·5
85·7
92·9
Weight percent of Na2O.SiO2

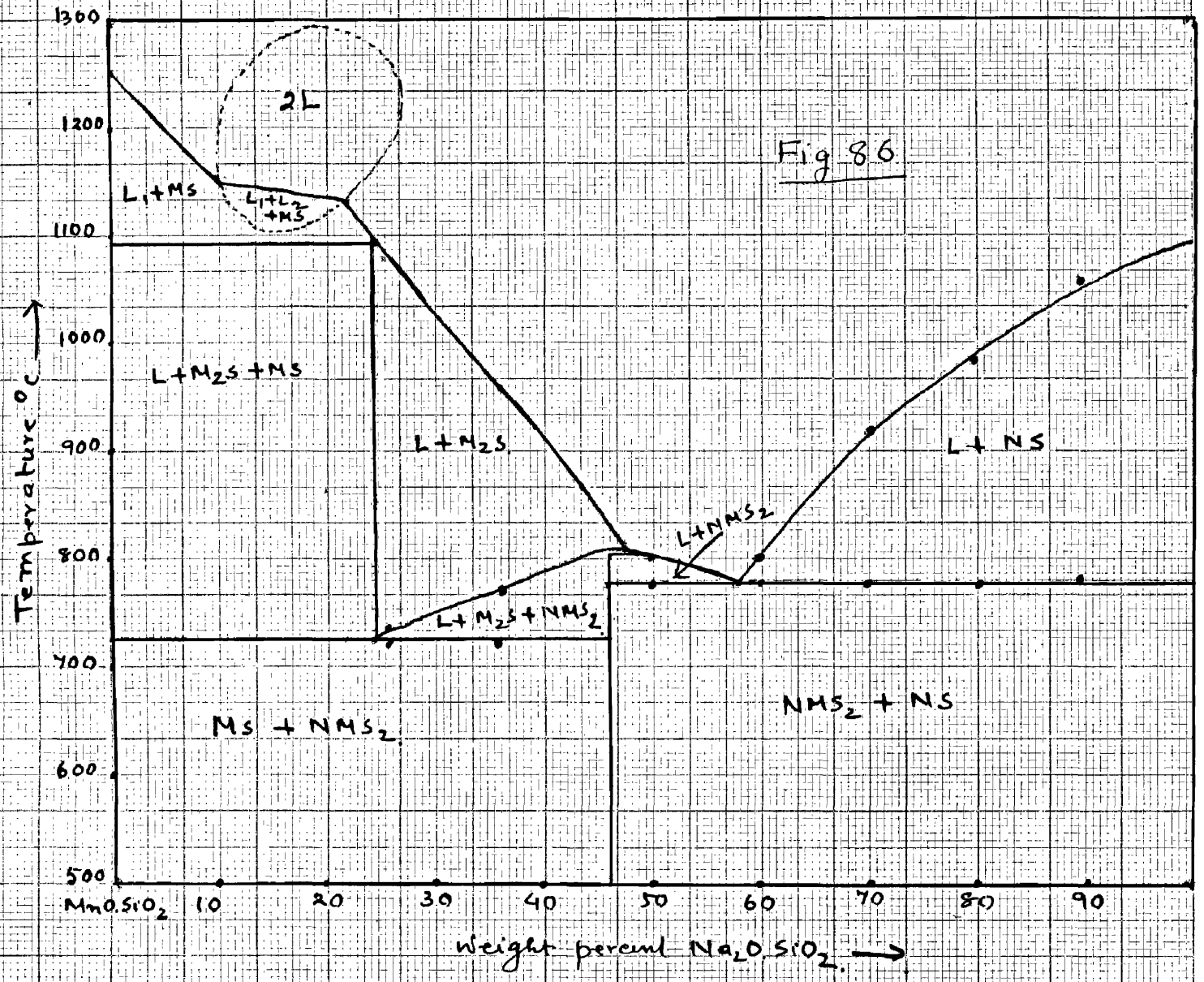
Fig 86
2L
L1+MS
L1+L2 +MS
L+M2S+MS
L+M2S
L+NS
L+NMS2
L+M2S+NMS2
MS + NMS2
NMS2 + NS
Temperature °C
1300
1200
1100
1000
900
800
700
600
500
MnO.SiO2
10
20
30
40
50
60
70
80
90
Weight percent Na2O.SiO2

CHAPTER 9.

LIQUID IMMISCIBILITY.

Fig 87

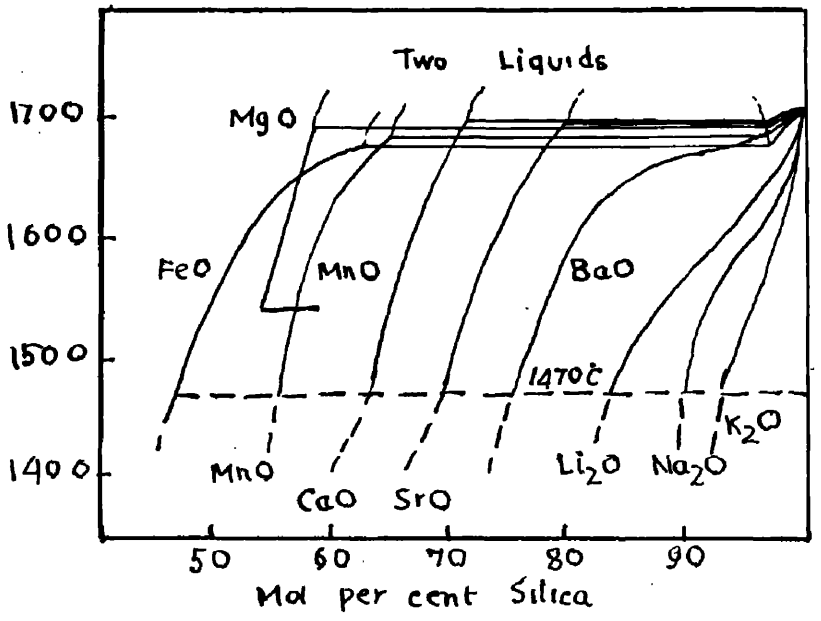
Two Liquids
1700
1600
1500
1400
MgO
FeO
MnO
BaO
1470°C
MnO
CaO
SrO
Li_2O
Na_2O
K_2O
50
60
70
80
90
Mol per cent Silica

LIQUID IMMISCIBILITY.

Liquid immiscibility is known to occur in many binary and more complex systems of silica with several basic oxides, e.g., FeO, MnO, CaO, MgO, SiO, ZnO, NiO and CoO. No immiscibility occurs in the binary alkali oxide-silica systems, nor in the $BaO-SiO_2$ and $PbO-SiO_2$ systems although the silica liquidus curves indicate that all the above systems except Rb_2O-SiO_2, Cs_2O-SiO_2 and $PbO-SiO_2$ show a tendency to separation into two liquids. Silica liquidus curves for these systems are shown in Fig.87.

The separation into two liquids in metal oxide-silica systems has been attributed by Warren and Pincus(34), to the need to satisfy the co-ordination requirements of Si^{4+} and the metallic cation. A state of lower free energy is attained when separation takes place into one liquid rich in silica in which the co-ordination requirements of Si^{4+} are satisfied and a second liquid which contains sufficient of the metallic oxide to enable the co-ordination requirements of the metallic cation to be satisfied. Thus in soda-silica melts with low soda content the interionic forces between silicon and oxygen tend to retain all the oxygen in a single phase. The attraction between Na^+ and singly bonded oxygen ions tends to cause separation of a second liquid phase richer in soda. As this second tendency is relatively weak no separation actually occurs. In the corresponding $CaO-SiO_2$ melts the interionic attraction forces between Ca^{++} and singly bonded oxygen ions are much stronger, and separation into two liquids takes place. The smaller the ionic radius of the metal ion, the larger is the metal-

oxygen ion attraction, and the greater will be the extent of the immiscibility gap. Warren and Pincus used the above explanation for two liquid formation to estimate the limit of immiscibility. Certain assumptions were made as to the maximum distance between Ca^{++} ions in $CaO-SiO_2$ glasses and the density of the melt. They obtained a value of 33 per cent by weight of CaO for the limit of the two liquid region which was regarded to be in satisfactory agreement with the experimental value of 28 per cent . A similar calculation for the $MgO-SiO_2$ system gave a value of 39 per cent by weight of MgO as compared with the experimental value of 31 per cent.

In ternary silicate systems in which both the binary metal oxide-silica systems show liquid immiscibility, the immiscibility gap extends across the diagram, e.g., $FeO-MnO-SiO_2$, $FeO-MgO-SiO_2$. Where only one of the binary systems shows liquid immiscibility, e.g., $Na_2O-MgO-SiO_2$, $CaO-Al_2O_3-SiO_2$, the gap is limited in area and extends only a short distance from the binary side showing immiscibility. It is believed that the effect of alkali oxides and alumina is to provide extra unsaturated oxygen ions. In the case of Na_2O the reason is obvious. With Al_2O_3 it is probable that the Al atoms enter the silicate network even though the Al^{3+} ion is trivalent.

Liquid immiscibility has also been observed in systems which do not contain silica, e.g., the binary systems $FeO-CaF_2$ and $CaO-B_2O_3$ and the ternary systems $FeO-CaO-P_2O_5$, $MnO-CaO-P_2O_3$ and $FeO-Na_2O-P_2O_5$. Thus in the $FeO-CaO-P_2O_5$ (35) system separation occurs into one liquid

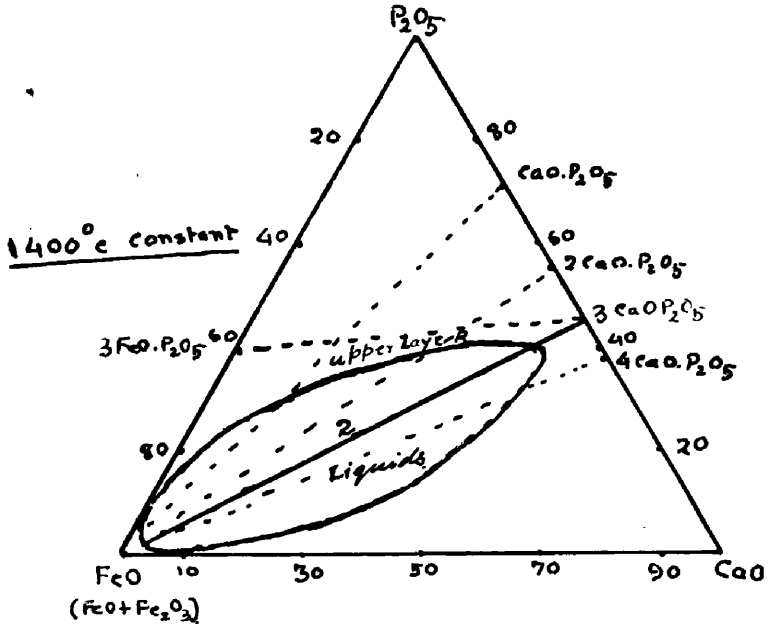
P_2O_5
1400°c constant
$CaO.P_2O_5$
$2CaO.P_2O_5$
$3CaO.P_2O_5$
$4CaO.P_2O_5$
$3FeO.P_2O_5$
upper layer
2 Liquids
FeO
$(FeO+Fe_2O_3)$
CaO

Fig 88

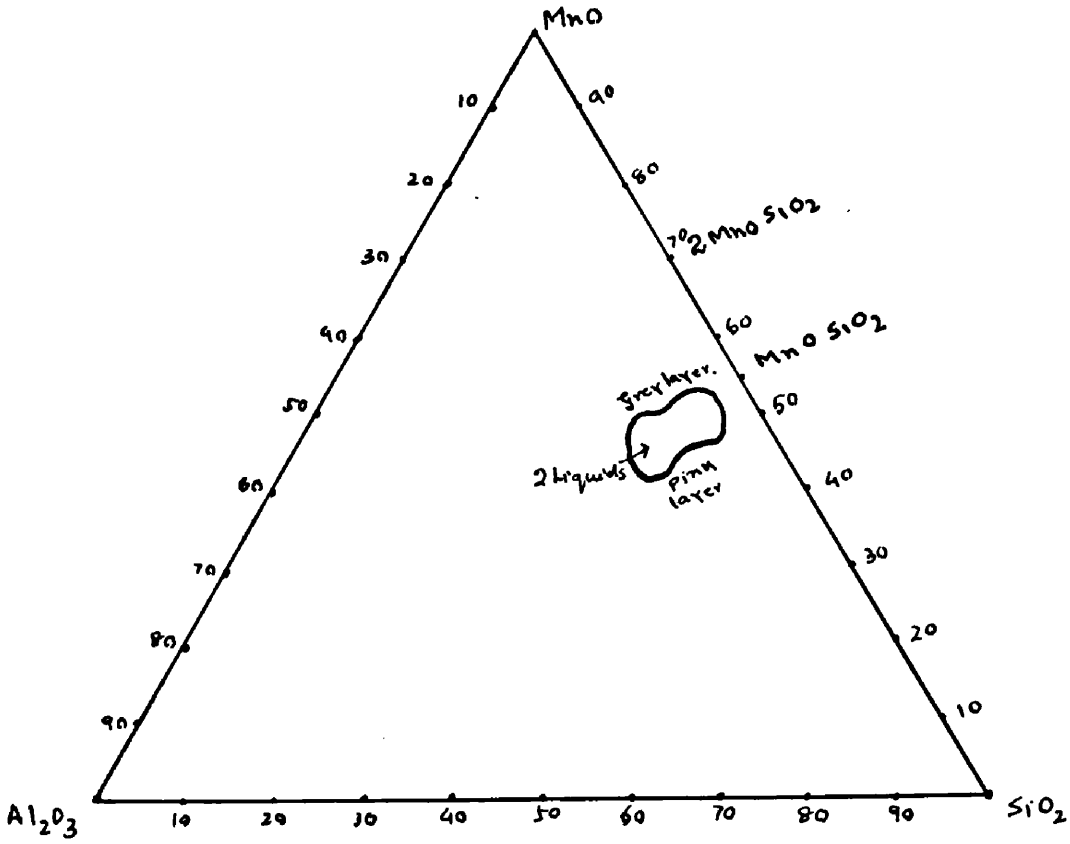
MnO
$2MnO\,SiO_2$
$MnO\,SiO_2$
Grey layer.
2 Liquids
pink layer
Al_2O_3
SiO_2

Fig 89

rich in FeO and the other liquid rich in $3CaO.P_2O_5$. As can be seen in Fig.88 no liquid immiscibility occurs in the binary systems although the FeO liquidus curve of the $FeO-P_2O_5$ system indicates a strong tendency to two liquid formation. Liquid immiscibility therefore shows itself as a closed lenticular shaped loop.

The satisfying of co-ordination requirements indicates that the states of lowest free energy will be obtained when the smaller Fe^{++} ions are mainly surrounded by smaller O^{++} ions and the larger Ca^{++} ions are associated with the larger PO_4 ions. The extent of this "sorting out" will depend upon the difference of free energy of formation from their constituent oxides of $3FeO.P_2O_5$ and $3CaO.P_2O_5$. In the $CaO-FeO-SiO_2$ system this type of immiscibility does not appear presumably because the difference between the free energies of formation of $2FeO.SiO_2$ and $2CaO.SiO_2$ is considerably smaller. Nevertheless Chipman(36) has shown that there is a strong positive deviation from ideality in the system as might be expected if a tendency to two liquid formation exists.

As has been described earlier a closed immiscibility loop appears in the $Na_2O-MnO-SiO_2$ system. An immiscibility gap was also found to occur in the $MnO-Al_2O_3-SiO_2$ system by Towers and Gworek(37) as shown in Fig.89, and it is probable that the reason for the gap is the same in both systems, for the main characteristics of the immiscibility gap are similar in the two systems. Thus the two layers found by Towers and Gworek were pink and gray, as in the present investigation and the

gap occurs at a corresponding part of the ternary diagram. No liquid immiscibility gap has been reported in the $MnO-SiO_2$ system, apart from the normal type at high silica contents, although recent experiments in which $MnO-SiO_2$ slags were melted in carbon crucibles at temperatures above the liquidus and cooled rapidly indicated that separation into two liquids in a composition range slightly less siliceous than $MnO.SiO_2$ occurs at temperature above the liquidus.

Mn^{++} occurs in 6-fold co-ordination in $2MnO.SiO_2$ but its state of co-ordination in Rhodonite ($MnO.SiO_2$) is uncertain. Voos(38) found that rhodonite formed an unbroken series of solid solutions with wollastonite in which Ca^{++} occurs in 8-fold co-ordination so that it is probable that Mn^{++} shows 8-fold co-ordination in rhodonite. On the other hand Fe^{++} and Mg^{++} only occur in 6-fold co-ordination, Ca^{++} shows 8 fold co-ordination in $CaSiO_3$ but its co-ordination state in more basic compounds is uncertain. However, Brandenberger(39) has assumed it to be 8-fold in γ -Ca_2SiO_4 and it may well be that Ca^{++} only occurs in 8-fold coordination in liquid slags.

Liquid immiscibility of the type under discussion may therefore be due to the occurrence of Mn^{++} in two different states of co-ordinatic in the liquid state, viz., 6-fold co-ordination in the liquid which gave rise to the grey layer and in which the silicate ions are possibly predominantly $Si_2O_7^{6-}$ and 8-fold co-ordination in the rhodonite type of liquid (corresponding to the pink layer) in which the silicate ions consists of $(Si_3O_9)^{6-}$ rings.

A C K N O W L E D G E M E N T.

The author wishes to thank Professor R. Hay and Dr. P.T. Carter for their help and advice during this investigation. The author also wishes to acknowledge the financial assistance received from the Union Carbide Corporation.

REFERENCES.

1. H.J.T. Ellingham. Trans. Soc. Chem. Ind. 1944 (63) p.125-133 Discussion Faraday Soc. No.4, 1948 p.129.

2. F.D.Richardson, and J.H.E. Jeffes. J.I.S.I., 1952(II) (171) p.165.

3. V.Giedroyc and T.E.Dancy. J.I.S.I., 1951(III) (160) p.353.

4. T.P.Colclough. Iron and Coal Trades Rev., 1936 (132) p.806.

5. T.P. Colclough. J.I.S.I., 1936 (134) p.547.

6. F.D.Richardson, J.H.E.Jeffes and G. Withers. J.I.S.I., 1950 (III) (166) p.213.

7. W.Oelsen and H.Wiemers. Mitt. Kaiser-Wilhelm Inst. Eisenforschung, 1942 (24) p.167.

8. W.R.Maddocks and E.T.Turkdogan. J.I.S.I., 1949 (162) p.249.

9. W.R.Maddocks and E.T.Turkdogan. J.I.S.I., 1952 (171) p.128.

10. C.Benedicks and H.Lofquist. "Non metallic inclusions in Iron and Steel" (Chapman and Hall) 1930, p.71.

11. P.Oberhoffer and K. d'Hurt. Stahl und Eisen 1919 (39) p.165, 196.

12. R. Hay, D.Howat, and J.White. J. Royal Tech. College (Glasgow), 1934, Vol.3, p.235.

13. British Iron and Steel Research Association, Annual Report 1954, p.64-65.

14. F.Doerinckel Metallurgie, 1911 (8) p.201.

15. J.W.Greig. Amer. Journ. of Sci. 1923 (13) p.133.

16. C.Benedicks and H.Lofquist. "Non Metallic Inclusions in Iron and Steel" (Chapman and Hall) 1930, p.98.

17. C.H.Herty. Metals and Alloys, 1930, p.883.

18. L. Pauling. "Nature of the Chemical Bond" 1940, p.352.

19. A.B. Murad. Ph.D. Thesis, Glasgow University, 1951.

20. F.C. Kracek. Journ. Phys. Chem. 1930 (34) p.1583.

21. G.W. Morey and N.L. Bowen. Journ. Phys. Chem. 1924 (28) p.1167.

22. J. Loffler. "Physical Chemistry of Silicates" Eitel, p.633 (1954).

23. E. Zintl. ibid. p.634.

24. V.W. Oelsen. Stahl und Eisen 1948 (68) p.75.

25. A. Dietzel. Glasstechnische Berichte 1948 (22) p.41.

26. H.B.Bell, A.B. Murad and P.T. Carter. Trans. A.I.M.E., 1952, p.718.

27. K.A. Fajan, and N.J. Kreidl. Journ. Amer.Cer. Soc., 1948 (31) p.105.

28. P.A. Niggli. "Physical Chemistry of Silicate" p.879, Eitel (1954).

29. G.F.Huttig and K.Dimoff. ibid. p.892.

30. W.E.S. Turner. Journ.Soc. Glass Tech. 1934 (18) p.143.

31. P.T. Carter and M.I.Ibrahim. ibid. 1952 (36) p.142.

32. G.R.Rigby. "Mineralogy of Ceramic Material" Rigby, p.47.

33. R. Hay, D.D.Howat, and J. White. Journ. Roy.Tech.College,(Glasgow), 1934 (3) 239.

34. A.G.Warren and B.E.Pincus. Jour. Amer.Cer. Soc., 1940 (23) 301.

35. W. Oelsen and H. Maetz. Mitt.Kaiser-Wilhelm-Inst. Eisenforschung 1941 (23) p.195.

36. C.R.Taylor and J. Chipman. Trans. A.I.M.E., 1943 (159) p.228.

37. H.Towers and J.Gworek. Journ. of West of Scotland Iron and Steel Inst. 1940-1944 (48-51) p.123.

38. E.B. Voos. Zeit. fur Anarg.Chemie, 1935 (222) p.201.

39. E.Brandenberger. "Physical Chemistry of Silicates" Eitel, 1954, p.20.

APPENDIX I.

RESULTS OF X-RAY DIFFRACTION.

ABBREVIATIONS.-

$2MnO.SiO_2$ = M_2S

$MnO.SiO_2$ = MS

$Na_2O.SiO_2$ = NS

$Na_2O.2SiO_2$ = NS_2

$2Na_2O.SiO_2$ = N_2S

$Na_2O.MnO.SiO_2$ = NMS

$2Na_2O.3MnO.3SiO_2$ = $N_2M_3S_3$

$Na_2O.MnO.2SiO_2$ = NMS_2

Intensity of X-ray Diffraction Lines.-

s = strong.

f.s. = fairly strong.

m = medium.

f.m. = fairly medium. (i.e., weak-medium)

w = weak.

v.s. = very weak.

$Na_2O.MnO.SiO_2$ (NMS)		$Na_2O.MnO.2SiO_2$ (NMS_2)	
Intensity	"d" values.	Intensity	"d" values.
s	3.012	m	3.647
m	2.858	s	3.281
s	2.728	v.s.	2.586
s	2.668	w	2.292
s	2.602	v.w.	2.207
m	2.438	m.	2.095
m	2.299	m	1.946
w	2.167	s	1.825
w	2.114	m	1.769
m	1.988	s	1.487
m	1.909	m	1.292
s	1.784	w	1.087
s	1.621		
w	1.566		
s	1.527		
w	1.458		
w	1.439		
m	1.389		
w	1.324		
w	1.304		
w	1.064		
w	1.137		

$2Na_2O.3MnO.3SiO_2$ ($N_2M_3S_3$)		Tephroite.	
Intensity	"d" values	Intensity	"d" values.
w	3.101	s	2.808
w	2.886	s	2.56
m	2.749	s	2.51
s	2.608	s	1.78
m	2.509	w	1.67
w	2.426	v.w.	1.615
w	2.343	m	1.54
w	2.128	m	1.52
m	1.860	m	1.43
m	1.687	w	1.37
s	1.517	w	1.35
w	1.315	m	1.06
m	1.177	m	1.04

$MnO.SiO_2$ (MS)		MnO	
Intensity	"d" values	Intensity	"d" values
s	2.991	s	2.564
s	2.773	s	2.22
m	2.608	s	1.57
m	2.249	s	1.341
m	2.18	s	1.284
m	1.816	m	1.111
m	1.72	s	0.994
m	1.61	m	0.9088
m	1.505	s	0.857
m	1.418	m	0.787
v.w.	1.316		
v.s.	1.263		

$Na_2O.SiO_2$ (NS)		$Na_2O.2SiO_2$ (NS_2)	
Intensity	"d" values	Intensity	"d" values
w	5.30	s	3.783
w	3.56	s	3.276
s	3.039	w	2.92
m	2.571	m	2.82
m	2.405	m	2.43
w	1.98	m	2.350
m	1.883	w	2.137
w	1.83	w	2.082
m	1.75	w	2.00
w	1.53	w	1.96
w	1.445	w	1.610
m	1.42	s	1.539
w	1.140	m	1.482
w	1.114	s	1.442
w	1.03	w	1.386
w	0.99	w	1.299
w	0.934	m	1.280
		w	1.16
		m	1.150
		s	1.136
		m	1.111
		m	1.04

MnO/NS = 50/50

Intensity	"d" values	Phases
m	3.011	NMS
f.m.	2.725	NMS
m	2.667	NMS
m	2.601	NMS
s	2.568	MnO
f.s.	2.218	MnO
f.m.	1.782	NMS
f.s.	1.567	MnO
m	1.525	NMS
m	1.338	MnO
m	1.282	MnO

MnO/NS = 40/60

Intensity	"d" values	Phas
s	3.013	NMS
w	2.860	NMS
s	2.726	NMS
s	2.669	NMS
m	2.602	NMS
m	2.566	MnO
m	2.219	MnO
w	1.986	NMS
s	1.783	NMS
f.s.	1.622	NMS
s	1.527	NMS
f.m.	1.339	MnO
f.m.	1.283	MnO

MnO/NS = 45/55

Same as slag
MnO/NS = 50/50.

MnO/NS = 35/65.

Intensity	"d" values	Phases
m	3.04	NS
f.m.	3.01	NMS
m	2.729	NMS
m	2.666	NMS
m	2.601	NMS
f.m.	2.574	NS
f.m.	2.404	NS
f.s.	1.785	NMS
f.s.	1.622	NMS
f.s.	1.525	NMS
w	1.748	NS
w	1.417	NS
v.w.	1.143	NS

MnO/NS = 30/70

Intensity	"d" values	Phases
m	3.04	NS
f.m.	3.01	NMS
f.m.	2.857	NMS
m	2.730	NMS
m	2.669	NMS
m	2.601	NMS
m	2.569	NS
m	2.402	NS
v.w.	1.978	NS
w	1.888	NS
w	1.746	NS
w	1.786	NMS
m	1.623	NMS
m	1.524	NMS
w	1.421	NS
w	1.388	NMS
v.s.	0.99	NS

MNO/NS = 25/75

Same as slag
MNO/NS = 30/70

MnO/NS = 20/80

same as slag
MnO/NS = 30/70

MnO/NS = 15/85

Intensity	"d" values	phases
s	3.038	NS
w	3.01	NMS
w	2.727	NMS
w	2.667	NMS
w	2.601	NMS
m	2.572	NS
m	2.403	NS
m	1.885	NS
w	1.783	NMS
f.m.	1.748	NS
w	1.62	NMS
v.w.	1.53	NMS
v.w.	1.444	NS
w	1.421	NS
v.w.	1.112	NS
v.w.	1.031	NS

MnO/NS = 10/90

same as slag
MnO/NS = 15/85

M_2S/N_2S = 92.9/7.1

Intensity	"d"values	Phases
s	2.808	M_2S
w	2.61	$N_2M_3S_3$
v.s.	2.56	M_2S_2 MnO
s	2.509	M_2S
s	2.222	MnO
s	1.78	M_2S
m	1.569	MnO
m	1.542	M_2S
m	1.52	M_2S
w	1.516	$N_2M_3S_3$
w	1.508	$N_2M_3S_3$
m	1.342	MnO
f.m.	1.283	MnO
m	1.058	M_2S
m	1.041	M_2S

M_2S/N_2S = 85.8/14.2

Intensity	"d"values	Phases
m	2.807	M_2S
m	2.607	$N_2M_3S_3$
v.s.	2.562	M_2S MnO
m	2.508	M_2S $N_2M_3S_3$
f.s.	2.221	MnO
w	1.859	$N_2M_3S_3$
m	1.779	M_2S
v.w.	1.688	$N_2M_3S_3$
f.m.	1.572	MnO
f.m.	1.516	$N_2M_3S_3$
f.s.	1.339	MnO
f.s.	1.284	MnO
v.w.	1.176	$N_2M_3S_3$
w	1.06	M_2S
w	1.041	M_2S
f.s.	0.995	MnO

M_2S/N_2S = 78.5/21.5

same as slag
M_2S/N_2S = 85.8/14.2

M_2S/N_2S = 71.5/28.3

Intensity	"d" values	Phase
v.w.	4.14	?
f.s.	2.607	$N_2M_3S_3$
s	2.566	MnO
f.m.	2.51	$N_2M_3S_3$
f.s.	2.22	MnO
f.m.	1.860	$N_2M_3S_3$
f.m.	1.686	$N_2M_3S_3$
m	1.569	MnO
m	1.516	$N_2M_3S_3$
f.m.	1.342	MnO
f.m.	1.283	MnO
w	1.176	$N_2M_3S_3$

M_2S/N_2S = 64.3/35.7

Intensity	"d" values	Phase.
f.s.	3.011	NMS
w	2.857	NMS
f.s.	2.727	NMS
m	2.666	NMS
m	2.609	$N_2M_3S_3$
s	2.565	MnO
f.m.	2.510	$N_2M_3S_3$
w	2.437	NMS
v.w.	2.425	$N_2M_3S_3$
f.m.	2.300	NMS
w	1.91	NMS
w	1.861	$N_2M_3S_3$
f.s.	1.783	NMS
f.m.	1.688	$N_2M_3S_3$
m	1.622	NMS
m	1.529	NMS
m	1.569	MnO
m	1.516	$N_2M_3S_3$
f.m.	1.340	MnO
f.m.	1.284	MnO
f.w.	1.176	$N_2M_3S_3$

$2MnO.SiO_2 : Na_2O.2SiO_2$
= 92.9:7.1

v.w.	3.646 NMS_2
w	3.280 NMS_2
w	2.990 MS
s	2.807 M_2S
w	2.773 MS
f.m.	2.585 NMS_2
s	2.509 M_2S
v.w.	2.25 MS
s	1.78 M_2S
f.m.	1.541 M_2S
f.m.	1.429 M_2S
w	1.825 NMS_2
w	1.466 NMS_2
f.m.	1.262 MS

Slag $2MnO.SiO_2 : Na_2O.2SiO_2$
= 85.8/14.2 and
78.5/21.5

same as $2MnO.SiO_2 : Na_2O.2SiO_2$
= 92.9/7.1

$2MnO.SiO_2 : Na_2O.2SiO_2$
= 71.5/28.5

w	3.646 NMS_2
f.m.	3.280 NMS_2
f.m.	2.990 MS
m	2.807 M_2S
w	2.773 MS
f.s.	2.585 NMS_2
w	2.25 MS
w	2.18 MS
w	2.096 NMS_2
w	1.945 NMS_2
f.m.	1.825 NMS_2
f.m.	1.78 M_2S
w	1.609 MS
f.m.	1.541 M_2S
w	1.505 MS
f.m.	1.466 NMS_2
m	1.429 M_2S
m	1.263 MS

Slag $2MnO.SiO_2 : Na_2O.2SiO_2$
= 64.3/35.7 and 57.2/42.8

Same as 71.5/28.5

$2MnO.SiO_2 : Na_2O.2SiO_2$
= 50/50

f.m.	3.646 NMS_2
m	3.280 NMS_2
f.m.	2.990 MS
w	2.773 MS
s	2.586 NMS_2
w	2.25 MS
w	2.18 MS
f.m.	2.096 NMS_2
w	1.946 NMS_2
f.m.	1.825 NMS_2
w	1.609 MS
w	1.505 MS
f.m.	1.486 NMS_2
v.w.	1.291 NMS_2
f.m.	1.263 MS

$2MnO.SiO_2 : Na_2O.SiO_2$
= 42.9/57.1

f.m.	4.301 Silica(Tridymite)
w	3.808 Silica(Tridymite)

Rest of the lines same as

$2MnO.SiO_2 : Na_2O.2SiO_2$
= 50/50

$2MnO.SiO_2 : Na_2O.2SiO_2$
$= 35.7/64.3$

f.m.	4.301 silica(Tridymite)
v.w.	4.08 silica)Tridymite)
f.m.	3.646 NMS_2
m	3.280 NMS_2
s	2.585 NMS_2
f.m.	2.096 NMS_2
w	1.946 NMS_2
f.m.	1.825 NMS_2
w	1.768 NMS_2
m	1.486 NMS_2

$2MnO.SiO_2 : Na_2O.2SiO_2$
$= 21.5/78.5$

m	4.30 (silica)Tridymite)
v.w.	4.08 (silica) "
v.w.	3.81 (silica) "
f.m.	3.782 NS_2
f.m.	3.646 NMS_2
f.m.	3.280 NMS_2
f.m.	3.276 NS_2
w	2.82 NS_2
m	2.586 NMS_2
w	2.43 NS_2
w	2.351 NS_2
w	2.096 NMS_2
w	1.946 NMS_2
f.m.	1.825 NMS_2
m	1.538 NS_2
w	1.486 NMS_2
v.w.	1.291 NMS_2
v.w.	1.281 NS_2
v.w.	1.151 NS_2
w	1.136 NS_2

$2MnO.SiO_2/Na_2O.SiO_2$
$= 92.9:7.1$

f.m.	3.280	NMS_2
s.	2.808	M_2S
f.m.	2.606	$N_2M_6S_3$
f.m.	2.584	NMS_2
s	2.56	M_2S
s	2.509	M_2S $N_2M_6S_3$
w	2.096	NMS_2
f.m.	1.826	NMS_2
f.s.	1.781	M_2S
f.m.	1.53	M_2S
w	1.516	$N_2M_6S_3$
w	1.488	NMS_2
v.w.	1.178	$N_2M_6S_3$
f.m.	1.05	M_2S

$2MnO.SiO_2:Na_2O.SiO_2 =$
$85.8:14.2$
same as
$2MnO.SiO_2:N_2O.SiO_2$
$= 92.9:7.1$

$2MnO.SiO_2/Na_2O.SiO_2$
$= 78.6:21.4$

v.w.	3.646	NMS_2
f.m.	3.281	NMS_2
m	2.807	M_2S
v.w.	2.750	$N_2M_6S_3$
f.m.	2.608	$N_2M_6S_3$
f.s	2.586	NMS_2
m	2.561	M_2S
s	2.51	M_2S $N_2M_6S_3$
w	2.095	NMS_2
w	1.945	NMS_2
w	1.859	$N_2M_6S_3$
f.m.	1.826	NMS_2
f.m.	1.78	M_2S
f.m.	1.53	M_2S
f.m.	1.516	$N_2M_6S_3$
w.	1.487	NMS_2
v.w.	1.178	$N_2M_6S_3$
f.m.	1.05	M_2S

$2MnO.SiO_2:Na_2O.SiO_2$
$= 71.5:28.5$
and $64.3:35.7$
same as
$2MnO.SiO_2:Na_2O.SiO_2$
$= 78.6:21.4$

$2MnO.SiO_2 : Na_2O.SiO_2$
$= 57.2 : 42.8$

f.m.	3.647	NMS_2
m	3.280	NMS_2
w	2.808	M_2S
w	2.749	$N_2M_8S_3$
m	2.607	$N_2M_8S_3$
f.s.	2.586	NMS_2
w	2.561	M_2S
m	2.51	M_2S $N_2M_8S_3$
w	2.095	NMS_2
f.m.	1.86	$N_2M_8S_3$
f.m.	1.826	NMS_2
w	1.78	M_2S
w	1.769	NMS_2
w	1.687	$N_2M_8S_3$
m	1.516	$N_2M_8S_3$
w	1.487	NMS_2
w	1.177	$N_2M_8S_3$

$2MnO.SiO_2 : Na_2O.SiO_2$
$= 50 : 50$

f.m.	3.647	NMS_2
m	3.280	NMS_2
m	3.011	NMS
w	2.858	NMS
w	2.749	$N_2M_8S_3$
m	2.607	$N_2M_8S_3$
m	2.728	NMS
m	2.667	NMS
f.m.	2.601	NMS
f.s.	2.585	NMS_2
w	2.509	$N_2M_8S_3$
w	2.095	NMS_2
f.m.	1.86	$N_2M_8S_3$
f.m.	1.826	NMS_2
m	1.785	NMS
w	1.769	NMS_2
w	1.687	$N_2M_8S_3$
w	1.621	NMS
m	1.516	$N_2M_8S_3$
w	1.487	NMS_2
w	1.177	$N_2M_8S_3$

$2MnO.SiO_2/Na_2O.SiO_2$
= 42.9:57.1

f.m.	3.647	NMS_2
f.m.	3.281	NMS_2
w	3.04	NS
f.s.	3.012	NMS
f.m.	2.858	NMS
f.s.	2.729	NMS
f.s.	2.668	NMS
m	2.602	NMS
f.s.	2.586	NMS_2
w	2.436	NMS
w	2.095	NMS_2
f.m.	1.826	NMS_2
m	1.785	NMS
v.w.	1.75	NS
f.m.	1.621	NMS
w	1.483	NMS_2
v.w.	1.419	NS
v.w.	1.388	NMS

$2MnO.SiO_2$: $Na_2O.SiO_2$ = 35.7/64.3
and 28.6/71.4
same as $2MnO.SiO_2/Na_2O.SiO_2$
= 42.9/57.1

$2MnO.SiO_2$:$Na_2O.SiO_2$
= 21.5:78.5

w	3.646	NMS_2
w	3.281	NMS_2
m	3.039	NS
f.m.	3.012	NMS
w	2.858	NMS
f.m.	2.73	NMS
m	2.668	NMS
w	2.602	NMS
w	2.585	NMS_2
w	2.571	NS
w	2.407	NS
w	1.882	NS
w	1.825	NMS_2
w	1.785	NMS
w	1.75	NS
w	1.42	NS
v.w.	1.141	NS
v.w.	1.032	NS

$2MnO.SiO_2$:$Na_2O.SiO_2$
= 14.3/85.7
same as $2MnO.SiO_2/Na_2O.SiO_2$
= 21.5/78.5

PETROLOGICAL DATA.

Phase	Refractive Index.	Birefringence	Crystal Habit.
$2MnO.SiO_2$	= 1.782 = 1.818	1st and 2nd order Colours	Orthorhombic
$MnO.SiO_2$	= 1.735 = 1.742	Maximum polarization Colour yellow.	Triclinic
$Na_2O.2SiO_2$	1.501	1st order yellow.	Orthorhombic
$Na_2O.SiO_2$	1.518	1st order orange.	Orthorhombic
$Na_2O.MnO.SiO_2$	1.653	1st order yellow.	Pseudo cubic.
$Na_2O.MnO.2SiO_2$	1.605	1st order yellow.	Pseudo cubic.
$2Na_2O.3MnO.3SiO_2$	1.674	1st order yellow.	Pseudo cubic.